5-2023

Identification of a role beyond iron acquisition for yersiniabactin during Yersinia pestis infection.

Sarah Price
University of Louisville

IDENTIFICATION OF A ROLE BEYOND IRON ACQUISITION FOR YERSINIABACTIN DURING

YERSINIA PESTIS INFECTION

By

Sarah LeAnn Price
B.S. University of Tennessee, 2012
M.S. University of Louisville, 2018

A Dissertation
Submitted to the Faculty of the
School of Medicine of the University of Louisville
in Partial Fulfillment of the Requirements
for the Degree of

Doctor of Philosophy in Microbiology and Immunology

Department of Microbiology and Immunology
University of Louisville
Louisville, Kentucky

May 2023

IDENTIFICATION OF A ROLE BEYOND IRON ACQUISITION FOR YERSINIABACTIN DURING

YERSINIA PESTIS INFECTION

By

Sarah LeAnn Price
B.S. University of Tennessee, 2012
M.S. University of Louisville, 2018

A Dissertation Approved on

March 31st, 2023

By the following Dissertation Committee:

_____
Dr. Matthew Lawrenz, PhD

_____
Dr. Yousef Abu-Kwaik, PhD

_____
Dr. James Collins, PhD

_____
Dr. Jon Warawa, PhD

_____
Dr. Deborah Yoder-Himes, PhD

ii

DEDICATION

This work is dedicated to those that believed in me at my lowest points, inspired me when I felt
life was dull, and taught me how to be a scientist.
Our failures do not define us, they create us.

Deb Eberle,
For me reminding me that science is the most creative outlet in the world.

Lucio Gama,
For providing me with the opportunity that changed my life forever.

Brandon Bullock,
For your advice, lack of patience, and cooking tips. You always understood me when
no one else did. INTJ.

ACKNOWLEDGEMENTS

ABSTRACT

IDENTIFICATION OF A ROLE BEYOND IRON ACQUISITION FOR YERSINIABACTIN DURING

YERSINIA PESTIS INFECTION

Sarah Price

March 31st, 2023

Yersinia pestis is a Gram-negative re-emerging bacterial pathogen that is responsible for bubonic, septicemic, and pneumonic plague. *Y. pestis* and other bacteria require transition metals, such as iron, zinc, and manganese, to maintain intermediary metabolism, transcriptional regulation, and virulence. To inhibit infection, eukaryotic organisms have developed distinct mechanisms, called nutritional immunity, to sequester these important nutrients from invading bacteria. For pathogens to colonize the vertebrate host, they have evolved dedicated acquisition systems for transition metals. During infection, *Y. pestis* overcomes iron limitation by secreting the siderophore yersiniabactin. Additionally, *Y. pestis* requires zinc for infection and utilizes high affinity transporters to overcome zinc restriction. The first zinc importer identified in *Y. pestis* was the ZnuABC transport system, which is essential for *in vitro* growth. Notably, ZnuABC is not required for *Y. pestis* virulence. Thus, while zinc acquisition is recognized as important for bacterial pathogenesis, there is a gap in our understanding of zinc uptake by *Y. pestis*. Recently, an unexpected role for the yersiniabactin system was identified for growth in zinc limited medium. Moreover, a *znuBC* mutant that lacks genes involved in yersiniabactin synthesis (e.g., *irp2*) was completely attenuated for virulence. These data suggested yersiniabactin might be involved in zinc acquisition during

infection. The findings I present here are the first to demonstrate a novel role for yersiniabactin in zinc acquisition in *Y. pestis*. I also show that this conceptually novel mechanism allows *Y. pestis* to overcome zinc nutritional immunity in both the mammalian and insect host. Furthermore, using a technically innovative approach called droplet Tn-seq, I was able to identify the primary secretion mechanism for yersiniabactin. These studies not only provide a significantly better understanding of the role for yersiniabactin-dependent zinc acquisition in *Y. pestis* virulence, but since yersiniabactin is a conserved virulence factor in other Gram-negative pathogens, also provide new insight into how a variety of other pathogens acquire zinc during infection. Furthermore, since yersiniabactin is essential for virulence, my identification of the yersiniabactin secretion system represents a novel target for the development of an anti-virulence therapeutic that could be used to combat infections by multiple bacteria.

TABLE OF CONTENTS

LIST OF FIGURES

LIST OF TABLES

CHAPTER 1

YERSINIA PESTIS AND METALS

INTRODUCTION

1.1 *Yersinia pestis*: the flea, the rat, the legend

In the bacterial family of Yersiniaceae, the genus *Yersinia* consists of 26 species, including the three human pathogens: *Yersinia pseudotuberculosis*, *Yersinia enterocolitica*, and *Yersinia pestis*. *Y. enterocolitica* and *Y. pseudotuberculosis* are enteric pathogens that lead to gastrointestinal illness and rarely cause fatal disease. These two bacteria are found free-living in the environment (1). *Y. enterocolitica* and *Y. pseudotuberculosis* are spread through the fecal-oral route for human transmission. The other *Yersinia* family member is *Y. pestis* and sequence homology shows that *Y. pseudotuberculosis* is an ancestor of *Y. pestis* (1). It has been estimated that *Y. pestis* diverged from *Y. pseudotuberculosis* around 1,500 to 20,000 years ago and shares around 97% gene homology (1–3). Despite the genetic similarity, the pathogenesis of *Y. pestis* is quite unique from *Y. pseudotuberculosis*. *Y. pestis* is the etiologic agent of an acute and rapid disease with significant mortality rates if left untreated, known as plague. Plague manifests in three forms of disease: bubonic plague, pneumonic plague, and septicemic plague (4).

Y. pestis has significantly impacted human history through three major pandemics, which are the Justinian Plague, the Great Mortality, and the Modern Pandemic. In the 6th century AD, the Justinian Plague spread around areas located near the Mediterranean Sea (5). The Great Mortality

occurred in the 14th century in Europe and continued intermittently for 300 years eliminating approximately one third of the population of the old world, with the Black Death occurring in the 1350s (4, 5). The most recent outbreak was the Modern Pandemic, which began in China in the 19th century and spread across the world (4). In 1894 during the Modern Pandemic, Alexandre Yersin identified and cultured the causative bacterium of plague (6). With its disturbing history, plague is often classified as an historical disease and only a concern of the past. However, the disease remains endemic in many parts of the world, including Africa, Asia, and the Americas, including the United States (5, 7). With the recurrence of the disease in several countries, plague has been categorized as reemerging pathogen by the World Health Organization (4).

Y. pestis is an enzootic pathogen that is naturally maintained in a cycle between the flea transmission vector and rodent hosts (4, 7). In these rodent populations, *Y. pestis* is endemic and these reservoirs are the cause of continuous and frequent outbreaks in places like Madagascar and the Democratic Republic of Congo (5, 8). These natural reservoirs include species such as rats, field mice, gerbils, and marmots (4, 8, 9). Humans can contract plague when bitten by an infected flea or inhalation of contaminated aerosols, including respiratory droplets that can promote person-to-person transmission – outbreaks have been reported that were initiated by flea transmission but rapidly spread through populations by aerosol transmission (10). The World Health Organization estimates that 2,000 to 4,000 cases of plague occur each year (9, 11). Although plague is currently treatable with antibiotics, this treatment option is only useful if the disease is diagnosed early. Unfortunately, there is no vaccine to prevent plague or stop the rapid transmission of *Y. pestis* through a population during an outbreak (12).

In the flea, *Y. pestis* infection is limited to the digestive tract. The digestive system of the flea is made up of an esophagus, proventriculus, midgut, and hindgut (13). The midgut is where all digestion and absorption of nutrients from a bloodmeal occurs and where *Y. pestis* must survive for transmission (13). Very little information is known about the physiological environment in the flea gut including pH, nutrient availability, osmotic pressure, and redox potential. Fleas do have very limited microflora in their digestive tract which may contribute to a difficult environment to

colonize (14). *Y. pestis* has unique mechanisms to allow for survival in this challenging environment. For transmission to the mammalian host, *Y. pestis* creates a solid mass that blocks blood flow in the proventriculus, which typically propels blood into the midgut, forcing the flea to regurgitate the blockage (13). While it has been shown that *Y. pestis* can survive on the mouth of the flea after a blood meal and be transmitted to the next host (15), biological transmission due to proventricular blockage is the most reliable means of spread of *Y. pestis* to a mammalian host (10, 15).

In the human host, the natural progression of disease initiated by an infected flea bite begins in the dermis of the skin (13, 16). Infection from a flea can occur with as few as 1-100 bacteria (4). From the site of inoculation, the bacteria travel through the lymphatic system to the draining lymph node. In the lymph node, the bacteria replicate rapidly to colonize the lymph node and the infected lymph node increases in size to cause a "bubo", which is a painful, swollen mass (12). The bubo is a hallmark symptom of bubonic plague, which is 40-60% lethal in 5-10 days post-exposure if left untreated. From the lymph node, *Y. pestis* can disseminate to the host's bloodstream to cause septicemic plague. This form of plague is 100% fatal if left untreated at the onset of symptoms (4, 11). In septicemic plague, the bacteria can further travel through the bloodstream to colonize the spleen, liver, and lungs (17). If the bacteria colonize the lung, secondary pneumonic plague will develop (4, 11). During pneumonic plague, the bacteria can easily spread from person-to-person through aerosol transmission leading to primary pneumonic plague, which can quickly lead to death in only 3 days. Plague manifests in all forms with flu-like symptoms with body aches, fevers, chills, and malaise (4).

1.2 A silent, yet deadly killer

To survive in each host, *Y. pestis* utilizes a plethora of virulence factors to establish infection in mammals or fleas. Each of these hosts presents distinctive environments that the bacteria must adjust to for colonization and transmission. While little is known about the atmosphere of the flea gut, the temperature inside the flea is 26 °C , which is significantly lower than the 37 °C of

mammalian body temperature (4). While the obstacles for colonization of the flea remain less understood, the mammalian host has a robust immune system to challenge *Y. pestis* pathogenesis.

1.2.a. Colonization of the flea

In the flea, three main virulence factors for transmission haven been characterized: Yersinia murine toxin (Ymt), hemin storage locus (Hms), and plasminogen activator (Pla) (18). Murine toxin is a cell-associated, phospholipase D protein released upon bacterial cell death and receives its name from the toxic effects is has on mice and rats during infection (19). Despite the known toxic effects of Ymt, an *ymt* mutant remains fully virulent for mice. In fact, the expression of Ymt is downregulated at 37 °C (20), suggesting an alternative importance for infection outside of the mammalian host. Specifically, Ymt has been shown to play a role in colonization of the flea midgut, which is a key step in transmission of *Y. pestis* (21). Another virulence determinant is the *hms* locus, which is located on chromosome on the pigmentation (*pgm*) locus that was defined by the pigmented color that the bacteria absorb in the presence of hemin or Congo Red at 26 °C (4, 22–24). The *hms* locus encodes for four genes responsible for hemin storage in the outer membrane of the bacteria and is essential for the development of the blockage in the flea required for transmission (25). When *hms* is present, *Y. pestis* forms a biofilm that supports proventricular blockage that a *hms* mutant cannot produce (21, 25–27). The blockage in the proventriculus improves transmissibility to a new host and is induced by a PhoP-PhoQ regulatory system (10, 28–30). The third virulence factor used by *Y. pestis* in the flea is *pla*, which is on the pCP1 plasmid and encodes a surface protease that leads to increased tissue invasiveness and systemic spread of the bacteria (31). In bubonic plague transmission, Pla is essential because it enhances dissemination of *Y. pestis* from the site of inoculation (32).

1.2.b. Virulence factors in the mammalian host

During infection of the mammalian host, *Y. pestis* utilizes several factors to evade the immune response and overcome the innate immune system (33–36). Since *Y. pestis* causes an acute infection with rapid disease progression, these interactions with innate immune cells, such as neutrophils and macrophages are important to pathogenesis. Early in infection, *Y. pestis* imposes

a non-inflammatory environment in the host. When the innate immune system responds, a cytokine

storm is released in the host by massive infiltration of antimicrobial products and cytokines (34, 37).

On the pCD1 plasmid, *Y. pestis* encodes for the type three secretion system (T3SS) that is

temperature regulated and only active at 37 °C in the mammalian host (4). The T3SS secretes

Yersinia outer membrane proteins (Yops) that interact with host signaling pathways to inhibit

phagocytosis and induction of a pro-inflammatory response (38–40). For translocation of Yops, the

T3SS directly interacts with host cells and forms a pore on the membrane for Yops to travel through

(39). Secreted Yops have been shown to target neutrophils, macrophages, and dendritic cells (41,

42). Once inside the host cell, Yop effectors function to inhibit bacterial phagocytosis through

interaction with the host cell cytoskeleton and to suppress the production of pro-inflammatory

cytokines by blocking activation of host signaling pathways (42–47). These stealthy interactions

allow *Y. pestis* to alter proper immune cell functions to inhibit an inflammatory response.

Toll-like receptors are key components of the immune system that identify pathogens

associated molecular patterns (PAMPS) to activate the host immune response (48).

Lipopolysaccharide (LPS) of Gram-negative bacteria is recognized by Toll-like receptor 4 (TLR4)

located on phagocytes, such as macrophages and dendritic cells. Recognition of LPS by TLR4

triggers a signaling cascade that leads to the production and secretion of pro-inflammatory

cytokines (49–51). *Y. pestis* evades this innate immune response by altering the structure of its

lipopolysaccharide (LPS) (4, 49, 52). Specifically, *Y. pestis* decreases the amount of acylation of

lipid A to remain unrecognizable to TLR4 (53). The cell wall composition of LPS differs between

infection in the flea and mammalian host, where the bacteria need to avoid the TLR4 response,

because the alteration of LPS is temperature-dependent (52).

Y. pestis also produces an antiphagocytic factor called the capsular antigen fraction 1 (Caf1)

(54, 55). Like the other immune evasion mechanisms, expression of Caf1 is induced upon infection

at 37 °C in the mammalian host (56). When activated, Caf1 prevents interactions between the

surface of *Y. pestis* and phagocytic cell receptors (57, 58). This inhibition blocks phagocytosis by

macrophages and monocytes (57, 58). While this factor contributes to virulence, unlike the T3SS and LPS alterations, Caf1 is not essential for virulence (59–62).

Another essential virulence factor used by *Y. pestis* for colonization of the mammalian host is Yersiniabactin (Ybt), a secreted siderophore that supports iron acquisition (63, 64). The genes involved in the Ybt synthesis and transport are located on a high pathogenicity island that is flanked by insertion elements and that can be spontaneously lost via natural recombination (24). However, *Y. pestis* mutants lacking Ybt are not virulent in bubonic or pneumonic plague mouse models and have been shown to only be virulent in mice by septicemic plague (64). However, if the host has iron readily available, such in the case of iron overload in the body, Ybt mutants are no longer attenuated and can cause lethal infection by bubonic and pneumonic (65). The essential nature of this siderophore highlights the importance for metal acquisition systems in virulence.

1.3 Bacterial pathogens require transition metals to grow

Transition metals, such as iron (Fe), zinc (Zn), and manganese (Mn), are involved in many crucial biological processes (66). The most studied metal ion at the host–pathogen interface is iron. This metal is critical for many cellular processes including respiration, DNA replication, and central metabolism. In vertebrates, Fe is mainly intracellular, and extracellular Fe is primarily bound to proteins. Zn is also predominantly intracellular, where it serves as a co-factor for many proteins and enzymes. In bacteria, metals play a role in everything from bacterial metabolism to virulence factor function and are frequently catalytic cofactors and are incorporated into metalloproteins including metalloenzymes, storage proteins, and transcription factors (67). Because bacteria require these metals, eukaryotic hosts have evolved to sequester and restrict access to these metals inhibit colonization by microbial invaders (68–72). Not surprisingly, pathogens have evolved to employ sophisticated mechanisms to acquire these limited metal ions in the vertebrate host.

1.4 Metal availability in the flea

Very little is known about the nutrient availability in the flea midgut. Directly after a bloodmeal, transition metal levels in the flea midgut would be expected to be high, due to nutrients in

mammalian blood. A study showed that Fe, magnesium (Mg), and calcium (Ca) levels are elevated in the midgut at 1 and 6 days post-blood meal (30). Although these nutrients are present, it is unknown if they are readily available to *Y. pestis*. However, from natural plague foci, researchers have been able to isolate *Y. pestis* that lack yersiniabactin (73, 74), indicating that the flea midgut has sufficient Fe available to support bacterial growth. This is further supported by laboratory studies with Ybt mutants that can colonize the flea (75). The availability of other metals are currently unknown but similar approaches with bacterial mutants deficient in the acquisition of other metals would allow researchers to define metal availability within the flea.

1.5 Metal homeostasis in vertebrates

Fe is the most abundant transition metal in the human body. There are 3 to 5 g of Fe in healthy adults and 65–75% is found in erythrocytes bound to heme (76). Similarly, Zn is an essential metal nutrient and nearly all Zn in the human body (95%) is found intracellularly where it plays a role in the structure and function of macromolecules (77, 78). Unlike Fe and Zn, only trace concentrations of Mn are found in human serum (<10 nM) and tissue (<4 μM) (79). Also, Mn-dependent enzymes are scarce and Mn can often be interchanged with another divalent cation (66). Because these metals are also required by invading pathogens, the concentrations of these metals in our bodies are tightly regulated.

Fe absorption in mammals is a very efficient process, which begins in the duodenum of the gut. Here, ferric Fe (Fe^{3+}) is reduced to ferrous Fe (Fe^{2+}), then imported into cells by natural resistance-associated macrophage protein 2 (Nramp2). After import, the fate Fe^{2+} depends on the cellular needs, where it can either be stored as ferritin, used in metalloenzymes, used in the biosynthesis of heme, or exported out of the cell through transporter ferroportin, the only known cellular iron exporter in vertebrates (80–83). Ferroportin is found on duodenal enterocytes, macrophages, and hepatocytes that store Fe^{2+} (80). This process is tightly controlled by the master regulator hepcidin, a peptide hormone produced in the liver, to ensure Fe homeostasis (84). Upon release, hepcidin binds to ferropotin to inhibit Fe^{2+} export and prevents pathogens from acquiring any free Fe in the body.

The importance of Fe homeostasis in limiting bacterial infection is highlighted by genetic defects that impact the host ability to maintain proper Fe concentrations. The most common genetic disorder for dysregulation of Fe metabolism is hereditary hemochromatosis, caused by at least five different mutations in iron metabolism genes, with mutations in the HFE gene being the leading cause for decreased expression of hepcidin. Individuals with hemochromatosis gradual accumulate iron in internal organs, especially the liver, heart, and pancreas, and suffer from cellular damage caused by the unfavorable redox effects of free iron that ultimately leads to organ failure. However, these individuals and are also at higher risk for bacterial infections, including *Yersinia* infections (65, 85, 86). Hemochromatosis has been shown to lead to increased disseminated *Y. enterocolitica* infection resulting in liver and spleen abscesses (87, 88) and in 2011 an accidental exposure to an attenuated *Y. pestis* strain unable to normally acquire iron resulted in the death of a laboratorian with hemochromatosis (89). The contribution of hemochromatosis to this death was confirmed using a mouse model of hemochromatosis (85).

Zn homeostasis is also tightly controlled and primarily regulated by cells of the liver. ZnT and ZIP transporters coordinate together to regulate cellular Zn homeostasis. ZnT transporters move Zn from the cytosol to the extracellular space and the lumen of intracellular compartments. In contrast, ZIP transporters function by refilling cytosolic zinc levels by mobilizing Zn from the extracellular space and the lumens of intracellular compartments. The total cellular zinc concentration is 10–100 µM, but almost all zinc ions (Zn^{2+}) in the cytosol are tightly bound to a host of metalloproteins and sequestered into or released from intracellular organelles by ZnT or vesicles by ZIP (77). Therefore, free Zn concentrations in the cytosol are very low. Both transporters coordinate fundamental roles in immune cell function through zinc signaling, and dysfunction or dysregulation of either transporter can lead to an abnormal immune system (90–92).

1.6 Nutritional immunity

The importance of metals spans all levels of life; thus, organisms dedicate substantial resources to acquire metals and maintain homeostasis. Despite the indispensable nature of metals, excess accumulation of these nutrients can be toxic. Teetering the balance between metal

starvation and toxicity is a meticulous challenge for bacterial pathogens because they face host defense mechanisms, called nutritional immunity, that take advantage of this dual nature of metals. The two arms of nutritional immunity either restrict metals or use excess amounts of metals to attack pathogens.

1.6.a. Metal restriction and nutritional immunity

In addition to general maintenance of metal homeostasis from our diet, innate immune cells, such as macrophages and neutrophils, play an important role in restricting metals from pathogens. Macrophages utilize an antiporter called natural resistance-associated macrophage protein 1 (Nramp1) to redirect Fe, Mn, and Mg out of the phagolysosome and into the cytoplasm (93). Nramp1 activity sequesters these metals from intracellular pathogens, such as *Y. pseudotuberculosis*, *Salmonella enterica* Typhimurium, and *Mycobacterium tuberculosis* (94–97). In the extracellular space, host cells secrete metal scavenging proteins including transferrin, lactoferrin, calprotectin and neutrophil gelatinase-associated lipocalin (NGAL or lipocalin 2) to inhibit growth of pathogens (67). Transferrin binds Fe^{3+} with a high affinity (K_d 10^{-20}M) at two domains and each domain can bind to one Fe^{3+} ion (98). Physiologically, transferrin is a major Fe transporter that shuttles Fe between storage sites and areas its needed (99). Lactoferrin is a member of the transferrin family and found within the specific granules of neutrophils and in biological fluids (100, 101). In the case of nutritional immunity, transferrin and lactoferrin sequester Fe from pathogens (99). Additionally, calprotectin is secreted to scavenge metals. Calprotectin is a heterodimer of two S100 proteins, S100A8 and S100A9, that binds and sequesters Zn, Mn, Fe, and Ni from pathogens (102–104). Calprotectin composes 50% of the cytosolic protein content in neutrophils (105) and are considered primary sources for this protein during infection. However, macrophages have been shown to produce calprotectin in response to infection (106). Another molecule that plays a role in nutritional immunity is lipocalin, a neutrophil gelatinase-associated protein. Lipocalin is secreted by neutrophils as an early response to infection and sequesters siderophores to neutralize Fe uptake by bacteria.

Metal sequestration by these host proteins have proven to be effective means to restrict bacterial infection. Calprotectin has been shown to have antimicrobial activity against bacteria, like *Staphylococcus aureus*, *Acinetobacter baumannii*, *Clostridium difficile, Helicobacter pylori*, and *M. tuberculosis* (107–112). Imaging of a *S. aureus* infection showed severe relocalization of Zn by calprotectin to uninfected areas of the tissue that were absent from the bacterial abscess in the liver tissue (107). In a study conducted with lipocalin-deficient mice, *E. coli* caused enhanced septicemia compared to infection in mice with lipocalin (113). However, some bacteria utilize stealth siderophores that allow them to avoid lipocalin. The main siderophore system utilized by *Y. pestis*, Ybt, is not affected by lipocalin activity (114). The host also induces mechanisms in immune cells to decrease intracellular Zn levels. The intracellular pathogen *M. tuberculosis* encounters Zn sequestration by macrophages, as these phagocytes pump Zn out of the cell to reduce intracellular levels (115). This action in macrophages leads to increased reactive oxygen species production to support antimicrobial activity (115). Transport of Zn into the cytosol of phagocytes from the extracellular space or out of the phagolysosome is curated by transporters in the ZIP family, specifically ZIP8 (116, 117). The direct effect of Zn sequestration by ZIP transporters on *Y. pestis* intracellular infection is unknown. The impact of calprotectin-mediated metal sequestration has not been tested against *Y. pestis*.

1.6.b. Metal toxicity and nutritional immunity

More recently, the toxic properties of metal have become appreciated as a mechanism against microbes. Through exploitation of the toxic properties of metal, vertebrates expand the repertoire of nutritional immunity to include metal sequestration and intoxication (107, 118–120). Zn has been shown to overtake the bacterial cell and compete with other metals or substrates by binding to non-cognate sites, thereby impairing proper function (121). The mis-metalating process has been shown to inhibit uptake of other important metals, prevent oxidative stress defenses, and inhibit catalytic activity of enzymes (121–127). To impose Zn toxicity, the host imposes an environment with excess Zn within immune cells. In macrophages, Zn is specifically trafficked into phagosomes containing intracellular bacteria by ZIP2/8 for intoxication (127–131). Mice that lack ZIP8 are unable

to control bacterial infections, with pathogens such as *Streptococcus pneumoniae* (116, 117). Macrophage induced Zn toxicity has been proposed to be driven by release of Zn intracellular stores (128), but is still not well understood. Neutrophils also utilize zinc toxicity to inhibit bacterial growth. During infection with group A *Streptococcus*, neutrophils mobilized zinc vesicles to poison the bacteria (132). Individuals with Zn deficiency have an increased susceptibility to infectious disease because not only do they not have fully functional immune systems but they lack the ability to enforce Zn toxicity against infections (133). Zn toxicity is an essential part of nutritional immunity and bacteria use Zn efflux systems to combat high concentrations of Zn (127, 130, 134–136).

1.7 *Y. pestis* uses metal acquisition systems to overcome nutritional immunity

Successful pathogens have evolved dedicated high-affinity metal acquisition systems to specifically overcome nutritional immunity. *Y. pestis* utilizes a plethora of acquisition systems to compete with nutritional immunity to acquire metals such as, Fe, Mn, and Zn. On the other hand, *Y. pestis* does have efflux systems that can be used when toxic levels of metals are encountered. Research with *Y. pestis* has been essential in our understanding of these mechanisms.

1.7.a. Regulating metal homeostasis in *Y. pestis*

Like the mammalian host, bacteria need to tightly regulate metal homeostasis to avoid potential toxic consequences of metal overload. The balance between metal starvation and toxicity in bacteria is maintained by a tight network of metal homeostasis pathways. Metal-responsive transcription factors, such as metalloregulators and metal-sensor proteins, coordinate these the activity of these systems and sense metal availability. When metal binds to a metalloregulator, the transcription factor can then bind to specific DNA sequences. These transcription factors are allosterically regulated by the specific metal they are responsible for (137). When the metalloregulator binds to their target metal, they will activate or repress the production of the corresponding metal homeostasis systems (138).

To adjust to altering Fe environments, bacteria utilize Fur (ferric uptake regulation) to regulate Fe acquisition (139). Fur is a transcriptional repressor of iron-regulated promoters, where it relies

on Fe^{2+} binding activity to attach to DNA (140). In the presence of high Fe, Fur inhibits transcription of target genes by a confirmational change occurring due to Fe binding to Fur (141, 142). Homologs of Fur have been identified in multiple Gram-negative bacteria, including *Y. pestis*, *Salmonella* Typhimiruim, *A. baumannii*, *Campylobacter jejuni*, *Pseudomonas aerugonisa* (143–145, 145, 146). In *Y. pestis*, Fur coordinates the regulation of 32 predicted operons (147).

Studies have shown a Zn requirement for *in vitro* growth of *Y. pestis* (148). Although Zn is required for optimal cellular function, Zn can also be toxic at high concentrations. Repression of transporters by Zur, a transcription factor, also occurs through allosteric regulation by two or more Zn ions binding to Zur. One atom serves to structurally stabilize Zur, and the other atom(s) supports a DNA-binding domain to fold allowing for the domain bind to the promoter of Zur-regulated genes (149, 150). Therefore, in an environment with high Zn concentrations, Zur inhibits transcription of target Zn transporters. Further, in a low Zn environment, Zur releases and transcription of Zn transporter genes can continue.

1.7.b. Iron acquisition in *Y. pestis*

To compete with Fe nutritional immunity, *Y. pestis* has multiple Fe acquisition systems (151–157). *Y. pestis* has several ABC transporters that share similarity to ones with proven roles in Fe acquisition in other organisms. Three ABC transporters, YfeABCDE, YfuABC and YiuABC, have activity during aerobic growth and thus transport Fe^{3+}. Yfu and Yiu show no significance to plague virulence (156). *Y. pestis* has three Fe^{2+} transporters, YfeABCDE, FeoABC and Fet, that have demonstrated activity under microaerobic conditions. The Yfe and Feo systems are utilized for Fe acquisition during intracellular growth (153). An *feoB* mutant was fully virulent in mouse models of bubonic and pneumonic plague, but an *yfe feoB* double mutant was fully virulent in pneumonic infection, but showed a loss in virulence during bubonic plague (152). Therefore, the Yfe and Feo systems may contribute to Fe acquisition during bubonic plague but are not essential in pneumonic plague.

Y. pestis can hijack Fe-containing molecules to acquire Fe. The *hmu* locus from *Y. pestis* allows it to use hemin as well as host hemoproteins including hemoglobin, myoglobin, hemin-albumin,

heme-hemopexin, and hemoglobin-haptoglobin as sources of Fe (158). Deletion of the *hmu* locus from *Y. pestis* lead to poor growth on iron-limited medium containing free hemin (158). Notably, Hmu is not essential for plague virulence (159).

Of all these systems, Ybt is essential for Fe acquisition during plague, signifying its importance as a virulence factor (64). Ybt is a secreted, siderophore that is synthesized by *Y. pestis* to acquire Fe. Ybt has a high affinity for Fe^{3+}, a formation constant of $4x10^{-36}$, and no affinity for binding Fe^{2+} (160). Unlike other siderophores, Ybt is not inhibited by lipocalin (114).

The *ybt* locus is encoded on the high-pathogenicity island, *pgm*, which is also found in *Y. enterocolitica*, and *Y. pseudotuberculosis* (161–163). In fact, almost 30 years ago, Ybt was first described in *Y. entercolitica* (161). Since then, the system has been well-defined and studied in the context of infection and Fe acquisition. Outside of *Yersinia*, the *ybt* locus is conserved in other pathogenic bacteria and these bacteria require Ybt for virulence including, pathogenic *Escherichia coli*, *Klebsiella pneumoniae*, and *Proteus mirabilis* (164–167).

The first gene in the *ybt* locus is the transcriptional regulator of the system is *ybtA* (168, 169) (Fig. 1-1A). Fur controls the expression of *ybtA* by a Fur-binding site near the *ybtA* promoter region (168). A mutation in the *ybtA* reduces expression of Ybt import and synthesis genes, *psn*, *irp1*, *irp2*, and *ybtE* (168). Intriguingly, it is speculated that the Ybt siderophore directly interacts with YbtA to activate transcription of the system, because both YbtA and Ybt must be present for induction of the Ybt system (168).

The synthesis complex of Ybt utilizes seven genes located in a 22kb region on the *ybt* locus (63) (Fig. 1-1A). These genes coordinate unique steps to generate the siderophore structure of a four-ring structure composed of salicylate, one thiazolidine, and two thiazoline rings with a malonyl linker separating the final thiazoline from the thiazolidine ring (Fig. 1-1B). First, YbtD transfers the 4′-phosphopantetheine moiety of coenzyme A to attachment sites on HMWP1 (*irp1*) and HMWP2 (*irp2*) for the substrates adenylated salicylic acid, three cysteines, and malonate (170). Then, YbtS coverts chorismic to salicylic acid, which is then adenylated by YbtE and attached to HMWP2. Here the complex is cyclized to form two thiazoline rings (171). Next, a malonyl linker is added by

HMWP1 to generate the final thiazoline ring and YbtU reduces the middle thiazolidine ring to a thiazoline ring to produce the final structure (172). YbtT cleans up the structure by removing irregular or mischarged molecules. Finally, HMWP1 releases the completed siderophore (170).

After synthesis and secretion of Ybt, the siderophore can steal Fe from lactoferrin and transferrin for Fe uptake. For import of Ybt bound to Fe (Ybt-Fe), *Y. pestis* utilizes *psn*, *ybtP*, and *ybtQ*. Psn (pesticin receptor) is located on the outer membrane of the bacteria and TonB provides the energy for active transport of Ybt-Fe across the membrane (173–175). Once in the periplasmic space, the Ybt-Fe complex is transported across the inner membrane by the ABC transporters, YbtP and YbtQ (176). After reaching the cytoplasm, Fe could be removed from Ybt by an enzyme that reduces Fe^{3+} to Fe^{2+} or degrades Ybt. The mechanism for Fe removal from Ybt still remains unknown and is a debated topic in the Ybt field. In fact, Fe could potentially be removed from Ybt at the cell surface by Psn, in the periplasm, or in the cytoplasm. There is support from studies with *E. coli* for the concept that metal is removed in the periplasm (177). These studies also show that Ybt is promiscuous and can bind to copper (Cu), which suggests the ability of Ybt to play a role in the transport of other metals (177–179). The ability of Ybt to bind Cu has been proposed to be a protective mechanism to prevent Cu toxicity in the bacteria (179). Further, Ybt has been shown to bind to nickel, cobalt, chromium, and gallium (178, 180). Even with the discovery of Ybt occurring thirty years ago, the system still has many unanswered questions.

Although the synthesis and import mechanisms of Ybt are well defined, the export system of Ybt remains unknown (Fig. 1-1C). This system remains unsolved because the *ybt* locus lacks genes for an export system (Fig. 1-1A). Recently, efflux pumps have been implicated in the secretion of other siderophores in bacteria like *E. coli*, *Vibrio cholerae*, *S. enterica* Typhimurium, *Pseudomonas putida*, and *M. tuberculosis* (181–185). Efflux pumps present a potential mechanism for Ybt export in *Y. pestis*.

During *Y. pestis* pathogenesis, Ybt is required for the development of bubonic and pneumonic plague (64). Notably, without Ybt, *Y. pestis* can cause septicemic plague due to the high amount of free Fe in the bloodstream. Fe acquisiton by Ybt is also significant to survival of *E. coli* and *K.*

pneumonia during infection (114, 186–188). Outside of direct Fe acquisition, Ybt can provide protection from reactive oxygen species (ROS) formation by scavenging Fe in phagocytes and preventing Haber-Weiss reactions (189).

1.7.c. Manganese acquisition in *Y. pestis*

Mn is important for intermediary metabolism, transcriptional regulation and virulence of bacterial pathogens (190, 191). Mn is largely known for its role as a cofactor for some free radical detoxifying enzymes, but can also plays a key role in central carbon metabolism (192). *Y. pestis* has two known Mn transporters, MntH and Yfe, that are also prominent in other Gram-negative bacteria. The MntH transporter, an Nramp1 family member, was first characterized in *Salmonella* and *E. coli* as a proton-dependent Mn transporter. Yfe, which was known for its role in Fe transport, was also shown to transport Mn into *Y. pestis* (151). It has been demonstrated that an *yfe* or *mntH* mutant did not significantly affect growth under Mn-limitation (193). However, an *yfe mntH* double mutant did show growth attenuation that was alleviated by supplementation with Mn (193). This mutant had a significant loss in virulence during bubonic plague but showed not attenuation in pneumonic plague (193). These data suggest that either Mn requirements change in different forms of infection, another Mn transport system can provide sufficient Mn for survival during bubonic infection, or that Mn sequestration differs at these infection sites.

1.7.d. Zinc acquisition in *Y. pestis*

Zn is an essential element and serves as an electrophilic catalyst for enzymes and a protein scaffold (194). It is estimated that 5–6% of bacterial proteomes consist of Zn binding proteins, emphasizing the need for mechanisms of zinc acquisition systems (195).

Y. pestis does have a Zur regulon, suggesting that Zur contributes to maintaining Zn homeostasis (196). In Zn-rich conditions, 154 *Y. pestis* genes were shown to be Zur-regulated by microarray expression analysis (196). These genes included *znuA*, *znuB*, *znuC*, and virulence-related genes, *psa* and *ail* (196). *Y. pestis znuABC* has also been shown to be repressed during *in vitro* growth in Zn-replete media (148). On the other side of Zn homeostasis, bacteria use Zn efflux systems to
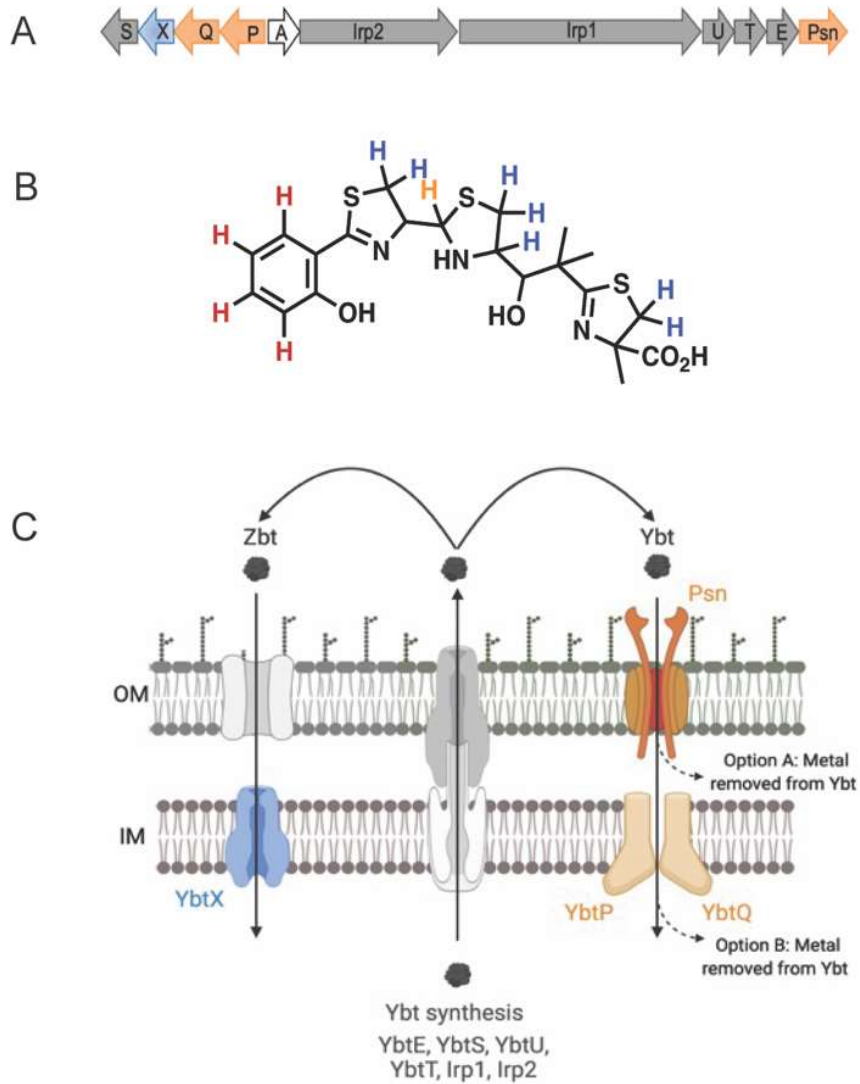
Figure 1-1. Yersiniabactin (Ybt) is the primary iron acquisition system in *Y. pestis*.

(A) Ybt operon encodes for genes in Ybt regulation (white), synthesis (gray), and import (orange and blue). (B) Schematic of Ybt molecule structure. (C) Schematic of Ybt and Zbt transport.

Zn out of the cell. *Y. pestis* has four homologs to well-described Zn efflux systems: ZntA (Y0410), ZntB (Y1994), ZitB (Y3050), and FieF (Y0060) (148). Studies have shown that a *zntA* mutant has decreased growth *in vitro* with macrophages but is not attenuated in bubonic or pneumonic plague (197). Further, transcription of *zntA* was detected in the lymph nodes of rats infected with *Y. pestis* but not during flea colonization, suggesting that Zn efflux by ZntA is important during bubonic plague (198, 199). Together, these results suggest that *Y. pestis* may not encounter toxic Zn levels during mammalian infection or that other Zn efflux systems can compensate for the loss of ZntA. Future studies need to be conducted to understand how *Y. pestis* maintains Zn homeostasis during infection.

On the other hand, bacteria also need to compete to acquire Zn. The ZnuABC transporter is the most well-studied high-affinity zinc transporters in Gram-negative bacteria. This system is used to transport zinc ions from the periplasmic space to the cytosol and for their accumulation in bacterial cells. The ZnuABC system has been shown to be required for pathogenesis in bacteria including, *Brucella abortus*, *C. jejuni*, *A. baumannii*, and *S. enterica* Typhimirium (200–204).

ZnuABC is composed of three proteins (Fig. 1-2). The first is ZnuA a periplasmic Zn^{2+} binding protein that contains a flexible region for binding Zn (205). The next two proteins provide movement across the inner membrane, a transmembrane channel domain, ZnuB, and an ATPase component called ZnuC (205). ZnuC is responsible for providing the energy to transport Zn ions across the membrane (149). The transporter functions by the flexible loop of the ZnuA protein delivering Zn to the ZnuBC transporter (206). The zinc uptake regulator, Zur, controls Zn uptake by the ZnuABC system. Zur functions by repressing ZnuABC to maintain zinc homeostasis in the bacterial cell (207, 208).

In *Y. pestis*, ZnuABC is the predominant Zn acquisition system during *in vitro* growth in Zn-limitation (0.4 μM), because a *znuBC* mutant shows a growth attenuation (148). In the presence of excess Zn (10 μM), growth of a *znuBC* mutant is fully restored (148). Surprisingly, under these high Zn conditions, the promoters for *znuA* and *znuC* are repressed in a *znuBC* mutant (148). This supports the idea of a second Zn transport system in *Y. pestis*, because without Znu actively

working to take in Zn, the system would not be repressed by high Zn concentrations. Additionally, elimination of ZnuABC shows a modest increase in survival in pneumonic or bubonic plague mouse model, suggesting that ZnuABC is not required for plague pathogenesis (148). Together these data indicate the presence of a second high affinity Zn transporter in *Y. pestis* that works together with ZnuABC.

To identify the second Zn acquisition system, mutants were generated in different known metal transporters in a *Y. pestis znuBC* mutant (148). Neither the MntH or YfeA system showed a growth phenotype for Zn (148). The first evidence that Ybt may contribute to Zn acquisition was that the *pgm* locus encoding the Ybt system was required for growth under Zn-limited conditions (209). When the synthesis gene *irp2* was deleted in a *znuBC* mutant, the mutant showed attenuated growth in Zn-limited media (209). However, the Psn receptor does not play a role in Zn acquisition, and it has been shown that a *znuBC psn* mutant grows better in Zn limitation than a *znuBC* mutant (209). These data indicate that without Psn, all available Ybt can be used for Zn acquisition. Instead, the putative inner membrane protein YbtX, a member of the Major Facilitator Superfamily, did have a growth attenuation in Zn limitation (209). YbtX is part of the *ybt* locus, but was not required for Fe uptake and despite many attempts to determine its function, the purpose of YbtX remained unknown (176, 209). Further, an *ybtX* mutant was not attenuated during bubonic or pneumonic plague, similar to a *znuA* mutant, however, a *znuA ybtX* mutant was significantly attenuated in both infection models (197). These data suggest that ZnuABC and YbtX are two high affinity Zn transport systems for *Y. pestis*.

The evidence of Ybt playing a role in Zn acquisition was very odd, because there was no evidence of Ybt binding to Zn by mass spectrometry, proton nuclear magnetic resonance, and ultra-violet visible spectrometry (178, 197). There was speculation that Ybt could exist in two isomeric forms each with unique metal binding properties (197). Notably, the siderophore pyochelin has two isomers that are transported by different systems in *P. aeruginosa* and *Pseudomonas fluorescens* (210). Similarly, by liquid chromatography mass spectrometry analysis, apo-Ybt has two peaks with retention times of 7.8 and 8.3 min, suggested two isomers of Ybt (197).

These data lead to two possible hypotheses for Zn import by YbtX. The first option is that another zincophore (Zbt) is secreted that can bind to Zn. *Y. pestis* does encode for another metallophore system that is genetically similar to the Staphylopine system in *S. aureus* that is involved in Co, Cu, Fe, Ni and Zn acquisition (211, 212). However, there was evidence that Staphylopine does not contribute to Zn acquisition (148) and the system has a frameshift that will likely make it unfunctional in *Y. pestis* (211, 212). These data indicate that the unknown Zbt molecule is not Staphylopine and the purpose of this system to *Y. pestis* remains unknown. The other option is that Ybt is enzymatically modified to bind to Zn to generate Zbt. An enzyme to alter the siderophore has not been identified.

Overall, YbtX is the import system for Zbt-dependent Zn acquisition, and Fe acquisition occurs through a totally separate system (Fig. 1-1C). However, the importance of Zbt-dependent Zn acquisition to virulence has never been shown, since Fe acquisition by Ybt is critical to the development of bubonic and pneumonic plague (64).
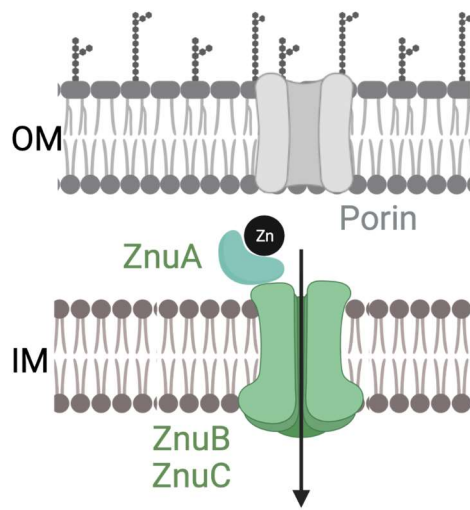
Figure 1-2. Zinc transport by ZnuABC in *Y. pestis*.

For Zn uptake, ZnuA binds to Zn in the periplasmic space. Then, Zn is shuttled through ZnuBC into the cytoplasm.

RESEARCH OBJECTIVES

Because transition metals are essential co-factors for bacterial growth and virulence, eukaryotic organisms use nutritional immunity to sequester metal from invading bacteria. To overcome nutritional immunity, pathogenic bacteria have evolved specialized systems to acquire transition metals. As these systems are critical for virulence, defining how bacterial pathogens acquire metals is imperative to understanding bacterial pathogenesis and may provide potential targets for novel antimicrobial strategies.

Fe acquisition has been well studied in *Y. pestis*, and the siderophore Ybt is essential for the bacterium to acquire Fe and cause disease. Unlike Fe, mechanisms for acquiring Zn by *Y. pestis* are less well understood. The primary transporter for Zn for *Y. pestis in vitro* is the ABC transporter ZnuABC. However, a *znu* mutant is still virulent in mouse models. This data suggests the possibility of a second Zn transport system in *Y. pestis* that contributes to virulence. Studies have shown that inactivation of the genes encoding the Ybt synthetase (e.g., *irp2*) and the *znuABC* acquisition system attenuates *Y. pestis* growth in Zn-limiting medium and during infection, suggesting that Ybt supports Zn acquisition. These data are the premise of my hypothesis that Ybt -dependent zinc acquisition contributes to *Y. pestis* virulence.

Additionally, the effect of metal sequestration by nutritional immunity on *Y. pestis* virulence has not been reported. Calprotectin is secreted by neutrophils to sequester Zn, Mn, and Fe at the site of infection. However, the role of calprotectin during plague infection has not been explored. I hypothesize that *Y. pestis* competed with Zn restriction by calprotectin through expression of ZnuABC and Ybt-dependent Zn acquisition.

Moreover, the secretion mechanism of Ybt remains unknown. I aim to use an innovative technique called droplet Tn-seq to identify additional genes required for Zn acquisition and define the role of these genes in Ybt secretion. Since other Gram-negative bacteria use efflux systems for siderophore export, I hypothesize that *Y. pestis* utilizes an efflux system to secrete Ybt for Zn acquisition.

My preliminary data suggested the presence of two Zn transporters in *Y. pestis* that serve vital but redundant roles in Zn acquisition. The completion of my dissertation will identify a novel mechanism for Zn acquisition by *Y. pestis* and the role of the system in virulence.

Research Objectives:

1. Determine the contribution of Ybt synthetase-dependent Zn acquisition during *Y. pestis* pathogenesis.

    a. Establish the importance Ybt synthetase-dependent Zn acquisition in flea colonization.

    b. Establish the importance Ybt synthetase-dependent Zn acquisition in virulence in the mammalian host.

2. Define the contribution of calprotectin to Zn restriction during *Y. pestis* infection.

    a. Determine if calprotectin restricts the growth to *Y. pestis in vitro*.

    b. Identify the impact of calprotectin on *Y. pestis* virulence.

3. Identify genetic elements responsible for secretion of Ybt.

    a. Identify genes required for Zn acquisition using droplet Tn-seq.

    b. Validate primary hits for defects in Zn acquisition using site-specific mutants.

    c. Determine contribution of genes to *Y. pestis* infection.

CHAPTER 2

YERSINIABACTIN CONTRIBUTES TO OVERCOMING ZINC RESTRICTION DURING

YERSINIA PESTIS INFECTION OF THE MAMMALIAN AND INSECT HOSTS[1]

SIGNIFICANCE

Transition metals are required for proper cellular function, which renders them a critical component for all life. To restrict bacterial infection, eukaryotic organisms actively sequester these transition metals, a concept referred to as nutritional immunity. Consequently, bacterial pathogens have evolved dedicated mechanisms to acquire transition metals in order to colonize the host. During human plague, *Yersinia pestis* overcomes iron limitation via production of the secreted siderophore yersiniabactin. Here we identify an iron-independent role for yersiniabactin in evading zinc-mediated nutritional immunity during mammalian infection and in *Y. pestis* colonization of the flea insect-vector. Importantly, yersiniabactin is found in several pathogens, indicating that it is used by a variety of bacteria to acquire multiple metals in order to overcome nutritional immunity.

SUMMARY

Yersinia pestis causes human plague and colonizes both a mammalian host and a flea vector during its transmission cycle. A key barrier to bacterial infection is the host's ability to actively

[1] Price, S. L., Vadyvaloo, V., DeMarco, J. K., Brady, A., Kehl-Fie, T. E., Garneau-Tsodikova, S., Perry, R. D., and Lawrenz, M. B. (2021). Yersiniabactin contributes to overcoming zinc restriction during *Yersinia pestis* infection of mammalian and insect hosts. *Proc Natl Acad Sci U S A* 118(44). PMID: 34716262.

sequester key biometals (e.g., iron, zinc, and manganese) required for bacterial growth. This is referred to as nutritional immunity. Mechanisms to overcome nutritional immunity are essential virulence factors for bacterial pathogens. *Y. pestis* produces an iron scavenging siderophore called yersiniabactin (Ybt) that is required to overcome iron-mediated nutritional immunity and cause lethal infection. Recently, Ybt has been shown to bind to zinc, and in the absence of the zinc transporter ZnuABC, Ybt improves *Y. pestis* growth in zinc-limited medium. These data suggest that in addition to iron acquisition, Ybt may also contribute to overcoming zinc-mediated nutritional immunity. To test this hypothesis, we used a mouse model defective in iron-mediated nutritional immunity to demonstrate for the first time that Ybt contributes to virulence in an iron-independent manner. Furthermore, using a combination of bacterial mutants and mice defective in zinc-mediated nutritional immunity, we identified calprotectin as the primary barrier for *Y. pestis* to acquire zinc during infection, and that *Y. pestis* uses Ybt to compete with calprotectin for zinc. Finally, we discovered that *Y. pestis* encounters zinc limitation within the flea midgut, and Ybt contributes to overcoming this limitation. Together, this is the first evidence that Ybt is a bona fide zinc acquisition mechanism used by *Y. pestis* to surmount zinc limitation during infection of both the mammalian and insect hosts.

INTRODUCTION

Yersinia pestis is a Gram-negative re-emerging bacterial pathogen that causes bubonic, septicemic, and pneumonic plague in humans. *Y. pestis* is a zoonotic pathogen maintained in the environment in rodent populations across the globe and is transmitted within these populations by a flea vector (4, 213, 214). As such, the bacterium has evolved specific factors that contribute to the colonization of both its mammalian and insect hosts (4, 213). Human bubonic plague manifests from the bite of an infected flea. After deposition into the dermis by the flea, *Y. pestis* disseminates to and colonizes the draining lymph nodes, resulting in the development of an inflamed lymph node referred to as a bubo. Primary septicemic plague occurs when bacteria are directly inoculated into blood vessels by fleas, or when bacteria disseminate from the lymph node to the bloodstream during bubonic plague (secondary septicemic plague). Via the blood, *Y. pestis* can spread to other

tissues, including the lungs, where infection can progress to the development of secondary pneumonic plague. Aerosolization of the bacteria from the lungs by coughing can further lead to person-to-person transmission causing primary pneumonic plague in naïve individuals (4, 215, 216). Without timely treatment, all three forms of plague are associated with high mortality rates. Because of the possibility for direct human-to-human transmission, the lack of an FDA-approved vaccine, and the potential for weaponization, *Y. pestis* is also considered a bioterrorism threat (11). Therefore, understanding the pathogenesis of *Y. pestis* will help in the development of new potential therapeutic approaches to protect against both environmental and man-made threats by *Y. pestis*.

Transition metals are essential nutrients required for proper cellular function, which makes them a crucial component for biological processes in all forms of life. Bacteria require transition metals in order to maintain intermediary metabolism, transcriptional regulation, and virulence for bacterial pathogens (70, 217–219). Since transition metals are vital for bacterial proliferation and infection, eukaryotic hosts sequester these essential nutrients from invading pathogens via a mechanism referred to as nutritional immunity (68, 217, 220). Nutritional immunity includes both tightly controlling systemic metal concentrations via regulation of metal absorption from the diet, and local restriction in response to infection through the release of metal binding proteins by innate immune cells (219, 221). For example, neutrophils responding to infection can release a variety of metal-binding proteins via both degranulation and a unique form of cell death called NETosis to restrict metal access by bacterial and fungal pathogens (222, 223). Calprotectin is one of these metal-binding proteins and is a heterodimer composed of two S100-family members, S100A8 and S100A9 (224–226). Via two metal binding sites, calprotectin is able to restrict microorganism access to manganese, zinc, and iron (102, 226–229). Zinc sequestration by calprotectin has been shown to be a major barrier to colonization by several bacterial pathogens, including *Salmonella enterica* Typhimurium, *Clostridioides difficile, Staphylococcus aureus*, *Acinetobacter baumannii*, and some strains of *Helicobacter pylori* (107, 109, 111, 228, 230, 231).

To overcome nutritional immunity, pathogens have evolved a variety of dedicated mechanisms to acquire transition metals during infection (221) and siderophores are some of the most robust mechanisms used by bacteria to specifically overcome host mediated iron limitation (232, 233). Yersiniabactin (Ybt) represents one class of siderophore used by *Yersinia* species, *Klebsiella pneumoniae*, pathogenic *Escherichia coli*, and other enteric pathogens to colonize the mammalian host (233–238). In *Y. pestis*, the synthesis and import machinery for Ybt are encoded on a high pathogenicity genomic island within the *pgm* locus on the chromosome (151, 239). Ybt is synthesized by the Ybt synthetase complex consisting of YbtE, YbtU, HMWP1, and HWMP2, and it is exported by the bacterium through an unknown mechanism (240, 241). Ybt binds to ferric iron (Fe) with a formation constant of 4×10^{36}, allowing it to outcompete for Fe with host nutritional immunity iron-binding proteins such as lactoferrin and transferrin (64, 240). Once bound to iron, Ybt-Fe is recognized by the outer membrane receptor Psn and imported across the outer membrane in a TonB-dependent manner (242). YbtP and YbtQ are then responsible for the import of the Ybt-Fe complex across the inner membrane (176). The importance of Ybt-mediated Fe acquisition to virulence has been demonstrated for *Yersinia*, *Klebsiella*, and *E. coli* by generating mutations in both the Ybt synthesis and import machinery (64, 188, 235). For *Y. pestis* specifically, Ybt mutants are significantly attenuated for growth in Fe-limited medium *in vitro* and in causing lethal infection in both bubonic and pneumonic plague models (64).

While originally described as an iron scavenging molecule, several recent studies indicate that Ybt can bind to other transition metals, suggesting that Ybt may also be used for the acquisition of metals other than Fe. Using purified Ybt and liquid chromatography mass spectrometry, Koh *et al.* showed that Ybt can bind several divalent transition metals, including nickel (Ni) and copper (Cu) (178). The same group later showed that *E. coli* can use Ybt to acquire Cu and Ni during metal-limitation and may also use Ybt to protect against Cu toxicity when Cu is present in excess (179, 180). Using a novel native spray metabolomics approach validated by NMR, Behnsen *et al.* demonstrated that Ybt can also bind to zinc (Zn), and further that expression of Ybt by the probiotic bacterium *E. coli* Nissle 1917 contributes to a selective advantage over *S.* Typhimurium under Zn-

limited conditions, including within the inflamed gut (69). A role for Ybt in Zn acquisition has been further supported by previous studies in *Y. pestis*. Specifically, while a *Y. pestis* mutant lacking the Zn importer ZnuABC is partially attenuated for *in vitro* growth in Zn-limited medium, a *znuBC irp2* mutant (*irp2* encodes the HMWP2 Ybt synthetase) is significantly more attenuated for growth in the same medium (148, 209). Moreover, the *znuBC irp2* mutant is attenuated in the septicemic plague model, a model in which *znuBC* and *irp2* are not individually required for virulence (209). Finally, Bobrov *et al.* also discovered that Ybt-dependent Zn acquisition does not require the Ybt-Fe transport machinery in *Y. pestis*, but instead requires the YbtX inner membrane protein (197, 209). The role of YbtX in Ybt-dependent Zn acquisition has been subsequently confirmed in *E. coli* Nissle 1917 (69). Together, these data strongly support a hypothesis that Ybt not only contributes to the acquisition of Fe but also Zn, and possibly other metals, during *Y. pestis* infection. Here, we test this hypothesis and demonstrate for the first time that Ybt contributes to *Y. pestis* virulence in the mammalian host independent of iron acquisition. Furthermore, we show that *Y. pestis* uses the ZnuABC and Ybt Zn acquisition systems to colonize the flea insect vector and to overcome calprotectin-mediated nutritional immunity during mammalian infection.

RESULTS

Yersiniabactin (Ybt) contributes to *Y. pestis* virulence independent of iron acquisition in the mammalian host.

 Y. pestis mutants lacking the Zn transporter ZnuABC (*znuBC*) and the ability to make Ybt (*irp2*) are significantly more attenuated than *znuBC* or *irp2* single mutants in the mouse model of septicemic plague (209), suggesting that Ybt contributes to Zn acquisition *in vivo*. However, because Ybt is also essential for Fe acquisition *in vivo* (64), infection of wild-type mouse models does not rule out the possibility that the *znuBC irp2* phenotype is an additive effect of limited Zn acquisition due to inactivation of *znuBC* and limited Fe acquisition due to inactivation of *irp2*. Therefore, to expand on these previous studies and more directly test the role of Ybt in Zn acquisition *in vivo*, we chose a mouse model of plague in which host-imposed Fe limitation is not a barrier to *Y. pestis* infection. Hemojuvelin deficient mice (Hjv$^{-/-}$) are unable to properly maintain Fe

homeostasis, resulting in increased absorption of Fe from their diet and accumulation of Fe within their tissues (Fig. 2-1A; Metal concentrations in Hjv$^{-/-}$ mice liver tissue Table 2-1) (86). Importantly, Quenee *et al.* previously showed that Hjv$^{-/-}$ mice are susceptible to infection by *Y. pestis* that have lost the pigmentation genetic locus (*pgm*) and are subsequently unable to produce Ybt, further demonstrating that Fe-mediated nutritional immunity is not a barrier to *Y. pestis* in this model (65). Therefore, infection of Hjv$^{-/-}$ mice should allow us to separate the role of Ybt in Fe acquisition from Zn acquisition in virulence. Toward this end, Hjv$^{-/-}$ mice were challenged intranasally with 10^5 colony forming units (CFU) of the KIM5+ *irp2* or *znuBC irp2* mutants. As anticipated, 100% of Hjv$^{-/-}$ mice infected with the *irp2* mutant succumbed to infection within 2.5 days (Fig. 2-1B). However, only one mouse from two independent studies developed a lethal infection when challenged with the *znuBC irp2* mutant ($p < 0.0001$). To determine if the route of infection impacted survival, separate groups of animals were challenged subcutaneously with 10^5 CFU of bacteria. In this model of bubonic plague, 70% of Hjv$^{-/-}$ mice succumbed to infection with the *irp2* mutant, while all mice survived infection with the *znuBC irp2* mutant (Fig. 2-1C; $p < 0.0001$). When the challenge dose was increased to 10^7 CFU, mortality increased to 90% for the *irp2* mutant, but still none of the mice infected with the *znuBC irp2* mutant developed a lethal infection (Fig. 2-1D; $p < 0.0001$). To further show that Ybt-dependent Zn acquisition is responsible for the attenuated phenotype, Hjv$^{-/-}$ mice were infected with a KIM5+ *znuA ybtX* mutant – YbtX is required for Ybt-dependent Zn acquisition *in vitro* but not Ybt-dependent Fe acquisition (197). When Hjv$^{-/-}$ mice were challenged with 10^5 CFU of the *znuA ybtX* mutant intranasally, all mice survived the 14-day infection period (Fig. 2-1B; $p < 0.0001$). This attenuated phenotype was also observed in the bubonic plague model, even when mice were challenged with 10^7 CFU (Fig. 2-1C and 2-1D; $p < 0.0001$). Importantly, genetic complementation of the *znuA ybtX* with an intact copy of the *ybtX* gene restored the virulence of the mutant (Fig. 2-1E and 2-1F). Of note, mice infected with the *znuBC irp2* or *znuA ybtX* mutants that survived to the end of these studies did not have any detectable bacteria present within their spleens, livers, or lungs. Collectively, these data demonstrate for the first time that Ybt contributes to infection independent of Fe acquisition and support the hypothesis that ZnuABC and Ybt are complementary Zn acquisition systems important for mammalian infection.
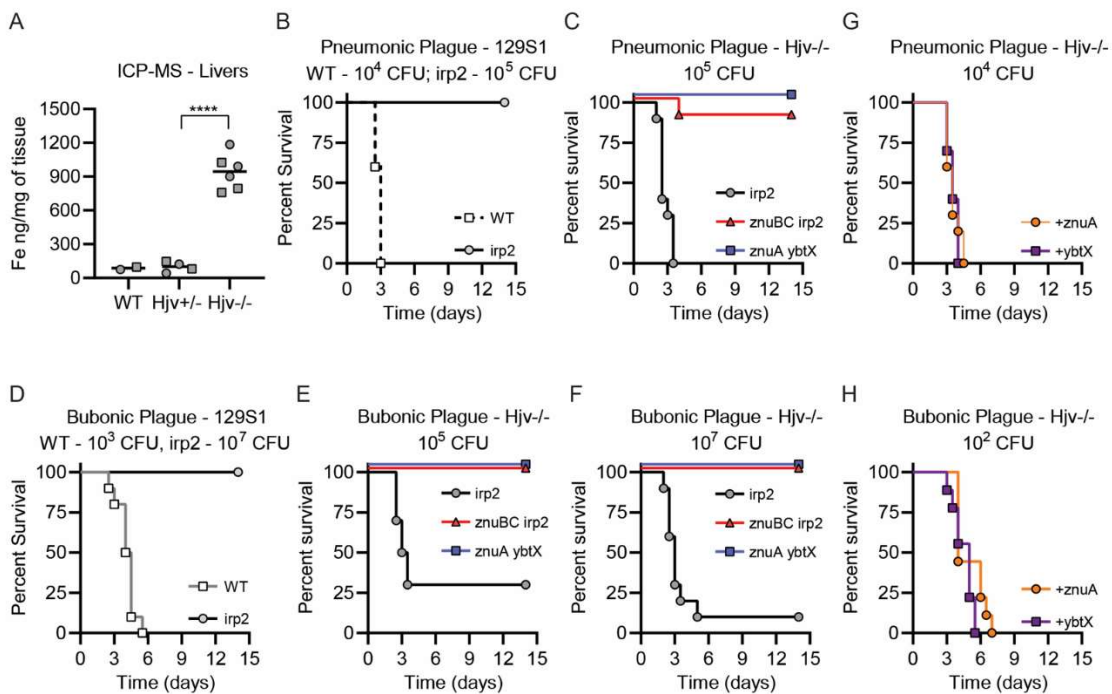
Figure 2-1. Ybt contributes to virulence independent of Fe.

(A) Fe concentrations of livers from C57BL/6J (WT), Hjv$^{-/+}$, or Hjv$^{-/-}$ mice as determined by ICP-MS. Male mice are represented by squares and female mice by circles. Unpaired two-tailed t-test, ****p<0.0001. (B) 129S1 mice were challenged intranasally with indicated inoculum of *Y. pestis* (WT; white squares) or *irp2* mutant (gray circles) and monitored every 12 h for the development of moribund disease for 14 days. (C) Hjv$^{-/-}$ mice were challenged intranasally with indicated inoculum of *irp2* (gray circles), *znuBC irp2* (red triangles)*,* or *znuA ybtX* (blue squares) mutants and monitored every 12 h for the development of moribund disease for 14 days. (D) 129S1 mice were challenged subcutaneously with indicated inoculum of *Y. pestis* (WT, white squares) or *irp2* (gray circles) and monitored every 12 h for the development of moribund disease for 14 days. (E-F) Hjv$^{-/-}$ mice were challenged subcutaneously with indicated inocula of *irp2* (gray circles), *znuBC irp2* (red triangles)*,* or *znuA ybtX* (blue squares) mutants and monitored every 12 h for the development of moribund disease for 14 days. (G-H) Hjv$^{-/-}$ mice were challenged with indicated inoculum of *znuA ybtX* complemented with *ybtX* (purple squares) or *znuA ybtX* complemented with *znuA* (orange circles) and monitored every 12 h for the development of moribund disease for 14 days. Results are combined data from 2 independent experiments (n=10 total).

<u>*Y. pestis* colonization of the flea vector requires ZnuABC and Ybt zinc acquisition systems.</u>

Despite the importance of the flea vector in *Y. pestis* transmission, metal availability in the flea midgut has been minimally characterized (30). Since the *znuA ybtX* mutant is extremely attenuated in its ability to grow in Zn-limited environments, and YbtX is not required for Ybt-mediated Fe acquisition, this mutant provides us a tool to specifically investigate the availability of Zn within the flea midgut and to determine the role of Zn transporters in flea colonization by *Y. pestis*. To this end, *Xenopsylla cheopis* fleas were co-infected using an artificial feeder system as previously described (243, 244) with a mixture of *Y. pestis* KIM6+ (which lacks the pCD1 virulence plasmid that is not required for flea colonization (244)) carrying a Kanamycin (Kan) resistance marker and *Y. pestis* with mutations in the Zn acquisition systems. Two h after feeding, a subset of fleas was euthanized, and bacteria were enumerated by replica plating on BHI agar with and without Kan to determine the ratio of KIM6+ to mutant bacteria initially ingested by the fleas during the blood meal. At 7- and 14-days post-infection, bacteria were enumerated from fleas in the same fashion to determine if the mutants had a fitness defect compared to KIM6+ bacteria, which would be indicated by an increase in the percentage of recovered KIM6+ bacteria (Fig. 2-2). During co-infections with *Y. pestis* KIM6+ and either the *znuBC* or *ybtX* mutants, no fitness advantage was observed in the parental strain (Fig. 2-3A and 2-3B). However, when fleas were co-infected with *Y. pestis* KIM6+ and the *znuA ybtX* double mutant, significantly more KIM6+ bacteria were isolated from the fleas than mutant bacteria at both 7- and 14-days post-infection compared to day 0 post-infection (Fig. 2-3C; $p<0.01$ and $p<0.001$, respectively). Together, these data indicate that Zn availability is limited within the midgut of the flea, and similar to infection of the mammalian host, *Y. pestis* uses the ZnuABC and Ybt systems to overcome Zn limitation to colonize the insect host.

<u>*Y. pestis* induces host calprotectin expression during infection.</u>

The inability of the *znuBC irp2* and *znuA ybtX* mutants to infect Swiss-Webster (197, 209) and Hjv$^{-/-}$ (Fig. 2-1) mice indicates that *Y. pestis* encounters Zn restriction during infection. One of the primary mechanisms used by the host to sequester Zn is through the release of calprotectin by
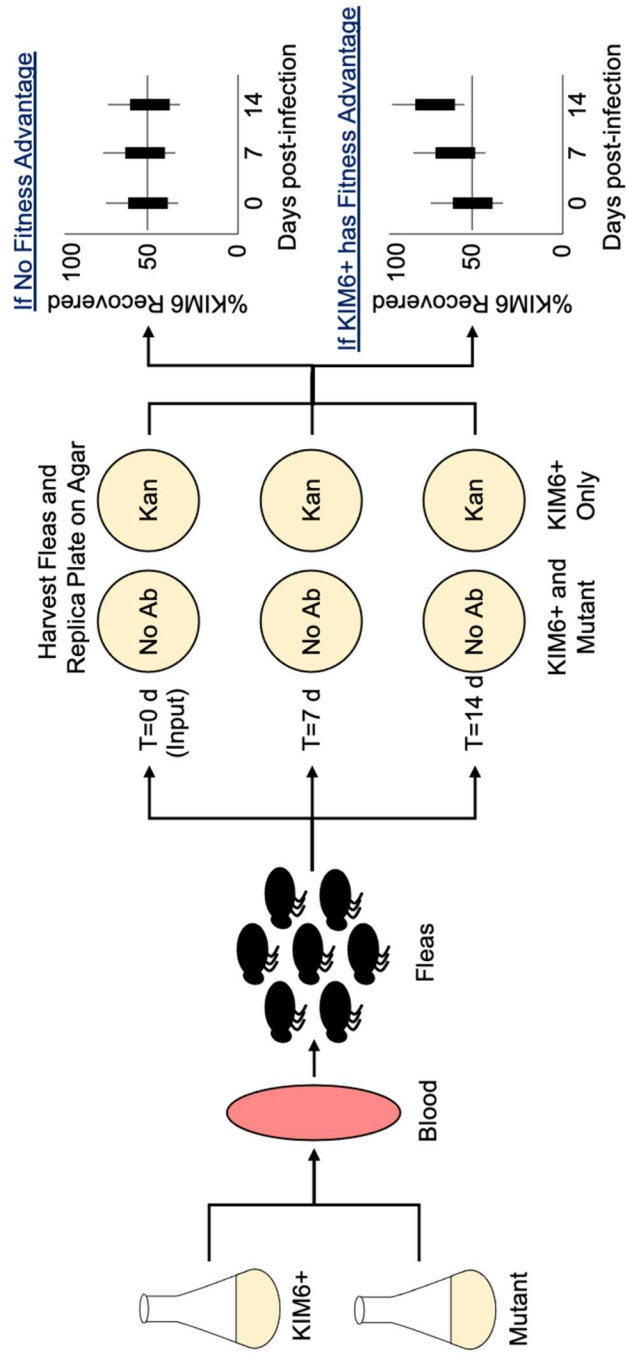
Figure 2-2. Schematic workflow to determine if Zn acquisition mutants have a fitness defect during flea colonization.

neutrophils and other host cells at sites of infection (224). To determine if *Y. pestis* encounters calprotectin during infection, C57Bl/6J mice were subcutaneously infected with *Y. pestis* CO92 (a fully virulent strain genetically similar to KIM5+ but in a different biovar) and the transcription of several nutritional immunity proteins within the draining lymph nodes was measured (Fig. 2-4A). Transcription of the siderophore binding protein lipocalin 2 and the Fe-binding proteins haptoglobin and lactoferrin increased within 36 h post-infection. However, we did not observe increased transcription of transferrin in the lymph nodes. Increased transcription of S100A8 and S100A9, the two subunits of calprotectin, was observed by 48 h post-infection. To determine if calprotectin is encountered by *Y. pestis* during pneumonic plague, C57BL/6J mice were infected intranasally with *Y. pestis* CO92 Lux$_{PcysZK}$ (245) and extracellular calprotectin was measured in the bronchial alveolar lavage fluid (BALF) over the first 48 h of infection (Fig. 2-4B). Compared to the mock-infected mice, significantly more extracellular calprotectin was recovered in *Y. pestis* infected BALF at 24 and 48 h post-infection ($p<0.01$ and $p<0.0001$, respectively). Together, these data indicate that calprotectin is present within *Y. pestis* infected tissues during both bubonic and pneumonic plague.

Zinc sequestration by calprotectin restricts the growth of *Y. pestis*.

Since our *in vivo* data indicated that *Y. pestis* encounters calprotectin during infection, we next asked if calprotectin could restrict the growth of *Y. pestis*. *Y. pestis* KIM6+ carrying the pGEN-*luxCDABE* luminescent bioreporter (245) was incubated with increasing concentrations of recombinant calprotectin and bacterial growth as a function of bioluminescence was monitored for 8 h to calculate the concentration of calprotectin that inhibited bacterial growth by 50% (IC$_{50}$). A dose-dependent inhibition of *Y. pestis* growth was observed, revealing an IC$_{50}$ of ~91 μg/ml of calprotectin for *Y. pestis* (Fig. 2-5A). To determine if calprotectin-mediated restriction of *Y. pestis* growth is dependent on metal sequestration, KIM6+ pGEN-*luxCDABE* was incubated with recombinant calprotectin inactivated for metal binding. Calprotectin has two metal binding sites designated Site 1 (S1; 6 His site) and Site 2 (S2; 3 His Asp site) (102, 228). S1 binds to Mn, Zn, and Fe (228, 246), while S2 appears to be specific for Zn binding (247, 248). Inactivation of both metal binding sites completely eliminated the ability of calprotectin to inhibit *Y. pestis* growth (Fig.
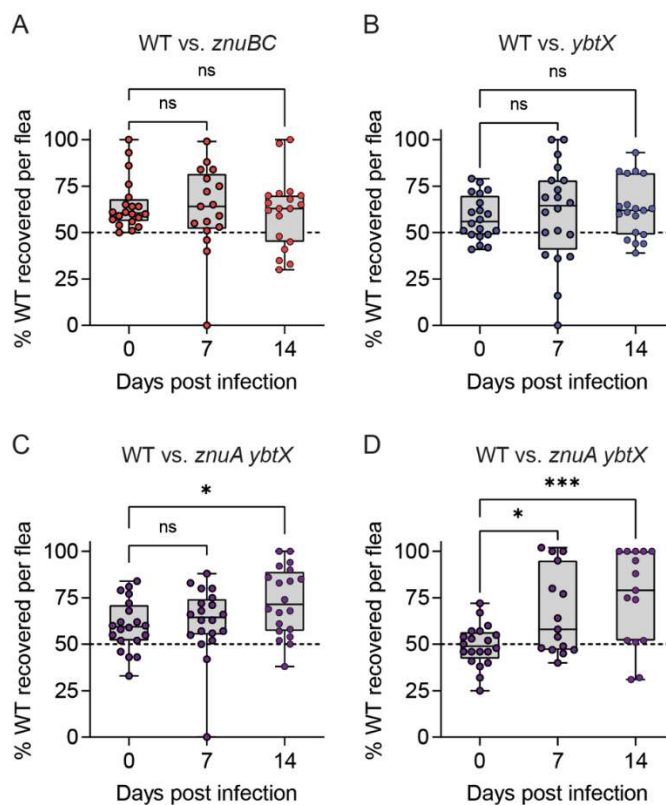
Figure 2-3. Mutants deficient in Zn acquisition are less fit to colonize the flea vector.

Xenopsylla cheopis fleas were infected using an artificial feeder with a mixture of *Y. pestis* (WT) and Zn acquisition mutants. At indicated time points, bacteria were enumerated, and the ratio of WT to mutant bacteria was calculated for (A) WT vs. *znuBC,* (B) WT vs. *ybtX,* or (C and D) WT vs. *znuA ybtX.* Greater recovery of WT at days 7 or 14 indicates that the mutant bacteria are less fit to colonize the flea. Each point represents bacterial enumeration from an individual flea; fleas in which infection was not established were excluded (n=15 to 20). One-way ANOVA with Dunnett's compared to day 0; ns=not significant, *p≤0.05 and ***p≤0.001. C and D represent biologically independent replicate experiments.

2-5B; IC_{50} >480 µg/ml; p≤0.0001), supporting that calprotectin restriction of *Y. pestis* growth is due to metal sequestration. To determine the contribution of specific metal sequestration by calprotectin on *Y. pestis* growth, KIM6+ pGEN-*luxCDABE* was incubated with recombinant calprotectin mutated in only one of the metal binding sites. Inactivation of only the S1 Mn/Zn/Fe binding site increased the IC_{50} of calprotectin by ~2-fold compared to WT calprotectin (Fig. 2-5B; IC_{50} = 182 (±9) µg/ml; p≤0.05). A similar ~2-fold increase in the IC_{50} was observed when the bacteria were incubated with calprotectin mutated only for the S2 Zn only binding site (Fig. 2-5B; IC_{50} = 190 (±9) µg/ml; p≤0.05). Moreover, the IC_{50} between the individual metal binding site mutant proteins was not statistically different. The similar IC_{50} for the S1 and S2 mutants indicate that calprotectin Zn sequestration is sufficient to restrict *Y. pestis* growth under these conditions.

ZnuABC and Ybt improve the ability of *Y. pestis* to grow in the presence of calprotectin.

Since calprotectin Zn sequestration appears to restrict the growth of *Y. pestis*, we next determined whether the ZnuABC and Ybt Zn acquisition systems improve the ability of *Y. pestis* to grow in the presence of calprotectin. While inactivation of either Zn acquisition system in *Y. pestis* decreased the IC_{50} of calprotectin compared to KIM6+, inactivation of *znuBC* appeared to have a greater effect on *Y. pestis* growth than inactivation of *irp2* or *ybtX* (Fig. 2-5C; p=0.0053 and p=0.0505, respectively). However, *Y. pestis* lacking both Zn acquisition systems (*znuBC irp2* or *znuA ybtX*) had significantly greater defects in growth in the presence of calprotectin than the single mutants (Fig. 2-5C; p≤0.0001). Complementation of the *znuA ybtX* mutant with *ybtX* restored the ability of the double mutant to grow in the presence of calprotectin. As observed for KIM6+, inactivation of either metal binding site in calprotectin resulted in an approximate 2-fold increase in the IC_{50} of calprotectin when incubated with the *Y. pestis* Zn acquisition mutants, but no significant differences were observed in the IC_{50} of the S1 and S2 mutant forms of calprotectin (Fig. 2-5D and 2-5E). Together, these data support that ZnuABC and Ybt are complementary Zn acquisition systems that improve the ability of *Y. pestis* to evade Zn-mediated growth restriction by host calprotectin.
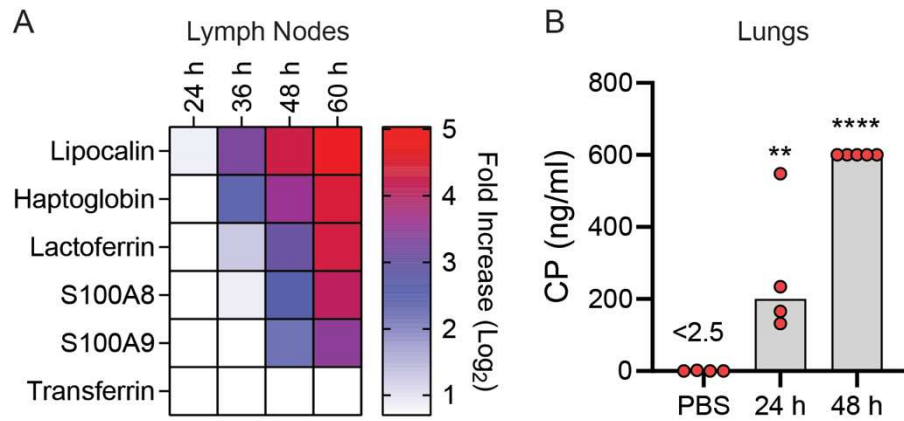
Figure 2-4. *Y. pestis* induces calprotectin expression during infection.

(A) C57BL/6J mice were infected subcutaneously with *Y. pestis* and draining lymph nodes were harvested at indicated time points (n=5) for RNA isolation and transcription analysis by microarray. Data is shown as transcriptional fold-change in infected tissues compared to lymph nodes from uninfected mice. (B) C57BL/6J mice were instilled with *Y. pestis* or PBS by intranasal installation, BALF was collected at 24 and 48 h, and extracellular calprotectin was measured. Each point represents an individual mouse and bars represent the mean. One-way ANOVA with Dunnett's compared to PBS control: **$p \leq 0.01$; ****$p \leq 0.0001$. For B, data is representative of two independent experiments.

<u>Calprotectin is the primary Zn sequestration barrier to infection by *Y. pestis*.</u>

Because *Y. pestis* appears to encounter calprotectin during infection and the *znuA ybtX* mutant is attenuated for both growth in the presence calprotectin *in vitro* and in Swiss Webster (197) and Hjv$^{-/-}$ mice (Fig. 2-1), we hypothesized that calprotectin is a barrier to Zn acquisition by *Y. pestis in vivo*. To test this hypothesis, C57BL/6J or S100A9$^{-/-}$ mice, which lack one of the subunits that compose calprotectin (249), were infected intranasally with 10^5 CFU of the KIM5+ *znuA ybtX* mutant and monitored for survival for 14 days (Fig. 2-6A). As previously shown for Swiss Webster (197) and Hjv$^{-/-}$ mice (Fig. 2-6B), C57BL/6J mice were completely resistant to infection. However, S100A9$^{-/-}$ mice were susceptible to infection by *znuA ybtX*, and the kinetics of survival mirrored that of KIM5+ infection. Similarly, S100A9$^{-/-}$ mice infected subcutaneously with 10^3 CFU of the *znuA ybtX* mutant to mimic bubonic plague were also susceptible to lethal infection, succumbing to infection at the same rate as mice infected with KIM5+ (Fig. 2-6B). Together, these data indicate that calprotectin represents a nutritional barrier to *Y. pestis* during both pneumonic and bubonic plague, and the ZnuABC and Ybt systems allow *Y. pestis* to overcome Zn sequestration by calprotectin to cause lethal infection.

DISCUSSION

Siderophores are essential for the virulence of a variety of pathogens (232, 250). Because of their high affinity for Fe, their role in virulence has been primarily linked to improved competition for Fe with host nutritional immunity mechanisms. However, while *in vitro* data indicates that siderophores can also bind metals other than Fe, the contribution of alternative metal binding by siderophores to virulence has been largely overlooked. In the case of Ybt, several independent groups have shown recently that Ybt can bind to Ga, Ni, Cu, Cr, and Zn, and to a lesser degree, Co, Pd, Mg, and Al, in addition to Fe (179, 180, 251). Moreover, Ybt has been shown to improve *in vitro* growth of *E. coli* in Cu-, Ni-, or Zn-limited media (69, 179, 180), and of *Y. pestis* in Zn-limited medium (197). However, direct evidence for a role of alternative metal binding by Ybt in virulence has been difficult to demonstrate for two reasons. First, many pathogens encode redundant metal acquisition systems that can mask the contribution of Ybt to metal acquisition. For example, several pathogens
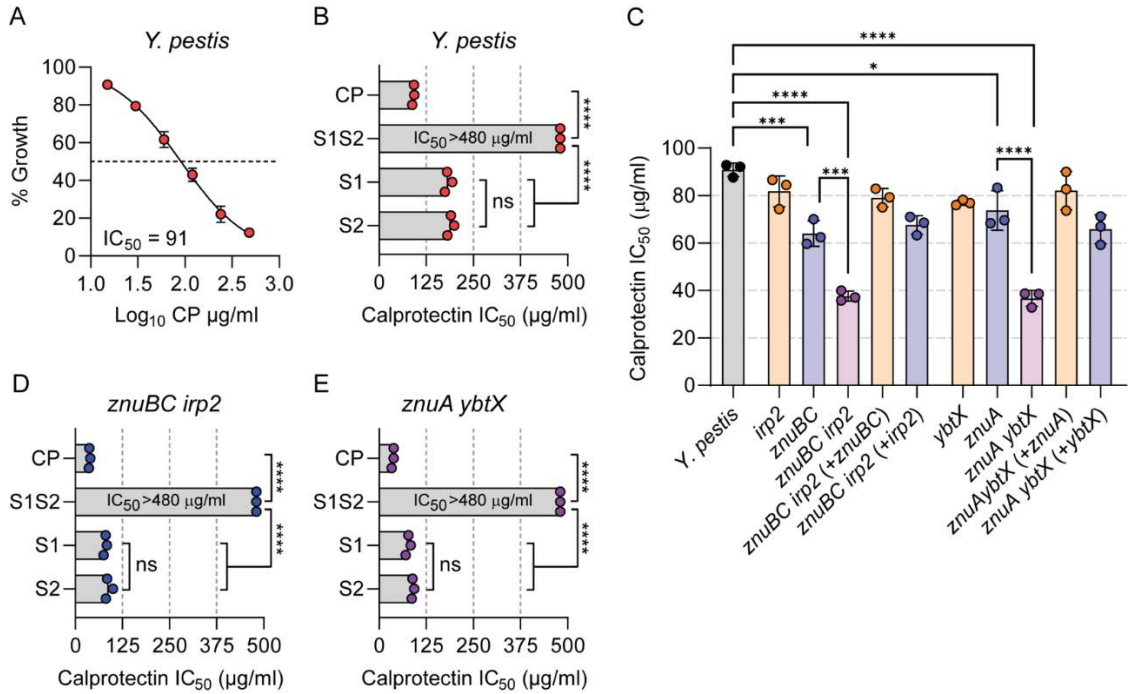
Figure 2-5. ZnuABC and Ybt both contribute to overcoming Zn sequestration by calprotectin.

(A) WT *Y. pestis* was incubated with increasing concentrations of calprotectin (CP), up to 480 µg/ml, and percent growth vs. untreated was determined at 8 h to calculate the IC_{50}. (B) IC_{50} of calprotectin containing mutations in metal binding Site 1 (S1), metal binding Site 2 (S2), or both metal binding sites (S1S2) when incubated with WT *Y. pestis*. (C) IC_{50} of calprotectin when incubated with indicated *Y. pestis* mutants. Complete statistical comparisons between all bacteria for 4C is in Supplementary Table 2. IC_{50} of calprotectin containing mutations in metal binding Site 1 (S1), metal binding Site 2 (S2), or both metal binding sites (S1S2) when incubated with (D) *znuBC irp2* or (E) *znuA ybtX* mutants. For B, D, and E the S1S2 mutant was unable to inhibit *Y. pestis* growth at the highest concentration tested (480 µg/ml). Each point represents the mean IC_{50} of a biologically independent experiment (n=3) and the bar represents the mean of the three independent experiments. One-way ANOVA with Tukey's comparison: ns= not significant; *p<0.05; ***p<0.001; ****p<0.0001.

that encode Ybt also encode the high affinity ZnuABC Zn transporter, which has been shown to at least partially compensate for growth defects under Zn limitation in the absence of Ybt in both *Y. pestis* and *E. coli* Nissle 1917 (69, 197). Second, for those pathogens that express Ybt, Ybt is the primary Fe acquisition system during infection, which makes it difficult to separate Fe-dependent contributions from other metal-dependent contributions to overall virulence. To overcome these hurdles, we used a combination of *Y. pestis* Ybt mutants lacking the ZnuABC Zn acquisition system and the Hjv$^{-/-}$ mouse strain defective in Fe-mediated nutritional immunity to clearly demonstrate for the first time *in vivo* that Ybt contributes to the virulence of *Y. pestis* independent of Fe acquisition. These data build upon the *in vitro* data by others described above and support the concept that Ybt should be considered more than a siderophore, and likely better described as a metallophore that can contribute to the acquisition of multiple metals during *Y. pestis* infection. Moreover, because Ybt and the Ybt transporter YbtX are conserved in other pathogenic bacteria, these data suggest that Ybt likely contributes to pathogenic potential for a variety of bacteria through an increased ability to compete with the host for not only Fe but other metals. This hypothesis is further supported by the improved competition of *E. coli* Nissle 1917 expressing Ybt over *S.* Typhimurium in the Zn-limited environment of the inflamed gut recently reported by Behnsen et. Al (69). Furthermore, the potential to increase the ability of bacterial pathogens to compete against multiple arms of the host nutritional immunity response during infection may also help to explain the hypervirulent phenotypes associated with *K. pneumoniae* clinical isolates that harbor the Ybt genetic loci (252–255). The application of similar strategies described here for *Y. pestis* in these other bacteria could be used to determine the contribution of alternative metal acquisition by Ybt to hypervirulence observed in certain clinical isolates that has been associated with the presence of the Ybt genetic loci.

While metal restriction has been established as an important barrier to bacterial infection in the mammalian host, a role for metal sequestration in restricting bacterial colonization of insect vectors has not been established. However, homologs of mammalian Fe-binding transferrins have been identified in several insects (256), and in a *Drosophila melanogaster* model system, transferrin 1
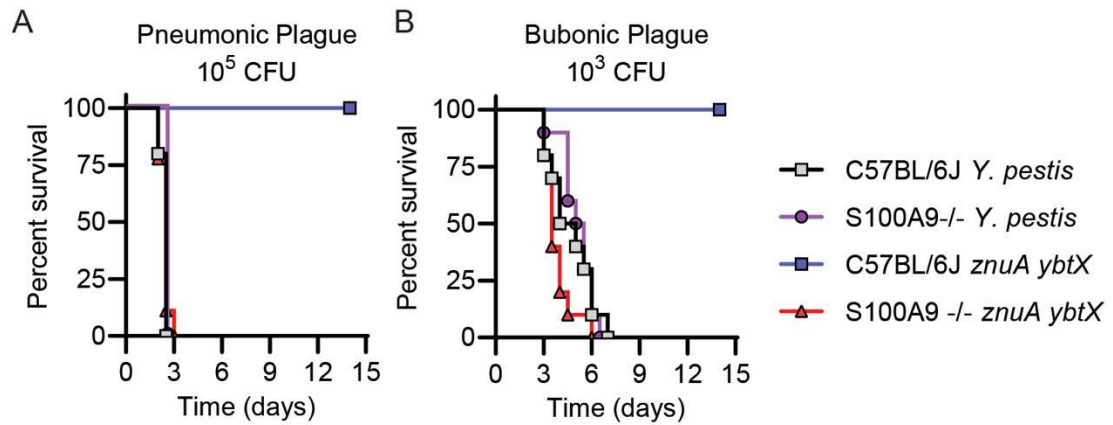
Figure 2-6. Calprotectin is the primary barrier to infection by the *znuA ybtX* mutant.

(A) C57BL/6J or S100A9$^{-/-}$ mice were infected intranasally with 10^5 CFU of WT *Y. pestis* or the *znuA ybtX* mutant. (B) C57BL/6J or S100A9$^{-/-}$ mice were infected subcutaneously with 10^3 CFU of WT *Y. pestis* or the *znuA ybtX* mutant. Results are combined data from 2 independent experiments (n=10 total). Log Rank Test revealed no significant differences in survival kinetics between S100A9$^{-/-}$ mice infected with WT *Y. pestis* or the *znuA ybtX* mutant, or C57BL/6J and S100A9$^{-/-}$ infected with WT *Y. pestis*.

sequesters iron and facilitates nutritional immunity to *Pseudomonas aeruginosa* (257), suggesting possible conservation of metal nutritional immunity in insects. Previous studies have shown that Ybt is not required for flea colonization by *Y. pestis* (25) and that Fe is not limited in the flea midgut (75). In contrast, we show here that the *znuA ybtX* mutant, which can acquire Fe but not Zn, is significantly attenuated in flea colonization compared to KIM6+ (Fig. 2-3). These data support that bacterial access to Zn is limited within the flea midgut but requires future biochemical analysis to directly measure metal concentrations within flea tissues to confirm limited Zn levels. Whether the flea is actively restricting Zn is not known. However, the first flea genome was recently published (258) and provides a new resource that may lead to the identification of potential nutritional immunity genes that could contribute to Zn-limitation based on homology with mammalian genes. Alternatively, *Y. pestis* may need high affinity Zn acquisition systems to compete for Zn with members of the microbiota of the flea digestive tract. How the microbiota of the flea effects transmission of *Y. pestis* has not been investigated, but similar to the mammalian host, it is likely the microbiota imposes selective pressures on pathogens that use these insects for transmission. Regardless of the mechanism for Zn limitation, these data are the first to demonstrate a role for Zn acquisition systems as transmission factors for *Y. pestis* and justify future studies to better understand metal restriction within fleas and other insects, and the potential impact of these systems on pathogen transmission.

The mammalian host produces a variety of proteins that can sequester Zn from invading pathogens (68, 220). In the mouse, calprotectin expression and release by host cells has been shown to occur during a variety of bacterial infections (108, 109, 111), and we observed evidence of increased calprotectin levels in *Y. pestis*-infected tissues during plague (Fig. 2-4). These data suggest that *Y. pestis* needs to overcome calprotectin-mediated nutritional immunity to proliferate in these tissues. This hypothesis is independently supported by observations published by other laboratories. Comer *et al*. reported a similar increase in S100A8 and S100A9 in the lymph nodes of rats infected with *Y. pestis* (259), and Nuss *et al*. reported increased transcription of these genes in the Peyer's patches during infection of the closely related enteric pathogen *Y.*

pseudotuberculosis (260). Despite these previous observations, the role of calprotectin in restricting *Yersinia* infections has not been previously tested directly. Interestingly, the kinetics of lethal infection of S100A9$^{-/-}$ mice with WT *Y. pestis* did not appear to differ from that of C57BL/6J or BALB/c mice that we have previously reported (245, 261, 262). This phenotype differs from what has been reported for other pathogens, in which S100A9$^{-/-}$ mice are more susceptible to infection than mice that produce functional calprotectin (107–109, 111). These data suggest that *Y. pestis* has evolved very effective mechanisms to overcome calprotectin mediated nutritional immunity, to which the ZnuABC and Ybt Zn acquisition systems appear to be major contributors. Future studies using the *znuA ybtX* mutant to identify the impact of calprotectin beyond overall host survival, such as monitoring of bacterial dissemination to and proliferation in different tissues, will allow us to specifically determine when *Y. pestis* encounters calprotectin-mediated Zn restriction during the progression of plague.

Calprotectin has been shown to sequester Mn, Zn, and Fe from bacterial and fungal pathogens (102, 108, 109, 228, 230). Using recombinant forms of calprotectin with different metal-binding abilities suggests that calprotectin-mediated sequestration of Zn is a barrier for *Y. pestis*, at least under the *in vitro* conditions in which we tested here. This is supported by the observation that inactivation of the S1 metal binding site, which binds Mn, Zn, and Fe, did not eliminate the ability of calprotectin to inhibit *Y. pestis* growth (Fig. 2-5B). Studies with other pathogens, such as *S. aureus*, have shown that Mn sequestration by calprotectin is necessary for maximal antimicrobial activity (108, 228), highlighting that the evolution of calprotectin to sequester multiple metals has resulted in a broad-spectrum antimicrobial protein that can restrict the growth of variety of pathogens that vary in their ability to acquire different metals. Like we have shown for Zn, *Y. pestis* also encodes multiple Mn acquisition systems, including the Yfe and MntH systems (193). In the absence of these Mn transporters, Mn binding via the S1 metal binding site might have a greater impact on growth restriction than observed here. However, an *yfe mntH* mutant is only partially attenuated during bubonic plague and does not appear to be attenuated during pneumonic plague (193), indicating that additional Mn acquisition mechanisms may be active during infection to

overcome calprotectin-mediated Mn sequestration. Alternatively, *Y. pestis* may be able to use other metals such as Fe to compensate for Mn restriction during infection as reported for *Streptococcus pneumoniae* (263).

While we observed an additive effect on the growth of *Y. pestis* in the presence of calprotectin when we inactivated both the Znu and Ybt Zn acquisition systems, the data from the single mutants suggest that the integral membrane ZnuABC transporter may be more effective at competing for Zn with calprotectin than secreted Ybt (Fig. 2-5C; *irp2* and *ybtX* mutants vs. the *znuBC* mutant). These data were unexpected, as previous studies with *S. aureus* have shown that staphylopine, a secreted Zn-binding metallophore, is more important for competition against calprotectin metal sequestration than AdaABC, a membrane bound Zn transporter (264). However, these results may be a reflection of Ybt expression by *Y. pestis* in these assays. For these studies, *Y. pestis* was cultured under metal replete conditions prior to incubation with calprotectin. Under these growth conditions, Ybt synthesis is minimal (146, 241). A greater contribution of Ybt may be observed if the bacteria are pre-grown under metal deplete conditions to increase the expression of Ybt in the *znuBC* mutant. Alternatively, while ZnuABC is a dedicated Zn transporter, Ybt also binds to Fe, and thus competition between different metals by Ybt may result in the appearance of a decreased contribution for Zn acquisition in these experiments. Importantly, we have previously shown that absence of the ZnuABC system does not impact virulence (148, 209), demonstrating that *in vivo*, Ybt is sufficient to compete for Zn with calprotectin.

Because the *znuA ybtX* mutant is not defective in Fe acquisition, this mutant provided us a powerful tool to directly test for the first time the role of calprotectin-mediated Zn restriction during plague. Inactivation of calprotectin by deletion of S100A9 in the host completely restored the virulence of this double mutant (Fig. 2-6). Moreover, we did not observe a significant difference between the kinetics of the infection with WT or *znuA ybtX* bacteria, indicating that calprotectin is the main barrier to Zn acquisition in mice during bubonic and pneumonic plague. These data also support that calprotectin is a potent barrier to bacteria attempting to colonize the host via intradermal or pulmonary routes. Because S100A8 and S100A9 comprise upwards of 40% of the

total cytosolic proteins in neutrophils (105, 265), and neutrophil-mediated calprotectin release has been linked to growth restriction of several pathogens (224, 231, 266), neutrophils tend to be considered the primary cells responsible for the release of calprotectin during infection. However, neutrophil inflammation in response to *Y. pestis* differs dramatically within the initial tissues colonized by *Y. pestis* during bubonic and pneumonic plague. During intradermal infection (bubonic plague), a rapid recruitment of neutrophils is observed to the infection site (267, 268). However, during pulmonary infection (pneumonic plague), infiltration of neutrophils is delayed (216, 269). These differences in neutrophil recruitment raise the possibility that calprotectin-dependent restriction may be mediated by different cells within different tissues. The role of cells other than neutrophils in mediating calprotectin restriction has been reported in the gut for *S.*Typhimurium and in the dermis for *Borrelia burgdorferi*, another vector-borne bacterium (106, 270), and our future goals are to use the *znuA ybtX* mutant to dissect the contribution of different cell types to the calprotectin response in specific tissues during bubonic and pneumonic plague.

In conclusion, we have directly demonstrated for the first time an Fe-independent role of the siderophore Ybt in *Y. pestis* virulence and colonization of both the mammalian and insect hosts. Because of the conservation of YbtX in enteric pathogens that produce Ybt, we expect that Ybt also contributes to Zn acquisition in other pathogens encoding the Ybt genetic loci, justifying that the concept of Ybt as merely a siderophore should be expanded to include a broader role for Ybt in the acquisition of other metals during infection (i.e., that Ybt should be considered a metallophore that binds and improves acquisition of at least two, and possibly multiple, metals). Furthermore, these data open the possibility that as a field, we need to examine whether other siderophores may also contribute to overall virulence through the acquisition of metals other than Fe.

METHODS

Ethics statement

Hjv$^{-/-}$ 129 (86) and C57BL/6J were originally purchased from The Jackson Laboratories and bred within the barrier facility at the Clinical and Translational Research Building at the University of Louisville, and C57BL/6 S100a9$^{-/-}$ mice (249) were bred at the University of Illinois at Urbana-

Champaign prior to transfer to the University of Louisville for infection. Groups contained both male and female mice, and no sex bias was observed during these studies. Animals were housed in accordance with NIH guidelines and all procedures were approved by the University of Louisville IACUC and the University of Illinois IACUC. Three days prior to challenge with *Y. pestis*, animals were transferred to University of Louisville's Center for Predictive Medicine Regional Biocontainment Laboratory ABSL-3 facilities to acclimate to the facility. Mice were maintained within ABSL-3 for up to 14 days post-challenge.

Bacterial strains and plasmids

The bacterial strains used in this study are listed in Table 2-3. *Y. pestis* was routinely grown for 15 to 18 h at 26 °C in Difco brain heart infusion (BHI) broth (BD Biosciences) with aeration. Strains transformed with the pGEN-*luxCDABE* plasmid (245) were grown in the presence of carbenicillin (50 μg/ml). Prior to pneumonic infection, *Y. pestis* grown at 26 °C was diluted to 0.05 OD_{600} in BHI broth with 2.5 mM $CaCl_2$ and grown at 37°C with aeration for 16 to 18 h (216). Bacterial concentrations were determined using a spectrophotometer and diluted to desired concentrations in 1x PBS for mouse infections or fresh medium for *in vitro* studies. Concentrations of bacterial inoculums for mouse studies were confirmed by serial dilution and enumeration on agar plates.

Inductively coupled plasma mass spectrometry (ICP-MS)

To determine the Fe concentrations in mice, livers were harvested from 8-week-old mice, and 10-20 mg of liver tissue was incubated at 65 °C in 70% nitric acid for 4 h, and then diluted 35-fold in Milli-Q purified, metal-free water. The solution was passed through a 100 μm filter, and Fe levels were measured by ICP-MS (Thermo Fisher Scientific X-Series II, Waltham, MA, USA) at the University of Louisville's Center for Integrative Environmental Health Science Toxicomics & Environmental Measurement Facility Core. Fe levels were calculated based on a standard curve and presented as ng/mg wet tissue.

Animal infections with *Y. pestis*

Mice were challenged with *Y. pestis* as previously described (245, 261, 262). Briefly, for intranasal challenge, mice were anesthetized with ketamine/xylazene and administered 20 µl of bacteria suspended in 1X PBS to the left nare. For subcutaneous challenge, mice were anesthetized with isoflurane and administered 20 µl of bacteria suspended in 1x PBS via subcutaneous injection at the base of the tail. Infected mice were monitored for the development of disease symptoms twice daily for 14 days. Moribund animals meeting predefined endpoint criteria were humanely euthanized by CO_2 asphyxiation and scored as succumbing to infection 12 h later.

Flea infections with *Y. pestis*

For flea infections, separate cohorts of *Xenopyslla cheopis* fleas were allowed to blood feed on infected sodium heparinized CD-1 mouse blood (BioIVT, New York, USA) using a previously described artificial feeding apparatus (243, 244). The bloodmeal was seeded with a 1:1 ratio of the *Y. pestis* KIM6+ *glmS-pstS*::kan[R] strain, and either the *ybtX*, *znuBC*, or *znuA ybtX* mutants to achieve a final concentration of 1.08×10^9 to 1.82×10^9 colony forming units (CFU)/ml blood. Only fleas that fed to repletion were selected. At 0-, 7-, and 14-days post-infection, co-infected fleas were processed to enumerate bacterial colonization (Fig. 2-2). To ensure optimal growth of the Zn acquisition mutants, agar plates were additionally supplemented with 10 µM $ZnCl_2$. Guidelines set forth by the U.S. National Institutes of Health (NIH) Guide for the Care and Use of Laboratory Animals and approved by the Washington State University IACUC were strictly applied when using mice in flea infection experiments.

Measurement of calprotectin during *Y. pestis* infection

To determine the expression of calprotectin during bubonic plague, C57BL/6J mice were infected subcutaneously with ~200 CFU *Y. pestis* CO92. At 24, 36, 48 and 60 h post-infection, the draining lymph nodes were harvested from five mice. Lymph nodes from each time point were combined, total RNA was extracted, and host transcriptional profiles were determined as previously described and compared to lymph nodes from uninfected mice (271). To determine extracellular levels of calprotectin within the lungs during pneumonic plague, mice were infected intranasally

with ~10^4 CFU of *Y. pestis* CO92 Lux$_{PcysZK}$ and at 24 and 48 h post-infection, groups of mice were euthanized, and bronchial alveolar lavage fluid (BALF) was collected as previously described (272). Host cells and *Y. pestis* were removed from the samples using a 0.45 µm syringe filter and total extracellular concentrations of calprotectin were determined using the Mouse Calprotectin SimpleStep ELISA Kit as described by the manufacturer (abcam, ab263885).

Determination of calprotectin inhibitory concentrations

Recombinant forms of calprotectin were produced in *E. coli* and purified as previously described (102, 228). To determine the concentrations of calprotectin to inhibit 50% growth of *Y. pestis*, bacteria were incubated with increasing concentrations of CP as previously described with modifications (102, 270). Briefly, overnight cultures of *Y. pestis* carrying the pGEN-*luxCDABE* plasmid grown in BHI at 26°C were diluted 1:50 in fresh BHI and grown for 4 h at 37 °C. 1×10^5 CFU were transferred to individual wells of a white 96-well plate (Greiner Bio-One) containing calprotectin in 38% BHI, 62% calprotectin buffer (20 mM Tris, pH 7.5, 100 mM NaCl, 3 mM $CaCl_2$). Plates were incubated at 37 °C and bacterial growth was measured after 8 h as a function of bioluminescence using a Biotek Synergy HT plate reader (0.5 s read, sensitivity of 135) as previously described (245).

Statistics

All animal experiments were repeated twice, and *in vitro* experiments were repeated three times to confirm reproducibility. Data are shown as the means ± standard deviations (SDs) from three independent experiments, unless otherwise noted. *P* values were calculated using Student's *t* test, one-way analysis of variance (ANOVA), or two-way ANOVA with appropriate posthoc testing as indicated. All statistics were completed using GraphPad Prism software.

ACKNOWLEDGEMENTS

46

Table 2-1. Concentration of metals in mouse livers (ng metal/mg tissue).

Metal	Wild-type		Hjv +/-		Hjv -/-	
	Mean	SD	Mean	SD	Mean	SD
9Be	0.00	0.00	0.00	0.00	0.00	0.00
23Na	1325.98	662.18	649.16	253.36	762.00	151.64
24Mg	247.30	52.34	200.35	89.85	175.26	43.05
27Al	2.98	2.24	2.87	1.19	2.62	1.04
39K	3884.08	1208.97	2587.88	1299.61	4151.59	790.63
44Ca	256.87	108.90	239.64	42.96	95.02	71.73
51V	0.06	0.04	0.01	0.01	0.11	0.03
52Cr	0.16	0.00	0.08	0.05	0.44	0.11
55Mn	1.71	0.94	1.19	0.78	2.28	0.33
57Fe	86.13	16.04	97.63	46.12	926.52	158.31
59Co	0.03	0.02	0.02	0.02	0.04	0.01
60Ni	0.07	0.03	0.12	0.07	0.06	0.03
65Cu	7.16	0.68	6.47	1.37	3.12	0.70
66Zn	41.98	19.63	28.40	11.84	22.62	11.71
75As	0.12	0.04	0.08	0.04	3.08	7.40
82Se	2.15	0.68	1.27	0.79	1.60	0.26
95Mo	0.83	0.06	0.91	0.53	2.67	1.49
107Ag	0.01	0.00	0.01	0.00	0.12	0.07
111Cd	0.01	0.01	0.01	0.01	0.09	0.13
121Sb	0.43	0.18	0.39	0.18	0.76	0.24
137Ba	0.68	0.13	0.58	0.12	0.02	0.32
208Pb	0.09	0.02	0.08	0.02	0.68	0.89

Table 2-2. Complete statistical comparisons between all bacteria for Fig. 2-5C.

	Y. pestis	irp2	znuBC	znuBC irp2	znuBC irp2 (+znuBC)	znuBC irp2 (+irp2)	ybtX	znuA	znuA ybtX	znuA ybtX (+znuA)	znuA ybtX (+ybtX)
Y. pestis	--	ns	***	****	ns	***	ns	*	****	ns	***
irp2		--	*	****	ns	ns	ns	ns	****	ns	*
znuBC			--	***	ns	ns	ns	ns	****	*	ns
znuBC irp2				--	****	****	****	****	ns	****	****
znu irp2 (+znuBC)					--	ns	ns	****	****	ns	ns
znu irp2 (+irp2)						--	ns	ns			ns
ybtX							--	ns	****	ns	ns
znuA								--	****	ns	ns
znuA ybtX									--	****	****
znuA ybtX (+znuA)										--	*
znuA ybtX (+ybtX)											--

*= p≤0.05; ***= p≤0.001; ****= p≤0.0001; ns=not significant

Table 2-3. Bacterial strains used in these studies.

Descriptive Name	Genotype	Identification Number	Source
Strains used for Hjv^{-/-} and S100A9^{-/-} mouse infections.			
KIM5+	(pCD1Ap)+, pgm+, pMT+, pst+	X17	(155)
irp2	X17 Δ*irp2*	X43	(151)
znuBC irp2	X43 Δ*znuBC*	X90	(209)
znuA ybtX	X17 Δ*znuA*, Δ*ybtX*	X103	(197)
znuA ybtX **(+*ybtX*)**	X103 complemented with *ybtX* in native site	X105	(197)
Strains used for flea infections.			
KIM6+ *glmS-pstS*::kan[R]	pCD1-, pgm+, pMT+, pst+ with kan[R] cassette inserted into the attTn7	VV670	(244)
KIM6+ *ybtX*	pCD1-, pgm+, pMT+, pst+, Δ*ybtX*	YPA262	(176)
KIM6+ *znuBC*	pCD1-, pgm+, pMT+, pst+, Δ*znuBC*	YPA154	(273)
KIM6+ *znuA ybtX*	pCD1-, pgm+, pMT+, pst+, Δ*znuA, ybtX*	YPA177	(197)
Strains used for calprotectin measurements in mice.			
CO92	pCD1+, pgm+, pMT+, pst+	YP003-1	(274)
CO92 Lux_{PcysZK}	YP003-1 with LuxCDABE_{PcysZK} inserted into attTn7	MBLYP-043	(245)
Strains used in *in vitro* calprotectin assays.			
KIM6+ *znuBC* pGEN-*luxCDABE*	YPA154 with bioluminescent reporter	YPA258	This work
KIM6+ *irp2* pGEN-*luxCDABE*	pCD1-, pgm+, pMT+, pst+, Δ*irp2* with bioluminescent reporter	YPA259	This work
KIM6+ *irp2 znuBC* pGEN-*luxCDABE*	pCD1-, pgm+, pMT+, pst+, Δ*irp2*, Δ*znuBC* with bioluminescent reporter	YPA260	This work
KIM6+ *ybtX* pGEN-*luxCDABE*	YPA262 with bioluminescent reporter	YPA265	This work
KIM6+ *znuA ybtX* pGEN-*luxCDABE*	YPA177 with bioluminescent reporter	YPA261	This work
KIM6+ *znuA ybtX* (+*ybtX*) pGEN-*luxCDABE*	YPA261 complemented with *ybtX* in native site	YPA290	This work

CHAPTER 3

DROPLET TN-SEQ IDENITIFIES THE PRIMARY SECRETION MECHANISM FOR

YERSINIABACTIN IN *YERSINIA PESTIS*

SUMMARY

Nutritional immunity is the process used by eukaryotic hosts to sequester transition metals such as iron, zinc, or manganese from invading bacterial pathogens. To overcome nutritional immunity, bacteria have evolved dedicated metal acquisition systems. *Yersinia pestis,* a Gram-negative bacterium that is the causative agent of plague, acquires iron and zinc by secreting the metallophore yersiniabactin (Ybt). Because Ybt is required for *Y. pestis* pathogenesis, defining the molecular mechanisms for the synthesis and transport of Ybt are essential to understanding this key virulence factor. The genes required for Ybt synthesis and import are well-defined, yet the genes required for secretion of Ybt have eluded identification. This mechanism has been difficult to identify because conventional pooled screening approaches are unable to connect genes involved in secretion with their function due to trans-complementation between mutants. To overcome this obstacle, we utilized a technique called droplet Tn-seq (dTn-seq). dTn-seq uses microfluidics to isolate individual transposon mutants in oil droplets, eliminating the potential for trans-complementation of secreted factors between bacteria, but still allowing for fitness comparisons of large transposon libraries. Using this approach, we demonstrated the applicability of dTn-seq to identify genes involved in secreted functions of bacteria. We then applied dTn-seq to

identify an AcrAB efflux system as required for growth in metal-limited conditions and demonstrated that this efflux system is the primary mechanism for Ybt secretion and required for virulence in the mouse model of plague. Together, these studies have finally revealed the secretion mechanism for Ybt that has eluded researchers for over thirty years and a potential anti-therapeutic target to combat plague and other infections by bacteria that rely on Ybt for metal acquisition.

INTRODUCTION

Plague is a disease that has impacted humankind through three major pandemics and remains a major public health concern (4, 213). The Gram-negative bacterial pathogen, *Yersinia pestis*, is the etiological agent of plague. The disease can manifest in three forms, which are highlighted by bacterial colonization of the lymph nodes during bubonic plague, the bloodstream during septicemic plague, and the lungs during pneumonic plague (215, 216). Without immediate antibiotic treatment, all forms of the disease can be fatal. Due to the ease of direct transmission between individuals in a population, potential for weaponization, and the lack of an approved vaccine, *Y. pestis* is categorized as a Tier 1 select agent (275). As a potential bioterrorism agent, understanding *Y. pestis* pathogenesis and discovering new therapeutic targets is a valuable research area.

Y. pestis requires transition metals to carry out proper cell function and metabolism. However, eukaryotic hosts use mechanisms referred to as nutritional immunity to restrict bacterial access to these metals to inhibit infection (68, 71, 220, 276). Consequently, *Y. pestis* has developed highly efficient systems to acquire iron (Fe), zinc (Zn), and manganese (Mn) to overcome the nutritional immunity (148, 151–153, 193, 197, 277). The most well-studied metal acquisition system utilized by *Y. pestis* is the secreted metallophore yersiniabactin (Ybt), which is essential for iron acquisition and contributes to zinc acquisition during infection (209, 278). The mechanisms involved in the synthesis and import of Ybt have been extensively studied (63, 171, 176, 197). The genes involved in these processes are all located in two operons within the pigmentation (pgm) locus, which is part of the high pathogenicity island on the chromosome of *Y. pestis* (Fig. 3-1A) (63). YbtA regulates the expression of the genes that comprise the Ybt enzyme complex responsible for the synthesis of Ybt (*irp1, irp2, ybtE, ybtS, ybtT, ybtU*) and the genes that encode the transporters involved in the

import of Ybt bound to iron (*psn, ybtP, ybtQ*) or Ybt bound to zinc (*ybtX*) (168, 176, 279). These operons are conserved in other species that synthesize Ybt, including pathogenic *Escherichia coli*, *Klebsiella pneumoniae*, and *Proteus mirabilis* (164–167, 280). Despite our extensive knowledge of this system, the molecular mechanism(s) responsible for the export of Ybt by bacteria has yet to be identified. Because Ybt is an essential virulence factor in all bacteria which synthesize it (277), identifying the Ybt export mechanism could reveal a therapeutic target for the development of anti-virulence-based therapeutics.

One of the reasons the Ybt export mechanism has eluded researchers for the last 30 years is that the mechanism is not encoded within the operons that encode the rest of the Ybt genes. Therefore, high-throughput genome screening techniques like transposon insertion sequencing (Tn-seq) are needed to identify these essentially unknown genes. Traditional Tn-seq uses a transposon to generate libraries of random mutants that include the inactivation of every non-essential gene in the genome (281). These libraries are then grown under selective conditions, for example metal limitation, and the fitness of individual transposon mutants can be calculated by quantifying their abundance within the population by deep sequencing (281). Transposon insertions into genes required to grow under the selective condition will be less fit and make up a smaller portion of the population after selection. While Tn-seq has proven to be a powerful discovery tool, conventional Tn-seq has a limitation that it is unable to identify genes for secreted factors. This is because all the mutants in a transposon library are grown together in one large pool. Within this pool, mutants in secreted factors required for growth under the specific selective conditions, for example Ybt needed by *Y. pestis* to grow under metal-deplete conditions, can "cheat" and use the secreted factors produced by their neighbors (also referred to as trans-complementation). Cheating allows these mutants to still grow under selective conditions, hiding their true phenotype, and eliminates the possibility of identifying genes of secreted factors via conventional Tn-seq. To overcome this limitation, we applied a recently described modified Tn-seq application called droplet Tn-seq (dTn-seq) (282) to identify mutants deficient in Ybt secretion. dTn-seq uses microfluidics to encapsulate individual transposon mutants inside a medium droplet surrounded by an oil layer

(282). The oil layer inhibits diffusion of Ybt, and other secreted factors, between droplets, allowing for the screening of a large library of mutants for growth defects under metal-limited conditions unaffected by neighboring bacterial cells. Using dTn-seq, we identified a role for an AcrAB-TolC efflux system for growth of *Y. pestis* in metal-limited conditions. Furthermore, by using a combination of *in vitro* and *in vivo* methods, we finally identified this AcrAB-TolC system as the primary export system for Ybt and show it is required for *Y. pestis* virulence.

RESULTS

<u>dTn-seq can overcome trans-complementation and identify factors involved in yersiniabactin synthesis.</u>

We have previously demonstrated that *Y. pestis* can grow within the microenvironment of the droplets needed for dTn-seq (282). For the Tn-seq library, we generated ~50,000 mutants using the HIMAR transposon as previously described (283) in a *Y. pestis* pCD1$^{(-)}$ *znuBC* background (representing >10x coverage of the genome). This background was chosen for two reasons. First, because the pCD1 plasmid is required for virulence but not for Ybt export, we can perform dTn-seq in this background at BSL-2. Second, while a *znuBC* mutant can grow in metal-limited conditions, a *znuBC irp2* mutant is extremely attenuated for growth in the same medium (209). Therefore, transposon mutants in genes required for the synthesis, import, or export of Ybt in a *znuBC* background should have significant fitness defects that can be easily differentiate from the *znuBC* mutant in droplets containing Zn-limited medium. The library was grown in BHI, passaged in metal-chelated PMH2 medium (cPMH2) to deplete intracellular stores of Zn, and then grown as a batch culture in cPMH2 or encapsulated into droplets of cPMH2 by microfluidics (Fig. 3-1B) (279). Genomic DNA was isolated from each culture condition, sequenced, and individual transposon mutant fitness was calculated as previously described (282). To validate that droplet encapsulation can overcome trans-complementation, we first determined fitness phenotypes for the known components of Ybt synthesis and import. Mutants with transposon insertions in *ybtA*, the master regulator of the Ybt system (168), or in *ybtX*, required for Ybt-Zn import (197), had significant fitness

A

B
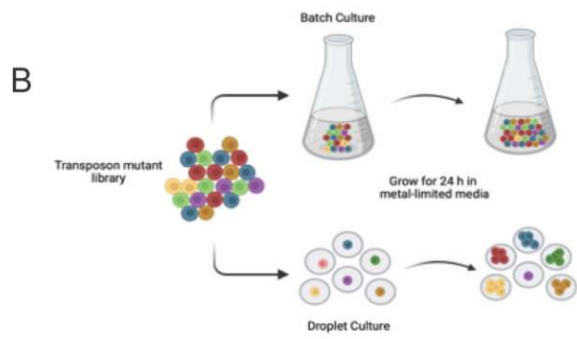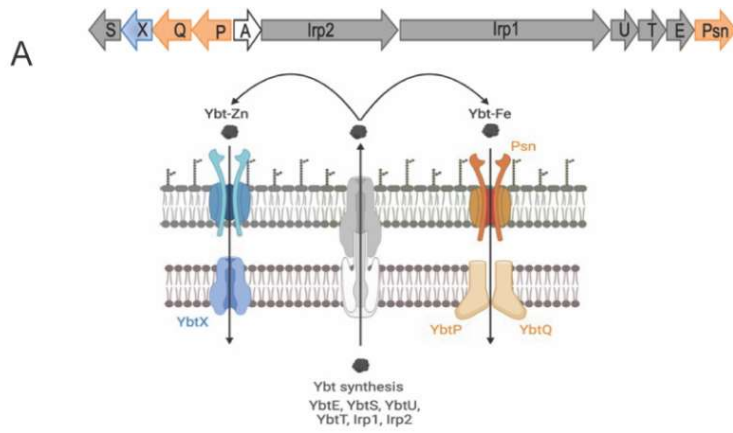
C

dTn-Seq can identify genes required for Ybt synthesis and transport.

Gene	Batch	Droplet	p-value	Description
y2395 (ybtX)	0.53	0.00	8.49E-02	Ybt-Zn importer
y2400 (irp1)	1.01	0.89	1.33E-05	Ybt biosynthesis
y2399 (irp2)	1.00	0.86	4.03E-05	Ybt biosynthesis
y2403 (ybtE)	0.98	0.79	1.48E-04	Ybt biosynthesis
y2401 (ybtT)	1.05	0.81	6.38E-02	Ybt biosynthesis

dTn-Seq can identify genes required for Ybt secretion.

Gene	Batch	Droplet	p-value	Description
y0704 (tolC)	1.01	0.86	4.84E-06	RND efflux (TolC protein)
y0703 (acrB)	1.00	0.88	1.87E-05	RND efflux (permease)

D
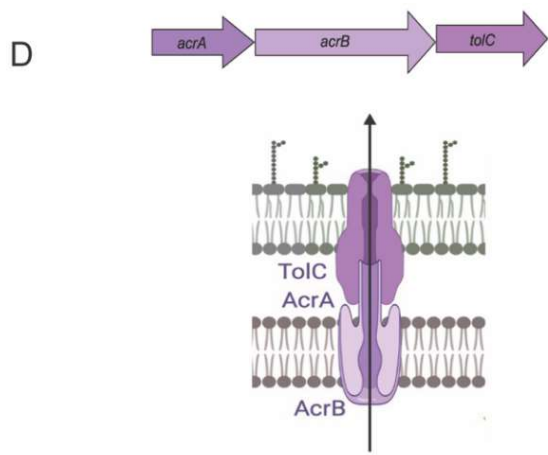
Figure 3-1. Ybt loci and droplet Tn-seq experimental design to identify Ybt secretion system.

(A) The Ybt operon contains genes for Ybt synthesis, import of Ybt bound to iron and import of Ybt bound to zinc. Synthesized Ybt is secreted through an unknown mechanism. (B) Experimental design for the dTn-seq experiment. The *Y. pestis* transposon mutant library was grown in batch culture and droplet culture in cPMH2 for 24 h. (C) Table of Ybt genes and genes in efflux systems identified as important for growth in metal limited conditions in the droplet environment by dTn-seq. (D) The AcrAB-TolC efflux system operon consists of three genes, *y0702* (*acrA*), *y0703* (*acrB*), and *y0704* (*tolC*). Schematic view of the AcrAB-TolC efflux system.

defects in batch culture (Fig. 3-1C). This was expected because these mutants do not express YbtX, and thus, are not able to import Zn even in the presence of Ybt (168, 197). In contrast, transposon insertions into the Ybt synthesis genes *irp1*, *irp2*, *ybtE*, or *ybtS* had no fitness defect in the batch culture, because despite not being able to synthesize Ybt, these mutants can still acquire Zn using Ybt synthesized from neighboring bacteria. However, in the droplets, both the import and synthesis mutants show significant fitness defects (Fig. 3-1C). These data validate that encapsulation of individual mutants prevents trans-complementation of Ybt between bacteria and support the use of dTn-seq to screen for genes involved in Ybt secretion.

<u>dTn-seq revealed that *y0703* and *y0704* are required for *Y. pestis* growth in zinc-limited medium.</u>

In total, 72 transposon mutants had statistically significant fitness phenotypes within the droplets (Table 3-1). We expect that mutations in the Ybt export system should have fitness phenotypes similar to the Ybt synthesis mutants - no fitness defect in the batch culture due to trans-complementation but a fitness defect in the droplets. From this list, two genes, *y0703* and *y0704* showed a fitness attenuation in the droplet and have homology to components of efflux pumps. Furthermore, closer analysis revealed that *y0703* and *y0704* are in an operon with *y0702,* and based on homology, are related to AcrAB-TolC efflux systems (Fig. 3-1D). Because similar efflux systems have been implicated in the export of siderophores in *Vibrio cholerae* and *E. coli* (183, 185), we prioritized our subsequent efforts to determine if these genes contribute to Ybt export in *Y. pestis*.

<u>*y0702-y0704* contributes to growth in metal limitation.</u>

To validate our dTn-seq data, we generated an in-frame deletion of the entire *y0702, y0703, and y0704* operon in the *Y. pestis* pCD1$^{(-)}$ *znuBC* background. The mutant was grown in Zn-limited cPMH2 and compared to a *znuBC* mutant. The *znuBC y0702-y0704* mutant was significantly attenuated for growth compared to the *znuBC* mutant (Fig. 3-2A; p = 0.01) but was not as attenuated as a *znuBC irp2* mutant, which cannot synthesize Ybt. Growth was restored to *znuBC* levels by genetically complementing back *y0702-y0704* into the native site on the chromosome (Fig. 3-2A) or by supplementation with excess Zn (Fig. 3-2B). Because Ybt is also involved in iron
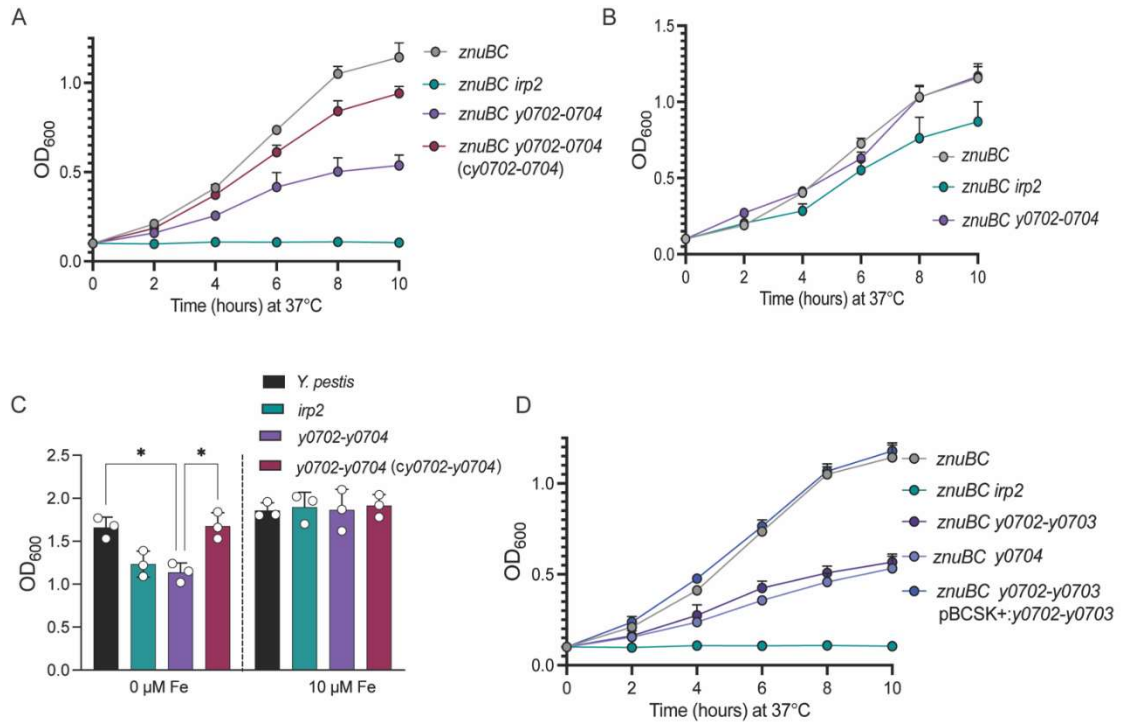
Figure 3-2. *y0702-y0704* contributes to growth during metal limitation.

The ability of *Y. pestis* KIM6+ *znuBC y0702-y0704* to grow in (A) zinc-limited medium (cPMH2) or (B) zinc-replete medium (cPMH2 + 10μM $ZnCl_2$). (C) OD_{600} of the *Y. pestis* KIM6+ *znuBC y0702-y0704* mutant at 24 h in iron-limited (cPMH2 + 0μM $FeCl_2$) or iron-replete (cPMH2 + 10μM $FeCl_2$) media. (D) The ability of *Y. pestis* KIM6+ *znuBC y0702-y0703* or *Y. pestis* KIM6+ *znuBC y0704* to grow in zinc-limited medium (cPMH2). For C, One-way ANOVA with Sidak's multiple comparison, *$p≤0.05$. Data represents the mean ±SD of three independent biological experiments. For some points, error bars are too small to visualize on the graph.

acquisition, we generated a *y0702-y0704* mutant in the *Y. pestis* pCD1[(-)] background to independently evaluate growth during iron limitation. Under these conditions the *y0702-y0704* mutant was significantly attenuated for growth in Fe limited conditions (Fig. 3-2C; p=0.0034) and had the same phenotype as the *irp2* mutant in both limited and excess Fe conditions. Together, these data support that the Y0702-Y0704 RND efflux system contributes to growth during both Zn and Fe limitation.

The *y0702-y0704* RND efflux system consists of an AcrAB inner membrane transporter (Y0702-Y0703) and TolC outer membrane transporter (Y0704) (Fig. 3-1D). To confirm that both components are required for growth under Zn limitation, single mutants were generated in each system in the *znuBC* background. Both mutants grew at the same rate as the *znuBC y0702-y0704* mutant, supporting that both components are required for growth under Zn limitation (Fig. 3-2D). However, due to the structure of the *y0702-y0704* operon (Fig. 3-1D), there was a chance that the deletion of *y0702-y0703* could have a polar effect on *y0704* and that only *y0704* was required. To eliminate this possibility, we trans-complemented the *znuBC y0702-y0703* mutant with *y0702-y0703* expressed on a plasmid. If there was a polar effect on *y0704*, then *y0702-y0703* expression from the plasmid would not be able to restore growth to the *znuBC* levels. However, genetic complementation on the plasmid was able to restore growth (Fig. 3-2D), demonstrating there was not a polar effect on *y0704* and that both the AcrAB and TolC components contribute to growth in metal-limited conditions.

<u>The Y0702-Y0704 efflux system is required for yersiniabactin secretion.</u>

Due to the decreased growth of a *znuBC y0702-y0704* mutant in Zn-limited media, we next tested if *y0702-y0704* is required for Ybt secretion. Since Ybt is secreted into the growth medium, strains secreting Ybt can trans-complement the growth of a *znuBC irp2* mutant during co-culture in metal-limited medium (279). Therefore, to determine if a *y0702-y0704* mutant secretes Ybt, we co-cultured a bioluminescent *znuBC irp2* mutant with either wild-type *Y. pestis*, an *irp2* mutant, or a *y0702-y0704* mutant and measured growth as a function of bioluminescence. If a strain secretes Ybt, then the *znuBC irp2* mutant will grow and bioluminescence will increase (Fig. 3-3A). As

expected, wild-type *Y. pestis* secretes enough Ybt to support the growth of the *znuBC irp2* mutant in Zn-limited medium (Fig. 3-3B). However, an *irp2* mutant, which cannot synthesize Ybt, did not support growth. Likewise, co-culture with the *y0702-y0704* mutant was unable to trans-complement the growth of the *znuBC irp2* mutant (Fig. 3-3B), supporting that the y0702-y0704 mutant is deficient in Ybt secretion. Complementation of the *y0702-y0704* system restored the ability of the strain to support growth of a *znuBC irp2* mutant (Fig. 3-3B).

Because Ybt binds to Zn (69), we can also indirectly measure Ybt levels in the bacterial supernatant by measuring Ybt competition of Zn-binding with 4-(2-pyridylazol)resorcinol (PAR) as previously described (284). PAR changes color when bound to Zn (absorbs light at 410 nm when unbound and 500 nm when bound to Zn), and therefore, the amount of free Zn within a sample can be measured by the change in the PAR absorbance. If a Zn-binding competitor is present, less Zn is available to bind to PAR, resulting in a decreased absorbance at 500 nm. For example, EDTA, a zinc chelator, can outcompete PAR for Zn binding, resulting in a significantly lower absorbance of PAR at 500 nm compared to PAR alone (Fig. 3-3C; $p<0.0001$). To test whether the supernatant from various *Y. pestis* strains could compete for Zn binding with PAR, bacteria were grown under metal-limited conditions and equal volumes of culture supernatant were harvested and filtered to remove bacteria. When compared to supernatant from wild-type *Y. pestis*, there was significantly higher PAR absorbance at 500nm in supernatants from the *irp2* and *y0702-y0704* mutants (Fig. 3-3C. $p<0.01$), further supporting that the *y0702-y0704* mutant is deficient in Ybt secretion.

Finally, to directly measure the amount of Ybt secreted by the *y0702-y0704* mutant, we used liquid chromatography mass spectrometry (LC-MS). Bacteria were grown in metal-limited medium for 8h, the OD_{600} of the cultures were measured (Fig. 3-3D), and Ybt was extracted with ethyl acetate from 10 OD_{600} equivalents of cell-free supernatant and analyzed by LC-MS as previously described (285) (Fig. 3-3E). Significantly less Ybt was present in the supernatant of the *y0702-y0704* mutant compared to wild-type *Y. pestis* (Fig. 3-3F; $p \leq 0.001$). However, there appeared to be residual Ybt detected in the supernatant of the *y0702-y0704* mutant above that of the *irp2* mutant (Fig. 3-3F). To determine if the *y0702-y0704* mutant was undergoing increased lysis due to Ybt
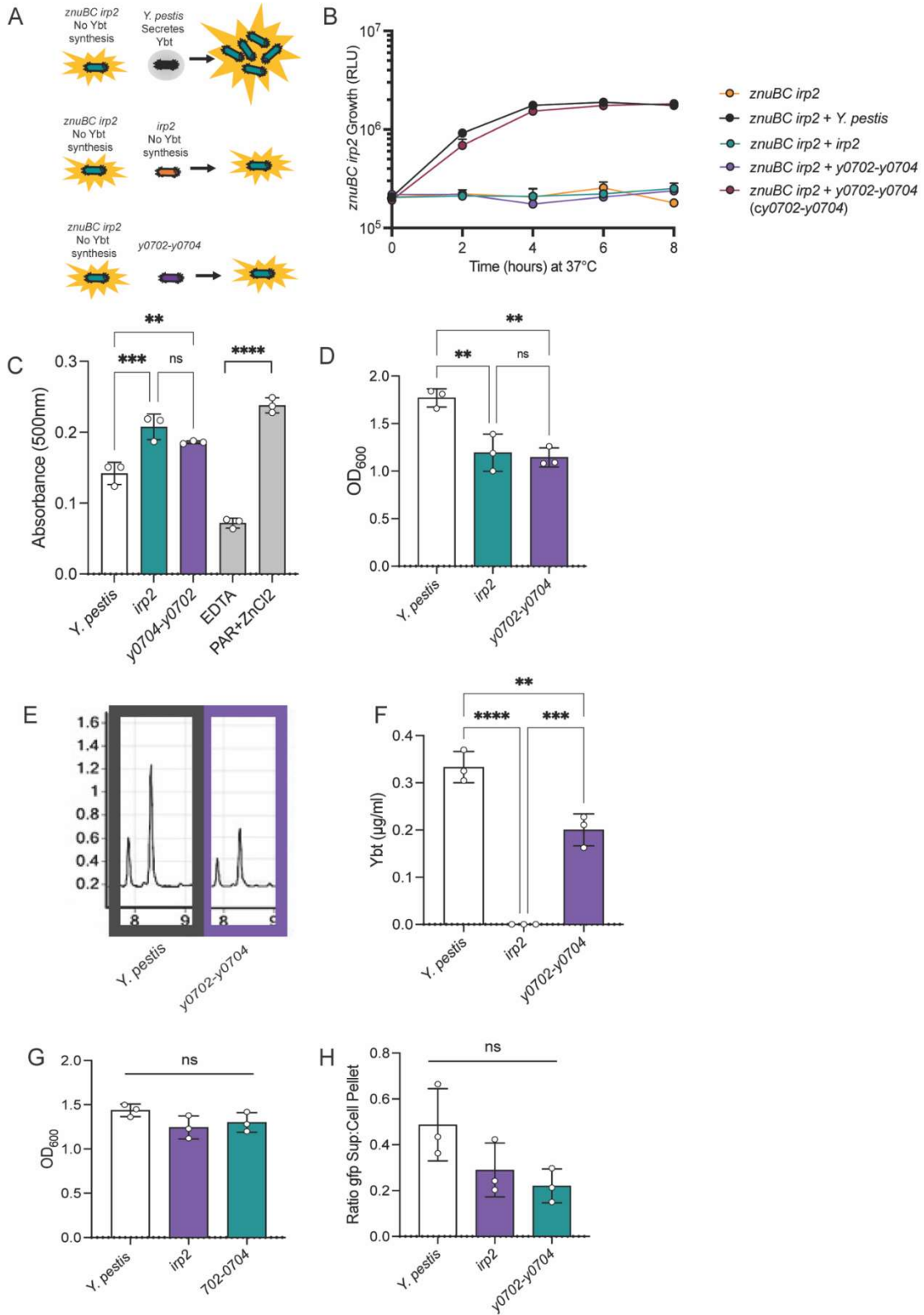
Figure 3-3. The AcrAB-TolC efflux system *y0702-y0704* is important for yersiniabactin secretion.

(A) Bioluminescent co-culture experimental design. (B) Growth of *znuBC irp2* pGEN*lux* in co-culture with another *Y. pestis* strain in chelex-treated PMH2 supplemented with 0.6μM $ZnCl_2$ at 37 ºC measured every 2 h for 10 h. Relative luminescent units (RLU) was plotted as the mean ±SD of three independent biological replicates. For some points, error bars are too small to visualize on the graph. (C) Absorbance at 500nm of PAR in the presence of *Y. pestis* supernatant. (D) Growth at 8 h in chelex-treated PMH2 supplemented with 0.6μM $ZnCl_2$ at 37 ºC. (E) LC-MS spectra of the two peaks of Ybt in the supernatant of *Y. pestis*. (F) Concentration of Ybt in the supernatant of *Y. pestis* quantified by LC-MS. (G) Growth of strains expressing GFP at 8 h in chelex-treated PMH2 supplemented with 0.6μM $ZnCl_2$ at 37 ºC. (H) Quantification of GFP protein in supernatant and cell lysates of *Y. pestis* strains. One-way ANOVA with Tukey test, **$p \leq 0.01$, ***$p \leq 0.001$, and***$p \leq 0.0001$. Mean ±SD of three independent biological replicates.

toxicity, which could result in release of Ybt, we transformed wild-type *Y. pestis* and a *y0702-y0704* mutant with a plasmid expressing GFP and measured the concentration of GFP in the culture supernatants by western blot. We observed no difference in the amounts of GFP between the supernatants (Fig. 3-3G and 3-3H), supporting that lysis of the *y0702-y0704* mutant did not occur at a higher rate than seen in wild-type bacteria. However, these data do not eliminate the possibility that the residual Ybt in the medium is not a result of release from normal bacterial lysis. Together, these data demonstrate that the *y0702-y0704* mutant is deficient in Ybt secretion and support that the Y0702-Y0703 RND efflux system contributes to Ybt export.

<u>The Y0702-Y0704 AcrAB-TolC efflux system is required for *Y. pestis* virulence.</u>

Ybt is required for Fe acquisition and contributes to the ability of *Y. pestis* to compete for Zn with the host protein calprotectin, and is thus essential for the development of lethal bubonic and pneumonic plague (64, 278). If the Y0702-Y0704 AcrAB-TolC system exports Ybt, then we expect it to be required for competition for metals with calprotectin and virulence. To determine if Y0702-Y0704 contributes to fitness in the presence of calprotectin, the concentration of calprotectin to inhibit 50% bacterial growth (IC_{50}) was determined for *Y. pestis*, *irp2*, *znuBC irp2*, or *znuBC y0702-y0704*. The IC_{50} of calprotectin was significantly lower for the *znuBC y0702-y0704* mutant compared to *Y. pestis* (Fig. 3-4A; $p \leq 0.01$), demonstrating that the mutant is less fit in the presence of metal restriction by calprotectin. Genetic complementation with *y0702-y0704* restored the ability of the mutant to grow in the presence of calprotectin. To determine if *y0702-y0704* is required for *Y. pestis* virulence, mice were infected with *Y. pestis* strains via either subcutaneous injection or intranasal instillation to mimic bubonic and pneumonic plague, respectively. As expected, all mice succumbed to infection with wild-type *Y. pestis* or the *znuBC* mutant but survived infection with the *znuBC irp2* mutant (Fig. 3-4B and 3-4C). Mice infected with the *znuBC y0702-y0704* mutant were more resistant to lethal infection, with a 50% survival rate in the bubonic plague model (Fig. 3-4B; $p \leq 0.001$) and 20% survival rate in the pneumonic model (Fig. 3-4C; $p \leq 0.0001$). Moreover, there was a significant delay in the mean time to death in the pneumonic plague model for the *znuBC y0702-y0704* infected mice (3.75 days) compared to those infected with wild-type or (2.5 days;

A

B

C

D

E

Time (hours): 12 24 36 48 60 72 84
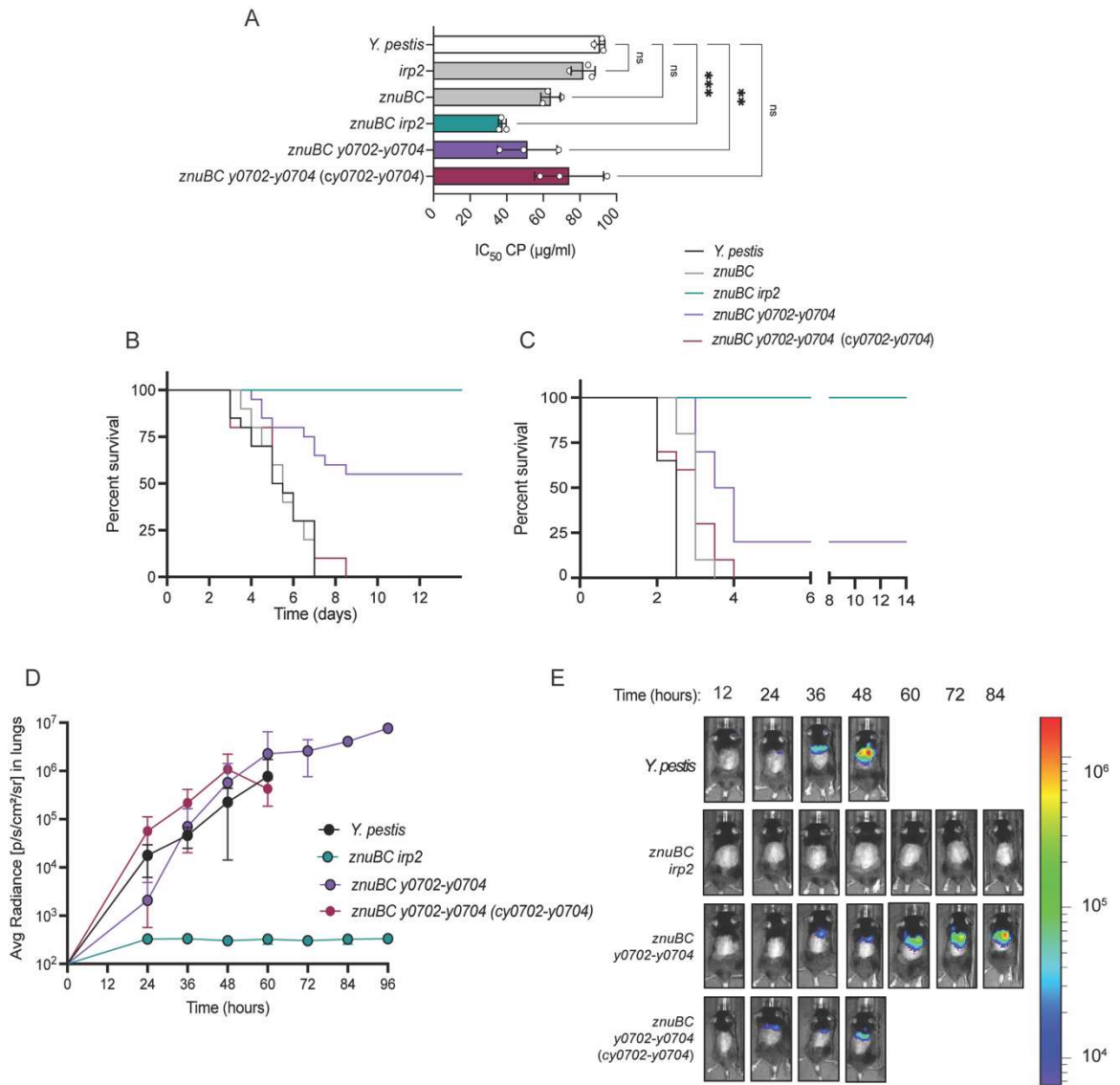
Figure 3-4. The AcrAB-TolC efflux system *y0702-y0704* contributes to *Y. pestis* virulence during plague.

(A) IC50 of calprotectin when incubated with *Y. pestis* strains. Each point represents the mean IC50 of a biologically independent experiment (n=3) and the bar represents the mean of the three independent experiments. One-way ANOVA with Tukey's comparison: ns= not significant, **$p<0.01$, ***$p=0.001$, and ****$p<0.0001$. (B) C57BL/6J mice were challenged subcutaneously with an inoculum of 10^2 CFU *Y. pestis* (WT; black), *znuBC* mutant (gray), *znuBC irp2* mutant (teal), *znuBC y0702-y0704* mutant (purple), and *znuBC y0702-y0704* (c*y0702-y0704*) (pink) and monitored every 12 h or the development of moribund disease for 14 days. (C) C57BL/6J mice were challenged intranasally with an inoculum of 10^4 CFU *Y. pestis* (WT; black), *znuBC* mutant (gray), *znuBC irp2* mutant (teal), *znuBC y0702-y0704* mutant (purple), and *znuBC y0702-y0704* (c*y0702-y0704*) (pink) and monitored every 12 h or the development of moribund disease for 14 days. (D) Bioluminescence measured every 12 h in the lungs of mice infected via pneumonic challenge with an inoculum of 10^4 CFU. Dashed line represents background relative luminescent units (RLU). (E) A representative mouse showing dissemination by bioluminescence after pneumonic challenge. Scale shows average radiance. Survival statistics were calculated by log rank test. For B, *znuBC y0702-y0704* vs. WT or *znuBC*, ***$p<0.001$. For C, *znuBC y0702-y0704* vs. WT, ****$p<0.0001$ and *znuBC y0702-y0704* vs. *znuBC*, **$p=0.0022$. Results are combined data from 2 independent experiments (n=10 total).

p≤0.0001) or the *znuBC* mutant (3 days; p=0.0022). Genetic complementation with *y0702-y0704* restored virulence in both models (Fig. 3-4B and 3-4C). Together, these data show that *y0702-y0704* contribute to virulence during bubonic and pneumonic plague.

Previous studies have shown that *Y. pestis* is unable to synthesize Ybt administered intranasally and does not proliferate within the lungs; however, a Ybt synthesis mutant can cause lethal infection via dissemination to the blood where metal availability is greater (63). Therefore, we next investigated whether the *znuBC y0702-y0704* mutant was defective in lung proliferation during pneumonic plague using a bioluminescent reporter and optical imaging to monitor *znuBC y0702-y0704* proliferation during infection (245). Similar to the wild-type *Y. pestis*, the *znuBC y0702-y0704* mutant was able to replicate efficiently in the lungs of mice that developed lethal disease (Fig. 3-4D and 3-4E), indicating that mice that succumbed to infection were developing pneumonic plague.

<u>Other AcrAB systems in *Y. pestis* do not contribute to yersiniabactin secretion.</u>

These data support that the Y0702-Y0704 AcrAB-TolC efflux system exports Ybt in *Y. pestis*, but the residual Ybt in culture supernatants and increased virulence of the *znuBC y0702-0704* mutant compared to the *znuBC irp2* mutant also indicates the presence of a secondary system for Ybt export. Genome analysis revealed *Y. pestis* has three other AcrAB systems, *y1049-1050, y3760-3759, and y3392-3393* (286). To determine if these systems are capable to export Ybt, we generated in-frame deletions in all three AcrAB transporters in the *znuBC* or *znuBC y0702-0704* backgrounds and determined the growth of the mutants in a Zn-limited medium. Deletion of all three AcrAB systems had no significant impact on the growth of either background (Fig. 3-5), indicating that Y0702-Y0703 is the only AcrAB efflux system capably of exporting Ybt in *Y. pestis*.

DISCUSSION

Thirty years after the first reports of Ybt as a siderophore produced by *Y. enterocolitica* (161), we have finally identified an AcrAB-TolC efflux system as the primary Ybt export mechanism in *Y. pestis*. We were able to accomplish this through the application of dTn-seq, which is uniquely suited to screen for mutations in secretion systems or factors that cannot be investigated with conventional
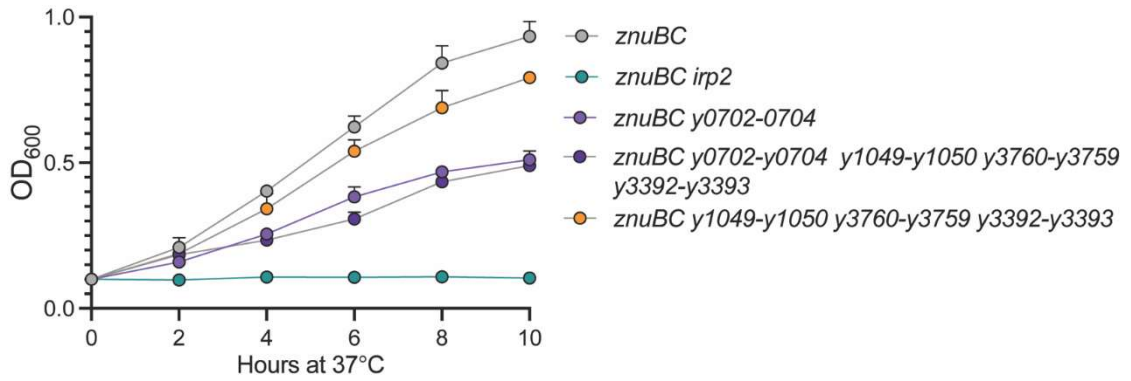
Figure 3-5. Other AcrAB transporters in *Y. pestis* do not contribute to yersiniabactin secretion.

Growth of other AcrAB transporter mutants in metal-depleted defined medium (chelex-treated PMH2) supplemented with 0.6µM $ZnCl_2$ at 37 ºC measured every 2 h for 10 h. Optical density at 600 nm (OD_{600}) was plotted as the mean ±SD of three independent biological replicates. For some points, error bars are too small to visualize on the graph.

Tn-seq approaches that suffer from trans-complementation hurdles. The successful application of dTn-seq in the identification of the Y0702-Y0704 Ybt export system establishes the utility of this system to be used by others to identify export systems or secreted factors produced by a variety of bacteria. However, some considerations need to be made when establishing the experimental design for dTn-seq. First, care needs to be taken to ensure a high frequency of the droplets produced contain single bacteria. This frequency can be influenced by the aggregative nature of the bacteria, the concentration of the culture used during the droplet formation, and the flow rate of the microfluidics system. Even under the best optimized parameters, a certain population of droplets will contain more than one bacterium, which can diminish absolute fitness phenotypes in mutants that can cheat. This is likely the reason that we still recovered some Ybt biosynthesis mutants in the droplets in our screen (Fig. 3-1C). However, despite these artifacts, the fitness defects of these mutants and *y0703* and *y0704* still rose to the top of our list of statistically significant hits, demonstrating that even these limitations can be overcome by the application of proper selective conditions and screen optimization. Second, the need to maximize single bacteria encapsulation will also influence the size of the libraries that can be generated by dTn-seq. While conventional Tn-seq often employs large transposon libraries (approaching 10^6 mutants or greater) to ensure genome saturation, current microfluidics technology needed to provide an appropriate frequency of droplets with individual bacteria limits individual libraries to approximately $5\text{-}7\times10^4$ mutants. Again, even at this library size, which represents approximately 10-fold coverage for *Y. pestis*, we were able to successfully identify *y0703* and *y0704*, but increasing the library size should improve confidence that all potential hits are represented in the screening process. While size of the individual pool cannot currently be increased, an alternative approach is to repeat the screen with multiple pools. Finally, the microenvironment of the droplet can affect bacteria differently than similar large volume culture conditions. Therefore, optimization of growth conditions in the droplets needs to be performed for each bacterial species prior to performing screens and may need to be further optimized if medium or selective conditions are changed. Despite these limitations, dTn-seq still represents a powerful new technique to identify secreted factors or systems that cannot be identified by conventional transposon mutagenesis strategies.

These studies demonstrated that the Y0702-Y0704 AcrAB-TolC efflux pump is required for growth in metal-limited media and Ybt secretion by *Y. pestis.* However, the *znuBC y0702-y0704* mutant was not as attenuated as the *znuBC irp2* mutant in Zn-limited medium and we were still able to recover Ybt from the *y0702-y0704* mutant cultures. While these concentrations were not sufficient for optimal growth during metal limitation or to trans-complement the growth of a *znuBC irp2* mutant in co-culture, it does indicate that some amount of extracellular Ybt is available for the bacteria. One possible source of Ybt in *y0702-0704* cultures could be Ybt released from dying bacteria. In *E. coli* and *V. cholerae*, inhibition of siderophore efflux leads to growth restriction, envelope stress, and induction of the Cpx stress response system but increased cell lysis was not reported (183, 287). It is likely that inhibition of Ybt secretion under conditions of increased Ybt synthesis (e.g., during metal limitation) would induce similar stresses in *Y. pestis* as the metallophore accumulates and sequesters metals within the bacterial cytoplasm. However, we tried to indirectly compare bacterial lysis between a *y0702-y0704* mutant and wild type *Y. pestis* by measuring the release of cytoplasmic expressed GFP but did not observe increased concentrations that would indicate elevated bacterial lysis of the mutant (Fig. 3-4). While this does not rule out the possibility that normal rates of bacterial death could be responsible for the residual Ybt recovered in *in vitro* culture, the *znuBC y0702-y0704* mutant is still partially virulent in the animal model, where bacterial lysis seems less likely to be sufficient to sustain bacterial colonization of a small population of bacteria. Therefore, it seems more likely that a secondary export system is responsible for the residual extracellular Ybt sufficient to support the intermediate virulence in the mouse model. We also eliminated the possibility that the secondary system is one of the other AcrAB homologs within the *Y. pestis* genome (*y1049-1050, y3760-3759, or y3392-3393)* but other RND efflux family members have been implicated in the efflux of other siderophores in *E. coli* and *Pseudomonas putida* (182, 185), and multiple RND efflux homologs and two additional TolC homologs are present in the *Y. pestis* genome that are viable candidates for a secondary system (286). Importantly, while none of these genes had fitness defects in the dTn-seq screen, this is likely because the Y0702-Y0704 system is the primary export system and masked any fitness defects in other systems. Moving forward, we will continue to search for this secondary export system by specifically targeting

these other RND/TolC homologs for inactivation or performing a second round of dTn-seq screening in the *znuBC y0702-y0704* mutant background.

The Ybt operon is not only found in the pathogenic *Yersinia* species but also in more clinically prevalent clinical isolates of *E. coli*, *K. pneumoniae, P. mirabilis,* and *S. enterica* serovars (164–167, 280). Our discovery that an AcrAB-TolC system is the primary exporter of Ybt in *Yersinia* and data from other laboratories showing RND efflux systems contribute to siderophore efflux (183, 185), strongly indicate that AcrAB-TolC efflux systems are the primary mechanisms for the export of Ybt in these other species. Because Ybt provides an important virulence advantage for these pathogens (164, 167, 235, 252, 288), a conserved export system makes for an attractive broad spectrum anti-virulence drug target, especially since many of these bacteria are also rapidly developing resistance to conventual antibiotics. Importantly, AcrAB and other RND efflux systems are also effective mediators of antibiotic resistance (289–294) and have previously been targeted to develop drugs that inhibit antibiotic efflux and increase the efficacy of current antibiotics (295–300). Thus, there are already several classes of drugs developed as antibiotic efflux inhibitors that might be repurposed as anti-virulence drugs that can be used as adjunct therapy to improve outcomes in the clinic for infections by bacteria that use Ybt to acquire metals. We are currently investigating the efficacy of different classes of RND efflux inhibitors on Ybt secretion.

In conclusion, using dTn-seq in *Y. pestis*, we have identified the AcrAB-TolC RND efflux pump Y0702-Y0704 as the primary secretion mechanism for Ybt. This successful utilization of dTn-seq brings a new technique to the field to identify unknown secreted factors in bacteria. Importantly, these data support previous studies that implicate efflux pumps as important metallophore export for other bacteria (182, 183, 185) and suggest a larger role for these pumps in bacterial pathogenesis and as potential drug targets.

METHODS

Ethics statement

C57BL/6J mice were purchased from The Jackson Laboratory and bred within the barrier facility at the Clinical and Translational Research Building at the University of Louisville. Groups contained both male and female mice and we observed no differences in outcomes based on sex during these studies. Animals were housed in accordance with NIH guidelines and all procedures were approved by the University of Louisville IACUC. Three days prior to challenge with *Y. pestis*, animals were transferred to the University of Louisville's Center for Predictive Medicine Regional Biocontainment Laboratory ABSL-3 facilities for acclimation. After infection, mice were observed for up to 14 days for the development of moribund disease and humanely euthanized if they met predefined endpoints.

Bacterial strains

The bacterial strains used in this study are listed in Table 3-2. *Y. pestis* was routinely grown in Difco brain heart infusion (BHI) broth (BD Biosciences) or under metal-deplete conditions in chelex-treated PMH2 supplemented with 1.0 μM $FeCl_2$, 1.0 mM $MgCl_2$, and 0.6 μM $ZnCl_2$ (cPMH2) (148). For metal-replete experiments, cPMH2 was supplemented with either 10 μM $ZnCl_2$ or 10 μM $FeCl_2$ as needed. Strains transformed with the pGEN-*luxCDABE* plasmid (245) were grown with carbenicillin (50 μg/ml) prior to co-culture. For infection, bacteria were grown overnight at 26 °C in BHI broth prior to subcutaneous challenge for the bubonic plague model. Prior to intranasal instillation, *Y. pestis* was diluted to 0.05 OD_{600} in BHI broth with 2.5 mM $CaCl_2$ and grown at 37 °C with aeration for 16 to 18 h (245). Bacterial concentrations were determined using a spectrophotometer and diluted to desired concentrations in 1x PBS for mouse infections. Concentrations of bacterial inoculums for mouse studies were confirmed by serial dilution and enumeration on agar plates.

Generation of transposon mutant library and site directed mutants

A transposon mutant library was generated in *Y. pestis* KIM6+ *znuBC* with the transposon delivery vector pSAM-DKm encoding the *mariner*-family transposon, *Himar1* C9 transposase, as previously described (283). Briefly, *Y. pestis* was transformed with pSAM-DKm by conjugation and transposon mutants were selected for on BHI agar plates with 50 mg/ml kanamycin and 2 mg/ml

irgasan and grown at 26 °C for two days. Colonies were enumerated and combined from multiple plates to generate a library containing approximately 50,000 mutants. The library was cryopreserved after growing in BHI broth with 50 mg/ml kanamycin, 2 mg/ml irgasan, and 1 μM $ZnCl_2$ shaking at 26 °C for two days. Random distribution of transposon insertions was confirmed by selecting 20 colonies before cryopreservation and comparing PCR products generated using nested PCR with transposon specific and random primers (283). Site specific and complemented mutants were generated using pSR47s and homologous recombination as previously described (301, 302). For trans-complementation, *y0702-y0703* was ligated into pBC-SK+, as previously described (303). Deletions were confirmed by PCR and sequencing.

Microfluidic device production for dTn-seq

Microfluidic devices were produced following the protocol described by Thibault *et al*. (2019) (282). Briefly, a microfluidic device mask with a single aqueous inlet and a 40 × 40 μm channel at the flow-focus junction was designed using AutoCad 2016 software. Glass photomasks were ordered from CAD/Art Services, Inc. (Bandon, OR). These masks were used to generate silicon molds by soft lithography that were used for the final microfluidic fabrication using polydimethylsiloxane (PDMS). The silicon mold and final microfluidic chip fabrication (including PDMS-glass plasma bonding) were performed at the Integrated Sciences Cleanroom and Nanofabrication Facility at Boston College.

Droplet production and culturing in droplets

The agarose droplets were produced following the protocol described by Thibault *et al*. (2019) (282). Briefly, 1% Seaplaque agarose (Lonza – 50101) was heated until dissolved in cPMH2 (148). The agarose solution was filtered (0.45 μm) and incubated at 37 °C. Transposon libraries were added at a suspension of 7.2×10^6 cell/ml and thoroughly vortexed. Syringe pump systems were incubated in a 37 °C for 2 h to prewarm them prior to droplet production. For oil and aqueous phases, a syringe pump rate of 500 μl/h was used, and the droplets were collected at 30 min. Before culturing, agarose droplets were gelled at 4 °C for 12 min with occasional shaking.

<u>Sample preparation, sequencing, and fitness calculations</u>

Genomic DNA (gDNA) was extracted from *Y. pestis* using the DNeasy Blood & Tissue Kit according to the manufacturer's guidelines (Qiagen). Illumina DNA sample preparation for Tn-Seq was performed as previously described (282). For cleanup, droplet DNA was cleaned using 10 µl of magnetic beads mixed with 20 µl PEG solution per sample followed by elution in 14.3 µl of dH_2O. Batch samples were cleaned and precipitated with phenol/chloroform method and resuspend in 26 µl H_2O. The ligation of DNA adapter barcodes was performed using T4 DNA ligase (NEB M0202L). The mix was combined with 13.12 µl DNA (droplet DNA) or 25 (batch DNA) to 1 µl of 1:5 diluted adapter, 1× T4 DNA Ligase Reaction Buffer, and 400 units T4 DNA ligase, followed by incubation at 16 °C for 16 h, 65 °C for 10 min, and held at 10 °C. In the droplet DNA sample, 10 µl magnetic beads were mixed with 20 µl PEG solution followed by elution in 36 µl of dH2O. Batch sample was used directly. Ligated DNA was PCR amplified using Q5 high-fidelity DNA polymerase (NEB – M0491L) using 34 µl of DNA (droplet DNA) or 1 µl of ligation mix added to 1X Q5 reaction buffer, 10 mM dNTPs, 0.45 µM of each primer (P1-M6-GAT-MmeI; P2-ADPT-Tnseq-primer), and one unit Q5 DNA polymerase (282). The samples were incubated at 98 °C for 30 s, then followed by 21 cycles of 98 °C for 10 s, 62 °C for 30 s, 72 °C for 15 s, followed by 72 °C for 2 min, and hold at 10 °C. According to the manufacturer's protocol, PCR products were gel purified and sequenced on an Illumina NextSeq 500. Sequence analysis was performed as previously described (281, 282, 304, 305).

<u>PAR Assay</u>

To test for competition for zinc binding with 4-(2-pyridylazo)resorcinol (PAR), bacteria were grown at 26 °C in BHI broth for 15 h, diluted to 0.1 OD_{600} in cPMH2, and grown with aeration at 37°C for 8 h. Each culture was passaged once more in cPMH2 for 15 h at 37°C. Cell free supernatant was isolated by filtration through a 0.02 µM filter to remove *Y. pestis* and incubated with 50 µM $ZnCl_2$ for 15 min. PAR was added at 200 µM and incubated for 5 min. Absorbance was read on a Biotek Synergy HT plate reader using a spectral read from 350-550 nm.

<u>Co-culture trans-complementation to measure rescue of *Y. pestis znuBC irp2* growth</u>

Bacteria were grown at 26 °C in BHI broth for 15 h, diluted to 0.1 OD_{600} in cPMH2, and grown with aeration at 37°C for 8 h. Each culture was passaged once more in cPMH2 for 15 h at 37 °C. Bacteria were resuspended into fresh cPMH2 at a final concentration of $1x10^6$ CFU/ml. 100 μL of *Y. pestis znuBC irp2* carrying the pGEN-*luxCDABE* bioluminescent reporter were aliquoted in to each well of a white 96-well plate (Greiner Bio-One). 100 μl of *Y. pestis*, *irp2*, or *y0702-y0704* were added to individual wells (n=3) and the plates were incubated at 37 °C. Growth of *Y. pestis znuBC irp2* as a function of increased bioluminescence was measured every 2 h for 8 h using a Biotek Synergy HT plate reader (0.5 s read, sensitivity of 135) as previously described (245).

Measurement of Ybt concentrations by LC/MS

Bacteria were grown at 26 °C in BHI broth for 15 h, diluted to 0.1 OD_{600} in cPMH2, and grown with aeration at 37°C for 8 h. Each culture was passaged once more in cPMH2 for 15 h at 37 °C. Bacteria were diluted to 0.1 OD_{600} in cPMH2 and grown for 8 h at 37 °C. 10 ml of cell-free supernatants were collected by centrifugation and filtration and mixed at a 1:1 ratio with ethyl acetate for extraction as previously described (285). The extract was dissolved in methanol and diluted in water for HPLC analysis as previously described (285).

Cell Lysis Measurement

Y. pestis strains expressing pGEN222gfp were grown at 26 °C in BHI broth for 15 h. Bacteria were diluted to 0.1 OD_{600} in cPMH2 and grown at 37 °C for 8 h. The culture was passaged once more in cPMH2 and grown for 15 h at 37 °C. 4 OD_{600} equivalents of cell pellets and cell free supernatants were collected. For supernatants, proteins were concentrated by trichloroacetic acid (TCA) precipitation (10% final concentration). Samples were incubated for 20 min on ice and proteins were pelleted at 13,000 RPM for 10 min. The proteins were washed with acetone, pelleted at 13,000 RPM for 2 min, and dried prior to resuspending directly in loading buffer. GFP was detected by slot blot using an anti-GFP antibody (Sigma No. G1544; 1:5,000).

Determination of calprotectin inhibitory concentrations

Recombinant forms of calprotectin were produced in *E. coli* and purified as previously described (102, 228). To determine the concentrations of calprotectin to inhibit 50% growth of *Y. pestis*, bacteria were incubated with increasing concentrations of calprotectin and bacterial growth was determined as previously described (278).

Animal infections with *Y. pestis*

Mice were challenged with *Y. pestis* as previously described (261, 262, 306). For intranasal challenge, mice were anesthetized with ketamine/xylazene and administered 20 µl of bacteria suspended in 1X PBS to the left nare. For subcutaneous challenge, mice were anesthetized with isoflurane and administered 20 µl of bacteria suspended in 1x PBS via subcutaneous injection at the base of the tail. Infected mice were monitored for the development of disease symptoms twice daily for 14 days. Moribund animals meeting predefined endpoint criteria were humanely euthanized by CO_2 asphyxiation and scored as succumbing to infection 12 h later.

Statistics

All *in vitro* experiments were repeated three times and data are shown as the means ± standard deviations (SDs) from the three independent experiments, unless otherwise noted. Animal experiments were repeated twice to confirm reproducibility and the data is represented as the combination of the two independent experiments. *P* values were calculated using Student's *t* test, one-way analysis of variance (ANOVA), or two-way ANOVA with appropriate posthoc testing as indicated. All statistics were completed using GraphPad Prism software.

Drs. Oleg Tsodikov, Juan Ortiz-Marquez, and Noemi Bujan Gomez for critical feedback and discussions of data. Finally, I would like to thank Dr. Ralph Isberg for discussions and introductions that lead to this collaboration between the Lawrenz and van Opijnen labs.

Table 3-1. Genes with significant difference in fitness between batch and droplet.

Protein	Fitness Batch	Fitness Droplet	Gene	Function	P-value
WP_071882759.1	1.01	0.89	-	LysM peptidoglycan-binding domain-containing protein	2.16E-16
WP_002231925.1	1.03	0.90	y0410 (zntA)	zinc/cadmium/mercury/lead-transporting ATPase	1.88E-12
WP_002210857.1	1.01	0.87	y1858	fimbrial biogenesis outer membrane usher protein	4.83E-11
WP_002214945.1	1.02	0.92	-	filamentous hemagglutinin N-terminal domain-containing protein	2.02E-09
WP_002211252.1	1.01	0.82	y2306	MULTISPECIES: alpha/beta hydrolase	1.35E-08
WP_002212885.1	**0.98**	**0.59**	**y2404 (psn)**	**MULTISPECIES: TonB-dependent siderophore receptor**	**1.84E-08**
WP_002209711.1	0.78	0.28	-	MULTISPECIES: chorismate synthase	3.62E-06
WP_002209121.1	0.98	0.86	dipZ	thiol:disulfide interchange protein DsbD	4.16E-06
WP_002214742.1	1.02	0.89	y3669	MULTISPECIES: type VI secretion system ATPase TssH	4.79E-06
WP_002209268.1	**1.01**	**0.86**	**y0704 (tolC)**	**TolC family protein**	**4.84E-06**
WP_002227857.1	1.00	0.90	-	phosphate ABC transporter permease	1.29E-05
WP_002212777.1	**1.01**	**0.89**	**y2400 (irp1)**	**MULTISPECIES: yersiniabactin polyketide synthase HMWP1**	**1.33E-05**
WP_002209267.1	**1.00**	**0.88**	**y0703 (acrB)**	**MULTISPECIES: multidrug efflux RND transporter permease subunit**	**1.87E-05**
WP_002209491.1	1.05	0.91	-	phosphoenolpyruvate carboxylase	2.06E-05
WP_002210856.1	1.02	0.89	y1859	MULTISPECIES: molecular chaperone	2.97E-05
WP_002212775.1	**1.00**	**0.86**	**y2399 (irp2)**	**MULTISPECIES: yersiniabactin non-ribosomal peptide synthetase HMWP2**	**4.03E-05**
WP_002208911.1	0.96	0.71	y3919	MULTISPECIES: redox-regulated molecular chaperone Hsp33	4.23E-05
WP_002215759.1	1.03	0.92	-	maltoporin	5.19E-05
WP_002211559.1	1.03	0.88	-	hypothetical protein	5.87E-05
WP_002208981.1	1.01	0.86	-	L-threonine 3-dehydrogenase	6.32E-05

WP_002211844.1	0.93	0.72	-	metal ABC transporter permease	1.00E-04
WP_002209138.1	1.02	0.76	-	MULTISPECIES: hypothetical protein	1.21E-04
WP_001088826.1	**0.98**	**0.79**	**y2403 (ybtE)**	**MULTISPECIES: yersiniabactin biosynthesis salycil-AMP ligase YbtE**	**1.48E-04**
WP_002361295.1	1.01	0.89	-	two-component sensor histidine kinase	1.75E-04
WP_002210924.1	0.86	0.65	-	transcription-repair coupling factor	1.80E-04
WP_002430108.1	0.96	0.57	-	hypothetical protein	2.15E-04
WP_002209795.1	1.01	0.89	-	MULTISPECIES: MFS transporter	2.21E-04
WP_002210228.1	1.01	0.82	y1683	MULTISPECIES: cation diffusion facilitator family transporter	3.07E-04
WP_002210231.1	1.05	0.87	-	MULTISPECIES: N-acetyltransferase	3.26E-04
WP_002211845.1	0.97	0.74	-	MULTISPECIES: metal ABC transporter permease	3.51E-04
WP_002209278.1	1.01	0.86	-	MULTISPECIES: sugar ABC transporter permease	5.88E-04
WP_002212016.1	1.03	0.92	-	MULTISPECIES: acetolactate synthase 2 small subunit	5.97E-04
WP_002209471.1	1.03	0.90	-	peptidoglycan editing factor PgeF	7.76E-04
WP_002216613.1	0.97	0.80	y1861	MULTISPECIES: spore coat U domain-containing protein	7.85E-04
WP_002209358.1	1.01	0.90	-	bifunctional glycosyl transferase/transpeptidase	8.50E-04
WP_002211556.1	1.02	0.85	-	MULTISPECIES: two-component system response regulator GlrR	9.52E-04
WP_002227896.1	0.95	0.81	y1897 (yfeA)	MULTISPECIES: metal ABC transporter substrate-binding protein	9.55E-04
WP_002209701.1	0.48	0.09	-	MULTISPECIES: phospholipid-binding lipoprotein MlaA	9.97E-04
WP_002215144.1	0.96	0.76	y3281	MULTISPECIES: membrane protein	3.56E-03
WP_002213192.1	1.03	0.81	-	gfo/Idh/MocA family oxidoreductase	5.83E-03
WP_002209833.1	1.04	0.82	hscB	MULTISPECIES: co-chaperone protein HscB	6.56E-03
WP_002208976.1	0.81	0.58	-	MULTISPECIES: protein-export protein SecB	8.94E-03
WP_002209272.1	1.05	0.81	y0707	MULTISPECIES: SCP2 domain-containing protein	9.45E-03

WP_002215049.1	1.00	0.44	y0544 (hemP)	MULTISPECIES: hemin uptake protein HemP	1.11E-02
WP_002210747.1	1.00	0.59	YPO1134	phosphate starvation-inducible protein PsiF	1.16E-02
WP_002210935.1	0.95	0.57	fabG	MULTISPECIES: 3-oxoacyl-ACP reductase FabG	1.17E-02
WP_002210121.1	0.55	0.00	-	MULTISPECIES: phospholipid ABC transporter ATP-binding protein MlaF	1.44E-02
WP_002214710.1	1.04	0.70	y2716	MULTISPECIES: hypothetical protein	1.80E-02
WP_002208509.1	0.54	0.15	-	sulfate/thiosulfate import ATP-binding protein CysA	1.95E-02
WP_002210093.1	0.96	0.65	y0179 (aaeX)	MULTISPECIES: DUF1656 domain-containing protein	2.47E-02
WP_002228074.1	0.94	0.57	YPO0788	MULTISPECIES: hypothetical protein	3.51E-02
WP_002210918.1	0.70	0.43	y1793 (phoQ)	MULTISPECIES: two-component system sensor histidine kinase PhoQ	3.75E-02
WP_002228199.1	1.03	0.73	YPO3540	hypothetical protein	3.89E-02
WP_002228136.1	0.93	0.55	YPO0205 (bfd)	MULTISPECIES: bacterioferritin-associated ferredoxin	4.96E-02
WP_002210145.1	0.47	0.81	-	osmotically-inducible protein OsmY	5.82E-02
WP_002212799.1	**1.05**	**0.81**	**y2401 (ybtT)**	**MULTISPECIES: yersiniabactin biosynthesis thioesterase YbtT**	**6.38E-02**
WP_002208738.1	1.05	0.73	y0929	MULTISPECIES: oxalurate catabolism protein HpxX	6.47E-02
WP_002208887.1	0.93	0.61	y3944 (nirD)	MULTISPECIES: nitrite reductase small subunit NirD	6.89E-02
WP_002210135.1	0.79	0.36	sspA	MULTISPECIES: stringent starvation protein A	7.05E-02
WP_002228733.1	1.00	0.70	-	MULTISPECIES: hypothetical protein	7.91E-02
WP_002210938.1	1.04	0.75	-	MULTISPECIES: hypothetical protein	8.03E-02
WP_001286280.1	**0.53**	**0.00**	**y2395 (ybtX)**	**MULTISPECIES: yersiniabactin-associated zinc MFS transporter YbtX**	**8.49E-02**
WP_002208599.1	0.90	0.64	y1066 (hemH)	MULTISPECIES: ferrochelatase	8.61E-02
WP_000140406.1	**0.63**	**0.00**	**y2398 (ybtA)**	**MULTISPECIES: yersiniabactin transcriptional regulator YbtA**	**8.97E-02**
WP_002214684.1	0.93	0.51	-	MULTISPECIES: (Na+)-NQR maturation NqrM	9.91E-02

WP_002210723.1	0.42	0.00	-	MULTISPECIES: succinate dehydrogenase membrane anchor subunit	1.22E-01
WP_002210123.1	0.55	0.00	-	outer membrane lipid asymmetry maintenance protein MlaD	1.38E-01
WP_002216002.1	1.04	0.73	y1139	hypothetical protein	1.72E-01
WP_071526452.1	1.06	0.75	-	coproporphyrinogen III oxidase	1.76E-01
WP_002211242.1	1.06	0.73	y2296	MULTISPECIES: DUF2583 domain-containing protein	1.81E-01
WP_000098391.1	**0.49**	**0.13**	**y2397 (ybtP)**	**MULTISPECIES: yersiniabactin ABC transporter ATP-binding/permease protein YbtP**	**1.82E-01**
WP_002210122.1	0.34	0.00	mlaE	MULTISPECIES: lipid asymmetry maintenance ABC transporter permease subunit MlaE	3.11E-01

Table 3-2. Bacterial strains used in these studies.

Descriptive Name	Genotype	Identification Number	Source
Strains used for *in vitro* assays.			
Y. pestis	pCD1-, pgm+, pMT+, pst+	YPA152	(307)
irp2	YPA152 Δ*irp2*	YPA153	(63)
znuBC	YPA152 Δ*znuBC*	YPA154	(148)
znuBC irp2	YPA154 Δ*irp2*	YPA157	(209)
y0702-y0704	YPA152 Δ*y0702-y0704*	YPA279	This work
y0702-y0704 (cy0702-y0704)	YPA279 ++*y0702-y0704*	YPA291	This work
znuBC y0702-y0704	YPA154 Δ*y0702-y0704*	YPA281	This work
znuBC y0702-y0704 (cy0702-y0704)	YPA281 +*y0702-y0704*	YPA292	This work
znuBC y0702-y0703	YPA154 Δ*y0702-y0703*	YPA302	This work
znuBC y0704	YPA154 Δ*y0704*	YPA301	This work
znuBC y0702-y0703 pBCSK+::y0702-y0703	YPA302 pBCSK+::*y0702-y0703*	YPA320	This work
znuBC y0702-y0704 y1049-y1050 y3760-y3759 y3392-y3393	YPA281 Δ*y1049-y1050* Δ*y3760-y3759* Δ*y3392-y3393*	YPA317	This work
znuBC y1049-y1050 y3760-y3759 y3392-y3393	YPA154 Δ*y1049-y1050* Δ*y3760-y3759* Δ*y3392-y3393*	YPA313	This work
Y. pestis pGEN-*luxCDABE*	YPA152 with bioluminescent reporter	YPA257	(278)
znuBC pGEN-*luxCDABE*	YPA154 with bioluminescent reporter	YPA258	(278)
irp2 pGEN-*luxCDABE*	YPA153 with bioluminescent reporter	YPA259	(278)
irp2 znuBC pGEN-*luxCDABE*	YPA157 with bioluminescent reporter	YPA260	(278)
znuBC y0702-y0704 pGEN-*luxCDABE*	YPA281 with bioluminescent reporter	YPA296	This work
znuBC y0702-y0704 (cy0702-y0704) pGEN-*luxCDABE*	YPA292 with bioluminescent reporter	YPA294	This work
Strains used for mouse infections.			
Y. pestis	pCD1+, pgm+, pMT+, pst+	X17	(242)
znuBC	YPA154 +pCD1	MBLYP-074	This work
znuBC irp2	X17 Δ*znuBC* Δ*irp2*	X90	(209)
znuBC y0702-y0704	YPA281 +pCD1	MBLYP-063	This work
znuBC y0702-y0704 (cy0702-y0704)	YPA292 +pCD1	MBLYP-070	This work

CHAPTER 4

MICRONEEDLE ARRAY DELIVERY OF *YERSINIA PESTIS* RECAPITULATES BUBONIC

PLAGUE

SUMMARY

Yersinia pestis, a Gram-negative bacterium, is transmitted through an enzootic cycle from a flea insect vector to a mammalian host. The flea deposits *Y. pestis* within the intradermal layer of the skin, which is colonized by the bacterium, leading to dissemination to the draining lymph node and the development of bubonic plague. Inoculation with a small gauge syringe needle can be used to recapitulate bubonic plague and study *Y. pestis* pathogenesis in the laboratory setting. However, the process to specifically target the dermis is tedious, error prone, and poses a safety risk for this highly pathogenic organism. Microneedle arrays (MNAs) are micron-scale polymeric structures that can disrupt the skin barrier and directly deliver materials to the dermis. MNAs have been used to deliver a variety of materials, including live bacteria and vaccine components to the dermis. However, MNAs are unable to span the thickness of standard nitrile/latex gloves, greatly reducing the risk of accidental exposure to the user. Our goal here was to determine if MNAs are a valid alternative to syringe-based inoculation strategies for *Y. pestis* to recapitulate bubonic plague and study bacterial virulence. To this end, we established the parameters required to establish a lethal inoculum of *Y. pestis* in a mouse model using MNAs. We also used whole-animal optical imaging to monitor bacterial proliferation and dissemination after inoculation with MNAs. Finally, using

MNAs to deliver *Y. pestis* zinc acquisition mutants, we demonstrated that calprotectin is an important nutritional immunity barrier encountered by *Y. pestis* within the dermis during bubonic plague. Together, these data demonstrate the utility of MNAs to safely inoculate mice with *Y. pestis* to recapitulate bubonic plague and study *Y. pestis* pathogenesis in the laboratory.

INTRODUCTION

The Gram-negative bacterium *Yersinia pestis* causes the disease bubonic plague, which is responsible for the most fatal pandemic in history known as the Black Death (4, 10, 308). Currently, bubonic plague cases still occur in areas in which the bacterium is endemic in animal populations, including the southwestern United States (5, 9). Within these environments, *Y. pestis* is maintained within an enzootic cycle in which the bacterium is transmitted between mammalian hosts by a flea vector. During the feeding process, infected fleas deposit *Y. pestis* directly into the intradermal skin layer (13, 309). These bacteria directly interact with host immune cells and rapidly disseminate from the skin to the draining lymph nodes (310, 311). Migration to the lymph nodes occurs minutes after infection and appears to be independent of intracellular trafficking by phagocytic cells (310, 311). Upon reaching the lymph nodes, *Y. pestis* evades clearance by resident immune cells and can replicate to high numbers. Eventually the bacteria breach the lymph node to disseminate into the bloodstream (312), which is an important step in the transmission of *Y. pestis* to a new flea vector and continuing the enzootic cycle. Spillover into human populations occurs when individuals come into contact with these infected fleas (28, 29). Despite the persistence of *Y. pestis* in many countries and potential for human spillover infections, no vaccine exists to prevent plague. A greater understanding of bacterial transmission and dissemination would significantly affect strategies for preventing and controlling the spread of *Y. pestis*.

In the past, subcutaneous injection of *Y. pestis* has been routinely used to model bubonic plague. While this approach has revealed many aspects of *Y. pestis* pathogenesis, growing evidence suggests that subcutaneous injection of *Y. pestis* does not completely recapitulate the disease kinetics of bubonic plague and lacks the ability to study important pathogen interactions at the initial site of infection in the dermis (310, 313). Therefore, investigators have started to employ

intradermal injection models that have proven to be more biologically reminiscent of flea transmission (18, 312, 313). Intradermal administration into the dermis of the ear has revealed that *Y. pestis* dissemination and kinetics of lethal infection is much quicker than rates observed from subcutaneous injection (310, 312). These studies highlight that upon *Y. pestis* intradermal infection, a few bacteria travel rapidly to the draining lymph node, where they replicate to high numbers forming a bubo (310, 312, 314). At the site of inoculation within the dermis, *Y. pestis* encounters neutrophils but the bacteria overcome the immune system to avoid clearance and eventually replicate at the infection site (268, 310, 311). Neutrophils have important roles in nutritional immunity through the release of proteins that restrict bacterial access to metals, including calprotectin that specifically sequesters zinc, manganese, and iron (108, 109, 111, 224, 231, 315, 316). Using subcutaneous administration of Y. pestis, we have previously shown that calprotectin is the primary zinc acquisition barrier for *Y. pestis* during bubonic plague (278). We also showed that he bacterium overcomes calprotectin metal restriction via the expression of two zinc acquisition systems, ZnuABC and yersiniabactin (278). However, the tissue in which *Y. pestis* encounters calprotectin restriction during bubonic plague remains to be determined and application of model that more closely mimics natural flea transmission, such as intradermal inoculation, will be informative.

While intradermal injection has proven to be a valuable tool to study plague, the application of intradermal injections presents a difficult challenge within the BSL-3 laboratory. The accurate application of a standard syringe needle to precisely infect the dermal layer of the skin while wearing appropriate personal protective equipment proves to be tedious and difficult. Moreover, these needles are significant potential safety hazards for laboratorians. Moreover, common administration volumes needed to ensure reproducible inoculations (>20 μl) can cause tissue damage within the intradermal space that may stimulate an immune response unrelated to bacterial infection (313). Therefore, a more efficient and safer technique to perform biologically relevant intradermal infections would significantly impact the adoption of the intradermal model for plague researchers. Microneedle arrays (MNAs) are micron-scale polymeric structures designed as

platforms for intradermal delivery for biological substrates (317). MNAs have been used extensively for vaccine and drug delivery, and more recently, have been adapted to specifically administer bacteria to the intradermal space (317–320). For drug delivery, MNAs have been utilized to study mechanisms to combat methicillin-resistant *Staphylococcus aureus* (MRSA) and distribute antibiotic vancomycin directly to the infected skin area (321). MNAs have been used for a variety of vaccine studies from immunizing with influenza antigen to stabilized dengue virus (319, 322, 323). Outside of studying infectious diseases, delivery by MNAs has shown an improvement for distribution of cancer vaccines and immunotherapies (317). Finally, MNAs have been adapted to mimic intradermal tick transmission inoculation of *Francisella tularensis* (320). The successful and reproducible intradermal delivery achieved in these studies suggest that MNAs may provide a useful tool to mimic flea transmission for the study bubonic plague pathogenesis in the BSL-3 laboratory.

Here we show that MNA administration of *Y. pestis* reproducible establishes intradermal instillation of *Y. pestis* that leads to lethal bubonic plague that mimics disease kinetics previously reported for intradermal needle and flea inoculation. Furthermore, we demonstrate the utility of MNA administration as a tool to study *Y. pestis* virulence by using this model to establish that host calprotectin effectively limits *Y. pestis* zinc acquisition within the dermis. Finally, using an attenuated strain of *Y. pestis*, we show that MNA administration within the dermis has potential as a vaccine delivery platform against pulmonary infection.

RESULTS

MNAs reproducibly deliver *Y. pestis* to the dermis.

Previous studies indicate that an infectious dose >200 colony forming units (CFU) of *Y. pestis* delivered via syringe inoculation to the ear pinna results in a reproducible lethal infection (313, 324). As such, our first step in adapting MNAs for *Y. pestis* inoculation was to establish conditions required to achieve reproducible inoculums within this range. The MNAs designed for this study were 650 μm from the MNA base to the tip to achieve penetration of the dermal layer (325). Unlike syringes, MNAs do not actively inject materials into the dermal layer. Instead, MNAs are coated

with the transported substances or microorganisms and pressed onto the skin for delivery into the puncture sites (320). Therefore, MNAs were incubated for 30 min with increasing bacterial concentrations (from $3x10^3$ to $3x10^8$ CFU/ml) to determine if an inoculum of 200-700 CFU could be achieved. After incubation, the MNA was placed on the bolus of the ear (Fig. 4-1A), applied for 5 seconds, and then removed. 15 min later, ears were harvested, 70% ethanol was applied with a sterile swab to remove external bacteria, and subsets of ears were either fixed in 10% formalin and imaged by two-photon microscopy or homogenized using a tissue tearer and plated on selective agar to enumerate CFU (the limit of detection was 100 CFU/tissue). Imaging of the ears revealed uniform needle inoculations across the dermal layer (Fig. 4-1B) that appeared to travel approximately 30 μm into the tissue (Fig. 4-1C). We were unable to recover any bacteria from ears inoculated with MNAs incubated with inoculums below $3x10^5$ CFU/ml (Fig. 4-1D), indicating that less than 100 bacteria were administrated by MNAs incubated at these concentrations. However, bacteria were recovered from tissues inoculated with MNAs incubated with $3x10^6$ CFU/ml and the number of CFU recovered increased as the inoculum increased to $3x10^8$ CFU/ml (Fig. 4-1D). Furthermore, we could detect rod-shaped bacteria at the inoculation site within the dermis layer (Fig. 4-1E). These data suggested that MNAs incubated with $3x10^7$ CFU/ml should deliver a dose within our desired range of ~500 CFU. To determine if these conditions yielded consistent reproducible inoculums, 15 mouse ears were infected with MNAs incubated with $3x10^7$ CFU/ml and inoculums were calculated 15 min later. Bacterial enumeration showed a mean 624 ± 129 CFU recovered from the tissue (Fig. 4-1F). Together, these data indicate that MNAs can consistently deliver *Y. pestis* into the dermis.

<u>MNA inoculation results in a lethal *Y. pestis* infection that mimics flea inoculation.</u>

Intradermal inoculation via flea bite or needle injection results in deposition of the *Y. pestis* into the dermis and rapid dissemination of a small population of bacteria to the draining lymph node (268, 310, 311). Despite recruitment of resident neutrophils, the bacteria that remain in the dermis are able to survive and undergo limited proliferation (310, 313, 326). To determine if MNA inoculation results in a similar disease manifestation, MNAs were used to inoculate mice with a *Y.*
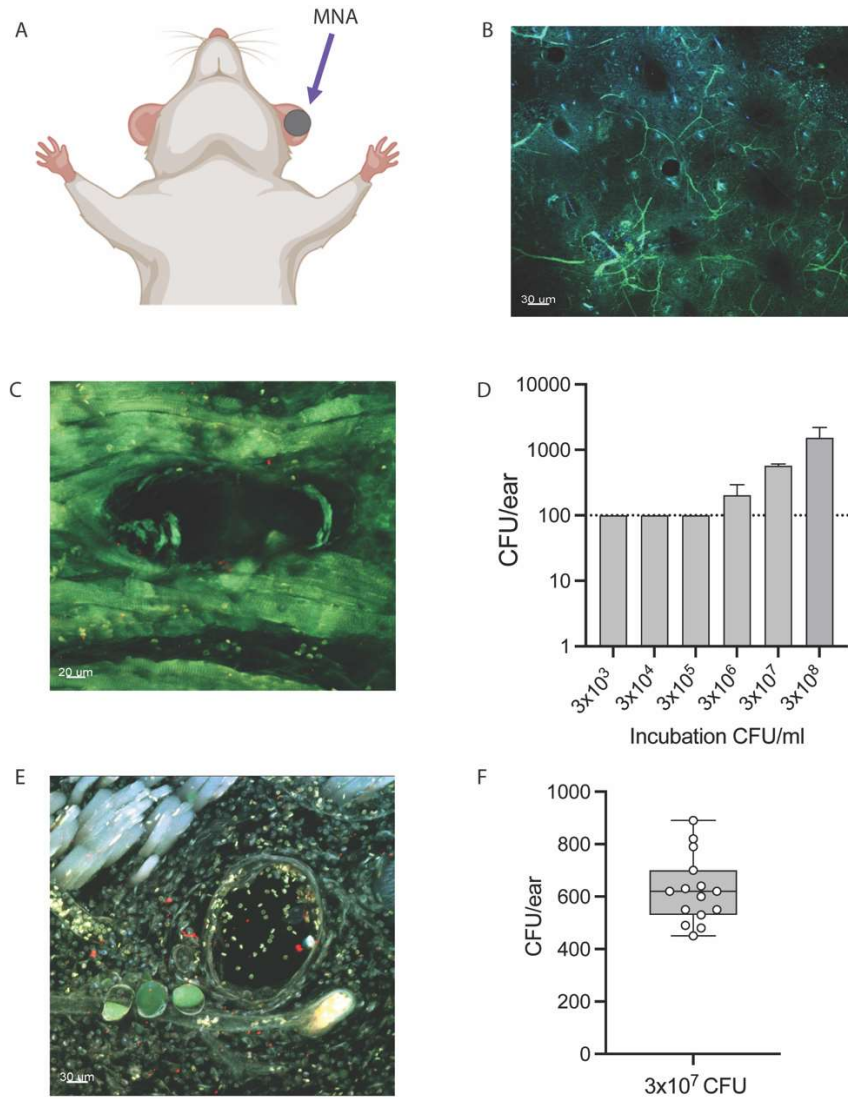
Figure 4-1. MNAs can reproducibly deliver *Y. pestis* to the dermis.

To determine inoculum by MNA infection, MNAs were incubated with increasing numbers of colony forming units (CFU) of *Y. pestis* for 30min. (A) After incubation, mice are infected by applying the MNA to the left ear and applying pressure for a few seconds. MNAs are removed with forceps after infection. (B and C) Image of ear inoculated with MNA without bacteria. (D) To determine inoculum CFU, ears were harvested at 15 min post-infection and bacteria were enumerated by serial dilution. Dotted line indicates limit of detection. (E) Image of MNA inoculation site with bacteria (red). (F) Inoculums for MNAs incubated with 3×10^7 CFU/ml was confirmed in two independent experiments (n=15).

pestis strain expressing a bioluminescent bioreporter (245). A subset of mice (n=3) was euthanized at 15 mins to confirm the inoculum (723 ± 384 CFU), and optical imaging was used to monitor bacterial proliferation and dissemination as a function of bioluminescence in the remaining animals (Fig. 4-2A-C). At 0.25 h, bioluminescent bacteria were detected in the ears but not the cervical lymph nodes. By 12 h post-infection the signal in the ears decreased, most likely due to loss of bacteria that were originally deposited on the ear surface, but we observed bioluminescent signal in the cervical lymph nodes indicating lymph node colonization by this time point. Bioluminescence in both tissues increased over the remaining course of the infection, with the signal from both tissues peaking at 48 h post-infection (Fig. 4-2A-C). Conventional bacterial enumeration at 48 h post-infection confirmed robust colonization of both tissues by *Y. pestis* (Fig. 4-2D). Furthermore, by 48 h post-infection bioluminescent signal was starting to be detected in other tissues, indicating that bacteria were beginning to disseminate into the bloodstream (Fig. 4-2C). Animals began to succumb to the infection by 60 h post-infection, with all animals meeting end point criteria by 80 h post-infection (Fig. 4-2E). The kinetics of the infection using MNAs for inoculation closely recapitulates what has been reported for intradermal needle inoculation or flea transmission (310, 326), supporting that MNA inoculation is a viable mechanism to model intradermal infections by *Y. pestis*.

MNA administration reveals the importance of calprotectin in restricting *Y. pestis* in the dermis.

Using a subcutaneous injection model, we have previously shown that calprotectin is the primary zinc sequestration barrier that *Y. pestis* needs to overcome to cause a lethal infection in mice (278). While these studies showed that calprotectin protects mice from lethal infection by *Y. pestis* zinc acquisition mutants, the study design did not inform which tissues *Y. pestis* encounters calprotectin-mediated zinc restriction during bubonic plague. Because neutrophils are a primary source of calprotectin (327) and rapidly recruited to the dermis during flea transmission of *Y. pestis* (326), we were curious if calprotectin restricts zinc availability for *Y. pestis* in the dermis. To test this hypothesis, C57BL/6J and S100A9$^{-/-}$ (deficient in calprotectin) mice were inoculated using the
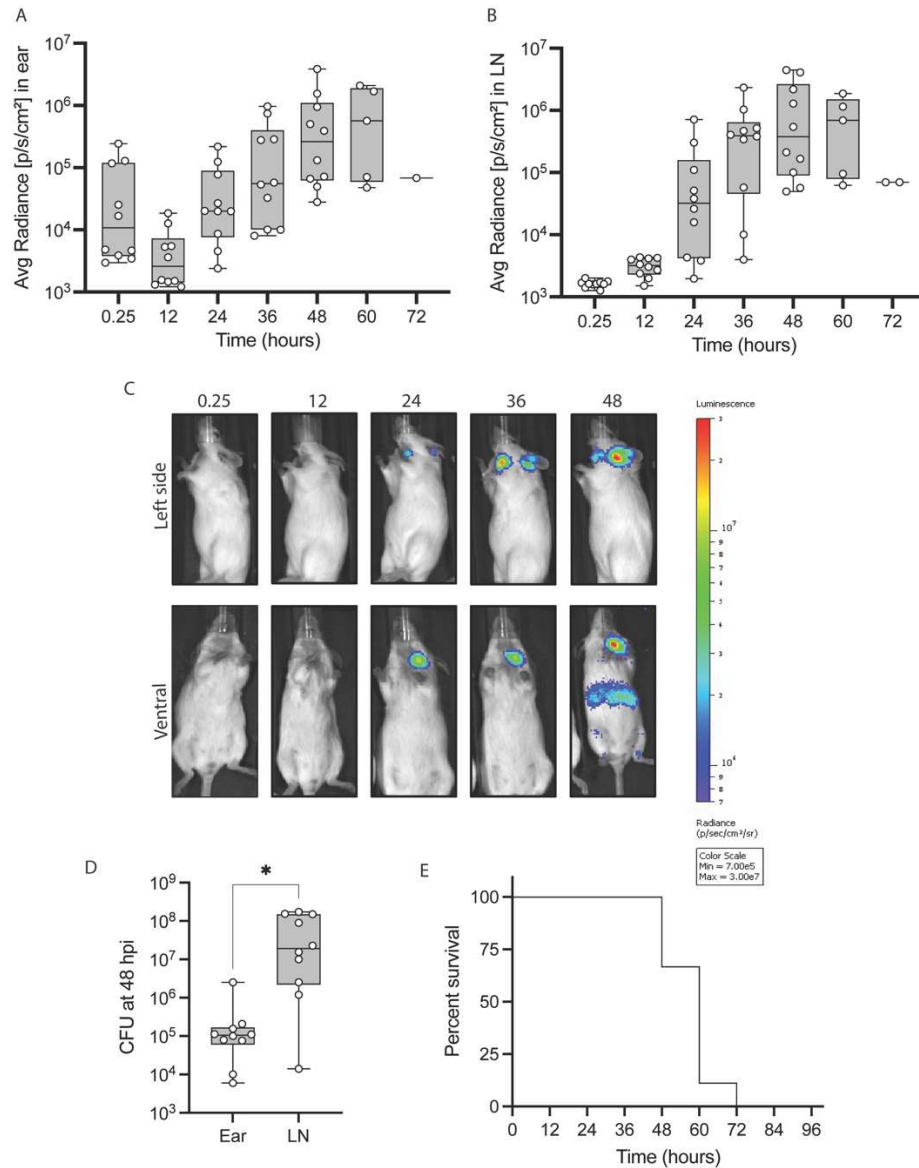
Figure 4-2. MNA inoculation results in a lethal *Y. pestis* infection that mimics flea inoculation.

To determine if *Y. pestis* infection follows similar kinetics of dissemination as a needle inoculation, Swiss Webster mice were infected intradermally with a bioluminescent strain of *Y. pestis.* Replication and dissemination were measured by optical imaging of the (A) ear and (B) draining LN at time of inoculation and every 12 h for 72 h. (C) Dissemination in representative mouse from the left side and ventral view. (D) Measurement of CFU in the ear and LN at 48 hpi for individual mice. Two-tailed t-test, p=0.0146.

MNAs as described above with *Y. pestis* or a *Y. pestis* zinc acquisition mutant (*Y. pestis znuA ybtX*) expressing a bioluminescent bioreporter (245). A subset of mice was euthanized at 15 min post-infection to confirm that equivalent inoculums were delivered (750 ± 117 and 526 ± 183, respectively), and bacterial proliferation and dissemination were monitored in the remaining mice by optical imaging. Greater bioluminescence was detected at each time point in the ears of S100A9$^{-/-}$ mice compared to C57BL/6J mice infected with *Y. pestis* (Fig. 4-3A), suggesting that calprotectin restricts bacterial proliferation within the dermis. Calprotectin restriction was further supported by infection with *the znuA ybtX* mutant, which was unable to replicate in the dermis of C57BL/6J mice but robustly replicated in the dermis of S100A9$^{-/-}$ mice (Fig. 4-3B and 4-3C). *Y. pestis* also appeared to more rapidly disseminate to the draining lymph node and/or was less able to proliferate within these tissues in S100A9$^{-/-}$ mice than C57BL/6 mice (Fig. 4-3D, 4-3E, and 4-3F). Moreover, S100A9$^{-/-}$ mice succumbed to infection with *Y. pestis* in a shorter period of time than C57BL/6J mice (Fig. 4-3G; mean time to death of 72 h vs. 90 h, respectively; p=0.109). As we reported previously using the subcutaneous injection model (278), S100A9$^{-/-}$ mice were unable to survive challenge by the *znuA ybtX* zinc acquisition mutant, while C57BL/6J mice survived (Fig. 4-3G; p<0.0001). Together, these data using intradermal instillation by MNAs demonstrate that calprotectin is an obstacle to infection of the dermis and a potent barrier to zinc acquisition within this tissue.

MNA delivery of attenuated *Y. pestis* increases survival to subsequent challenge.

MNA delivery of vaccine candidates to the dermis has been shown to effectively mount a robust immune responses that can protect against pulmonary challenge with influenza A virus and *F. novicida* (320, 322). Because the *znuA ybtX* mutant is severally attenuated for bubonic plague, we were curious if the mice that survived MNA administration with the *znuA ybtX* mutant might generate an immune response that would protect them from subsequent pulmonary infection with *Y. pestis*. Therefore, C57BL/6J mice were inoculated with *Y. pestis* or *Y. pestis znuA ybtX* and monitored for the development of moribund disease for 14 days. As expected, all mice challenged with *Y. pestis* succumbed to infection while those challenged with the *znuA ybtX* mutant survived the infection (Fig. 4-4A). Optical imaging showed a similar pattern of proliferation and dissemination

A

B

C

91

D

Avg Radiance [p/s/cm²/sr] in LN

Time (hours)

Y. pestis C57BL/6J
Y. pestis S100A9−/−
znuA ybtX C57BL/6J
znuA ybtX S100A9−/−

E

Y. pestis   *znuA ybtX*

C57BL/6J

F

Y. pestis   *znuA ybtX*

S100A9−/−

G

Percent survival

Time (hours)

Y. pestis S100A9−/−
znuA ybtX S100A9−/−
Y. pestis C57BL/6J
znuA ybtX C57BL/6J
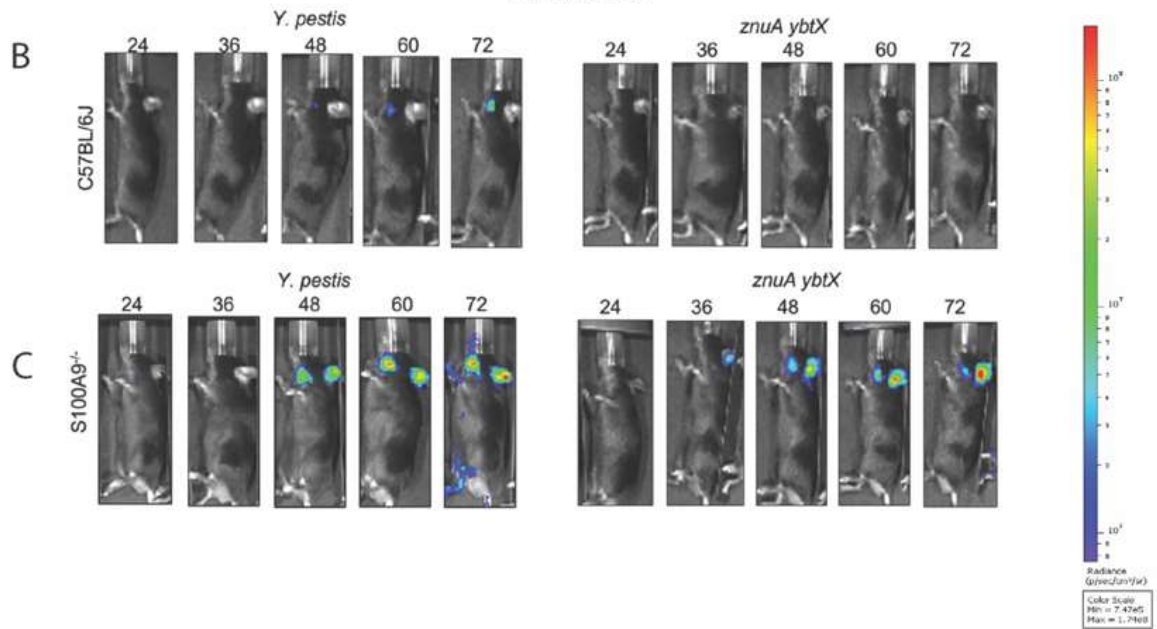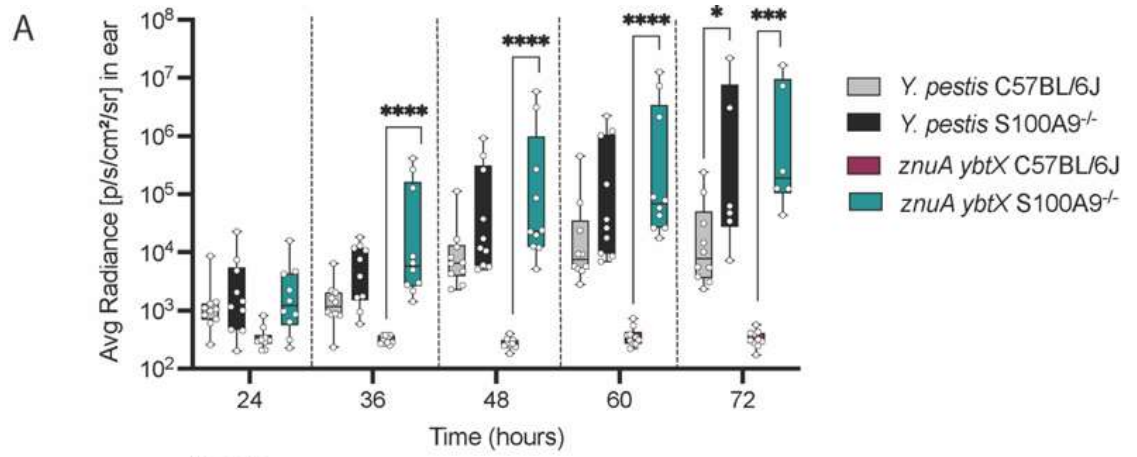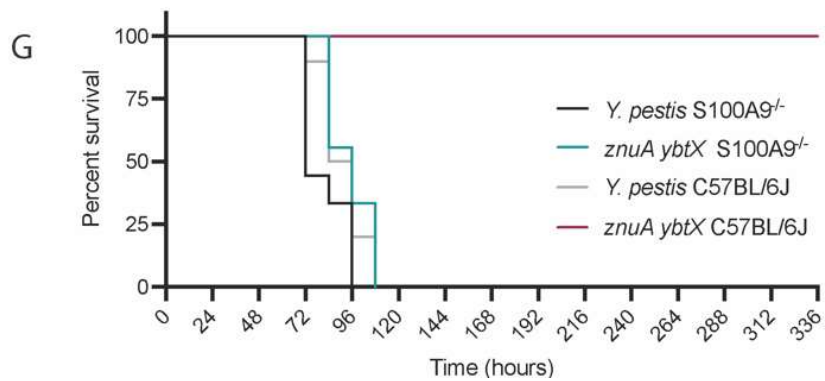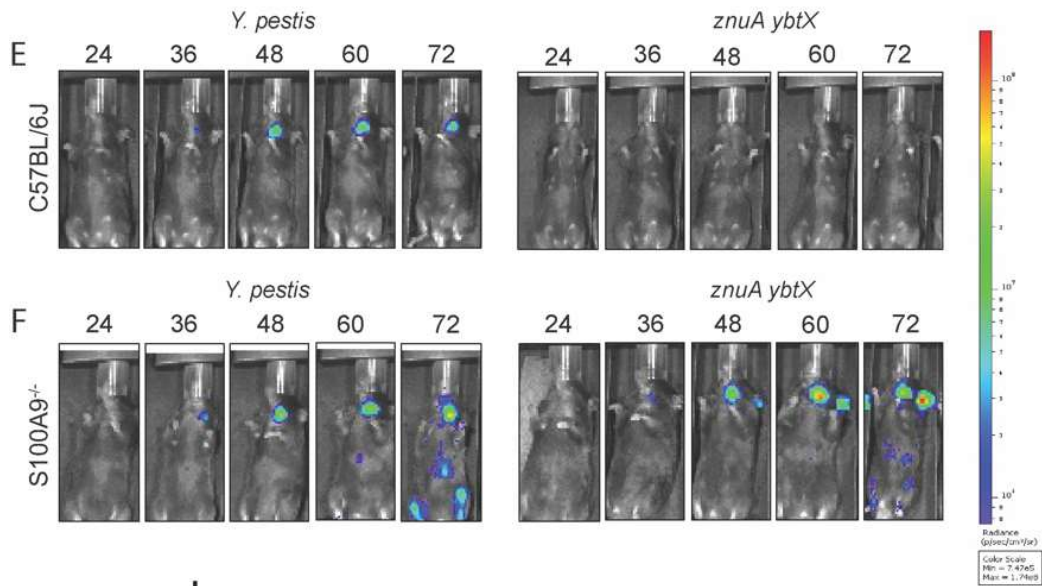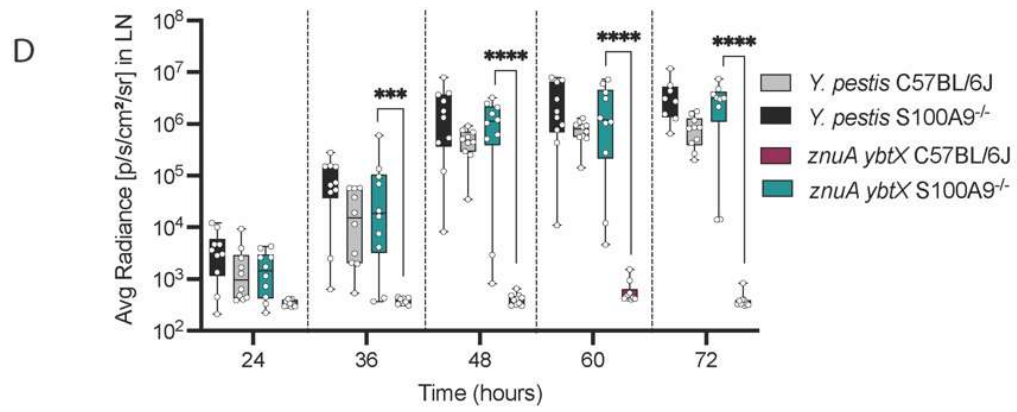
Figure 4-3. MNA administration reveals the importance of calprotectin in restricting *Y. pestis* in the dermis.

To determine the calprotectin barrier, C57BL/6J or calprotectin knockout (S100A9$^{-/-}$) mice (n=10) were infected intradermally with bioluminescent strains of *Y. pestis* or a *znuA ybtX* mutant. (A) Dissemination of bacteria was monitored and measured by bioluminescence via IVIS imaging in infected ear. Representative (B) C57BL/6J and (C) S100A9$^{-/-}$ mouse from *Y. pestis* or *znuA ybtX* mutant infections showing infected ear. (D) Dissemination of bacteria was monitored and measured by bioluminescence via IVIS imaging in the draining LN. Representative (E) C57BL/6J and (F) S100A9$^{-/-}$ mouse from *Y. pestis* or *znuA ybtX* mutant infections showing LN. (G) Survival was monitored every 12 h for 14 days for C57BL/6J and S100A9$^{-/-}$. Two-tailed t-test; *=p<0.042, ***=p<0.001, ****= p<0.0001. Log-rank test: C57BL/6J *Y. pestis* vs. C57BL/6J *znuA ybtX* p<0.001; C57BL/6J *znuA ybtX* vs. S100A9$^{-/-}$ *znuA ybtX* p<0.001.

in the ears and draining lymph nodes as observed in Fig. 3 (Fig. 4-4B and 4-4C), and importantly, no bioluminescence signal was detected in the tissues of *znuA ybtX* infected mice (Fig. 4-4B and 4-4C). On day 14, the mice that were infected with the *znuA ybtX* mutant by MNA inoculation and a naïve group of mice were infected with bioluminescent *Y. pestis* by intranasal administration and monitored by optical imaging and for the development of lethal infection. Optical imaging of the thoracic cavity indicated slower proliferation of *Y. pestis* in the lungs of animals that were previously exposed to the *znuA ybtX* mutant, but ultimately the mice were not able to inhibit bacterial proliferation (Fig. 4-4D). However, slower proliferation in the *znuA ybtX* exposed mice directly correlated with a significant delay in lethality compared to naïve infected mice (Fig. 4-4E; mean time to death of 96 h vs 60 h, respectively; p=0.0002). Together, these data indicate that despite the inability of the *znuA ybtX* mutant to proliferate and disseminate, mice were mounting a systemic immune response to the bacteria, though a longer time or repeated MNA administration may be required to generate a fully protective response.

DISCUSSION

While subcutaneous inoculation has been a valuable tool to study bubonic plague pathogenesis, intradermal inoculation is more biologically relevant to natural flea transmission of *Y. pestis* (328). Previously, MNAs have been used for mouse infections with *F. novicida* (320), another bacterium transmitted by an insect vector. Building on these studies, we developed and characterized a similar model for *Y. pestis* inoculation in the ear pinna using MNAs, which is a safer and more efficient tool than typical needle inoculation (318). Our first goal was to ensure that infection with MNAs would provide dissemination kinetics similar to those reported in studies of flea or other intradermal infection models with *Y. pestis* (310–312). These previous studies suggest that upon infection in the dermal layer, a few bacteria immediately travel via lymphatic vessels to the draining lymph node and begin to replicate to establish infection (310–312). In a direct comparison between intradermal and subcutaneous routes of infection, Gonzalez *et al*. demonstrated that lymph node colonization occurred more rapidly with the intradermal infection route (313). Using bioluminescent imaging, we recapitulated these results from Gonzalez *et al*. and observed lymph
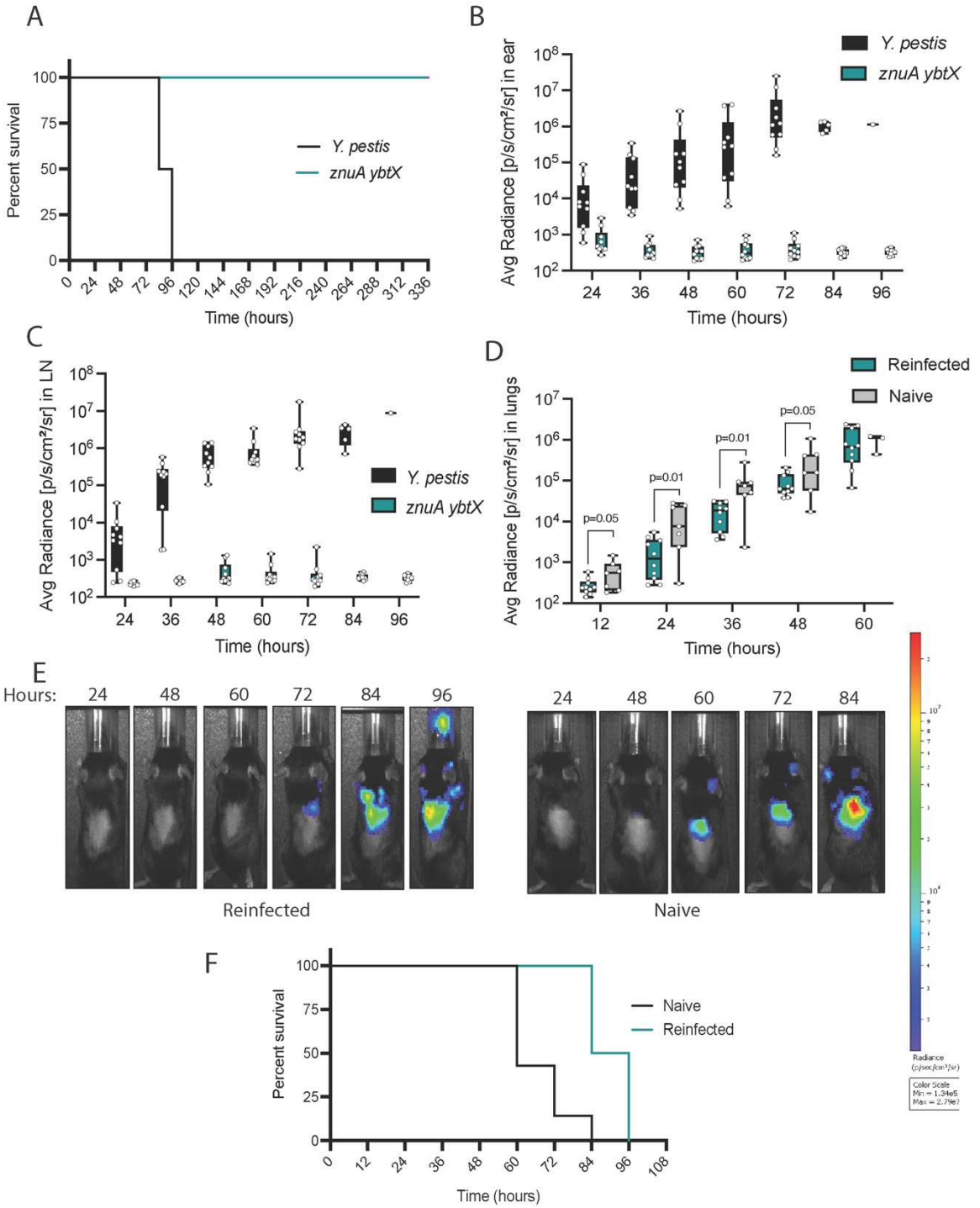
Figure 4-4. MNA delivery of attenuated *Y. pestis* increases survival to subsequent challenge.

 To determine the potential for using MNA infection with the *znuA ybtX* mutant as a vaccine platform, (A) C57BL/6J mice (n=10) were infected via MNAs with *Y. pestis* and *znuA ybtX* (inoculum=1x10^2) and monitored for 14 days. (B and C) Bioluminescence was monitored every 12 h in the inoculated ear and draining LN. On day 14, mice were reinoculated with a bioluminescent strain of *Y. pestis* via intranasal instillation and disease progression was compared to naïve C57BL/6J (n=10). (D) Replication of bacteria in the lungs was measured by bioluminescence via optical imaging. Two-tailed t-test. (E) Representative mice from reinoculation with *Y. pestis*. (F) Survival was monitored every 12 h for 14 days. Log-rank test: p=0.002.

node colonization within 12 hours of inoculation, with the peak bioluminescence observed at 48 h post-infection. Importantly, these data are also similar to infection with *Y. pestis* by flea inoculation (311). Furthermore, our MNA infection model shows a rapid progression to lethality, which correlates with previous needle intradermal infections for plague pathogenesis (313). It has been speculated that lethality in the intradermal bubonic model is faster than subcutaneous injection because of greater presence of, or access to, lymphatic vessels in the dermal layer of the skin (313). It is also important to note that the volume administered by needle inoculation can also influence the host response, with larger volumes (>2 μl) causing tissue damage and potential administration beyond the intradermal space (313, 329, 330). Not only does a smaller inoculation match more to a flea bite and cause less tissue damage, it also is less favorable to the bacteria (313). Importantly, because the microneedles do not deposit large volumes into the tissue, the bacteria are delivered directly within the intradermal space without similar concerns on mis localization of bacteria due to changes in inoculum volumes (318). Overall, these data support that the MNA infection model is biologically applicable to bubonic plague infection that is administered through a flea bite.

Using MNAs, we recapitulated previous findings that calprotectin is the main obstacle for zinc acquisition during *Y. pestis* infection (Fig. 4-3) (278). However, by combining MNA administration with optical imaging of bacterial mutants, we were able to expand on these initial studies and show that *Y. pestis* encounters calprotectin-mediated zinc sequestration within the dermis during bubonic plague. These data indicate that *Y. pestis* needs to rapidly adjust to metal limitation upon flea transmission, and that zinc acquisition is essential for the bacterium to colonization of the dermis. Moreover, these data also demonstrate that we can use *Y. pestis* MNA administration to better define host-pathogen interactions specifically within the dermis, which have different cell types and responses than other tissues. For example, while neutrophils have been implicated as the primary source for calprotectin during immune responses in the lungs and liver (102, 228, 266), a study using skin biopsies of Lyme disease patients suggests that other cell types are the primary source for calprotectin-mediated metal limitation in the dermis (106). With the establishment of this

reproducible dermal model of infection, moving forward we will use *Y. pestis* as a tool to better understand the mechanisms involved in nutritional immunity within the dermis.

With plague cases still to occurring worldwide, there remains a need for a vaccine. Due to differences in lymphatic vascularization between the dermal layer and subcutaneous level in the skin (331), intradermal and subcutaneous inoculations show differences in immune responses, with intradermal vaccines generating a more robust mucosal immune response (313, 332–334). Recent successes with MNA-delivered vaccines suggest a MNA platform can provide a strong mucosal immune response (320, 322). While vaccination was not the primary goal of these studies, we were able to show that intradermal delivery of an attenuated *Y. pestis* strain had any impact on subsequent pulmonary challenge – slower replication and a delay in the development of lethal infection. While a change in overall survival was not observed, likely because of the limited time frame that mice were allowed to recover from challenge and generate a robust immune response, these studies provide preliminary data that MNA delivery of a vaccine may result in effective protection against pneumonic plague and justify future studies specifically designed for vaccination (i.e., prime boost scenarios, measurements of immune responses, different vaccine formulation, etc.).

METHODS

Ethics statement

C57BL/6J mice were purchased from The Jackson Laboratory and Swiss Webster were purchased from Charles River. S100A9$^{-/-}$ mice were bred at the University of Illinois at Urbana-Champaign prior to transfer to the University of Louisville for infection. Groups contained both male and female mice, and no sex bias was observed during these studies. Animals were housed in accordance with NIH guidelines and all procedures were approved by the University of Louisville IACUC and the University of Illinois IACUC. Three days prior to challenge with *Y. pestis*, animals were transferred to University of Louisville's Center for Predictive Medicine Regional Biocontainment Laboratory ABSL-3 facilities to acclimate to the facility. After infection, mice were

observed for up to 14 days for the development of moribund disease and humanely euthanized if they met predefined endpoints.

Bacterial strains

Y. pestis KIM6+ (63) and Y. pestis znuA ybtX strains (197) were routinely grown in Difco brain heart infusion (BHI) broth (BD Biosciences). Strains transformed with the pGEN-luxCDABE or pGEN222-dsRed plasmids (245) were grown in the presence of kanamycin (50 µg/ml). For infection, bacteria were grown overnight at 26 °C in BHI broth prior to intradermal challenge. Prior to intranasal instillation, Y. pestis was grown over night at 26 °C, diluted to 0.05 OD_{600} in BHI broth with 2.5 mM $CaCl_2$, and grown at 37 °C with aeration for 16 to 18 h (261, 262). Bacterial concentrations were determined using a spectrophotometer and diluted to desired concentrations in 1x PBS for mouse infections. Concentrations of bacterial inoculums for mouse studies were confirmed by serial dilution and enumeration on agar plates.

MNA Preparation

Microneedle arrays (MNAs) were prepared as previously described (320). Following preparation, MNAs were sterilized with ethylene oxide before use in subsequent mouse studies.

MNA incubation with Y. pestis

Prior to infection, MNAs were incubated with Y. pestis for infection as previously described (320). Briefly, Y. pestis was diluted to desired concentration (CFU/ml) in BHI. MNAs were fully submerged in 1 ml of culture in a 24 well-plate and incubated for 30 min with rocking at room temperature. Any bubbles from the culture were gently removed from the MNAs prior to incubation using a pipet tip. Prior to infection, excess medium was removed from the MNAs using a sterile cotton swab.

Animal infections with Y. pestis

Mice were challenged with Y. pestis as previously described (245, 261, 262). Briefly, for intradermal challenge, mice were anesthetized with isoflurane and inoculated by MNA on the left ear. MNA was pressed on the ear for 5 seconds and the removed with forceps. For intranasal

challenge, mice were anesthetized with ketamine/xylazene and administered 20 µl of bacteria suspended in 1X PBS to the left nare. For optical imaging, mice were anesthetized with isoflurane and imaged using the IVIS Spectrum imaging system (Caliper Life Sciences, Hopkinton, MA). Average radiance (photons/sec/cm2) was calculated for ear and lymph nodes as previously described (245). Infected mice were monitored for the development of disease symptoms twice daily for 14 days. Moribund animals meeting predefined endpoint criteria were humanely euthanized by CO_2 asphyxiation and scored as succumbing to infection 12 h later.

Measurement of bacterial burden in the ear and lymph node

Bacterial numbers in the ear dermal layer and lymph nodes were determined by conventional bacterial enumeration using serial dilutions. Ears were wiped with 70% ethanol wipe prior to removal to eliminate viable skin-resident bacteria. All tissues were homogenized in sterile PBS using a tissue homogenizer (Omni). Tenfold serial dilutions were made in PBS, and 10 µl were plated in triplicate onto Difco BHI agar (BD Biosciences) plates. Colony forming units (CFU) were counted after incubation at 26 °C for 48 h.

Imaging of ear with two-photon microscopy

Mouse ears were collected immediately upon infection with *Y. pestis*. Ears were placed into tissue cassettes in 10% formalin for 24 h. Following fixation, tissue cassettes with ears were washed once with PBS and stored in PBS. Ears were stained with anti-*Y. pestis* serum (1:1,000). *Y. pestis* was visualized by ds-Red with mouse ear structures and immune cells visualized by autofluorescence in GFP.

Statistics

Animal experiments were repeated twice to confirm reproducibility and the data is represented as the combination of the two independent experiments. *P* values were calculated using Student's *t* test, one-way analysis of variance (ANOVA) with appropriate posthoc testing as indicated. All statistics were completed using GraphPad Prism software.

ACKNOWLEDGEMENTS

CHAPTER 5

GOT ZINC? A DISCUSSION OF A NOVEL ROLE FOR YERSINIABACTIN

5.1 Summary of major findings

In summary, my dissertation work demonstrates a role for Ybt during *Y. pestis* infection beyond Fe acquisition. My work began by identifying the contribution of Ybt to Zn acquisition during *Y. pestis* infection in the mammalian host and insect vector. During plague, *Y. pestis* encounters the Zn-sequestering protein calprotectin and uses ZnuABC in tandem with Ybt to compete with calprotectin for Zn. Notably, calprotectin restriction represents the main Zn barrier to plague infection, and during plague, calprotectin sequestration occurs at the site of infection. Additionally, my work focusing on the Ybt system identified the secretion mechanism of Ybt as a RND efflux pump, Y0702-Y0704. While this pump is the primary mechanism, my data indicates that a secondary mechanism may also contribute to Ybt export, as a *y0702-y0704* mutant does have some residual Ybt secretion. Together my findings have significantly furthered the knowledge of how bacteria compete with nutritional immunity to acquire Zn and how the Ybt system functions in *Y. pestis* and other bacteria.

Figure 5-1. *Y. pestis* has two redundant Zn acquisition systems, ZnuABC and Ybt.

During bubonic and pneumonic plague, ZnuABC and Ybt work together to compete with calprotectin to acquire Zn. For Zn and Fe acquisition, Ybt is secreted out of the cell by Y0702-Y0704, an AcrAB-TolC RND efflux pump. An unknown secondary exporter supports Ybt secretion. Outside the cell, Ybt can bind to Fe or Zn. For Ybt-dependent Fe acquisition, the Ybt-Fe complex binds to the Psn receptor to cross the outer membrane and is transported across the inner membrane by YbtPQ. For Ybt-dependent Zn acquisition, the Ybt-Zn complex is imported across the outer membrane by an unknown receptor. Inside the periplasm, the Ybt-Zn complex is imported into the cytoplasm by YbtX.

The study of nutritional immunity has mostly focused on the restriction of Fe from bacteria by the host. More recently, restriction of other metals has been recognized as essential in preventing infection by bacteria. My studies are the first to describe an Fe-independent role for Ybt during virulence and define a conceptually innovative mechanism in *Y. pestis* to overcome Zn nutritional immunity. Moreover, I used a novel application of a hemochromatosis animal model that allowed us to specifically define the role of Zn acquisition during *Y. pestis* virulence. The data I have generated is a significant improvement in understanding *Y. pestis* Zn acquisition during infection. Importantly, the Ybt system is a conserved virulence factor in other Gram-negative pathogens, including multidrug resistant strains of *Klebsiella pneumoniae* and uropathogenic *E. coli*. Since YbtX is conserved across bacterial genomes, Ybt most likely contributes to Zn acquisition in other bacterial pathogens as well, which is further supported by data from *E. coli* Nissle (69). Therefore, these findings concerning Ybt-dependent Zn acquisition contribute to a better understanding of Zn import by this system and virulence in other pathogens. Now that Ybt has been shown to contribute to the acquisition of metals besides Fe, there is a possibility that other siderophores can binds to more metals, but this has been masked by a strong Fe phenotype. Thus, these systems could play a role in the acquisition of other metals during infection.

In addition to identifying the role for Ybt in Zn acquisition, I also sought to identify genes involved in the secretion of Ybt. Unfortunately, conventional Tn-seq methods performed in batch cultures cannot be used to identify genes involved in the production of secreted molecules due to trans-complementation by neighboring cells. To overcome this hurdle, I employed a technically innovative approach called droplet Tn-seq, which isolates individual bacteria to eliminate trans-complementation, but still allows for high throuput competition-type screening. With this system, I was able to use a non-bias transposon mutagenesis approach to identify novel genes involved in Ybt secretion that has evaded researchers for over 30 years. This research demonstrates that similar approaches can be applied to identify genes involved in other secreted factors for variety of bacteria. Moreover, because Ybt is an essential conserved virulence factor found in several Gram-

negative bacteria with high clinical relevance, knowledge of the secretion system for Ybt opens up targeting this secretion system for the development of efflux inhibitors that can serve as anti-virulence therapeutics to combat these infections.

Finally, I have also demonstrated that MNAs are a new tool to study intradermal infections by *Y. pestis*, which provide a more biologically relevant look at how *Y. pestis* infects the mammalian host through a flea bite. Specifically, I showed that the calprotectin barrier to Zn acquisition during *Y. pestis* intradermal infection occurs at the site of inoculation in the dermis. This opens opportunities for future researchers to study immune responses to *Y. pestis* and direct interactions between *Y. pestis* and immune cells safely, and more effectively in the dermal layer upon infection.

Overall, this work has not only improved our understanding of Y. pestis virulence but contributed beyond the *Yersinia* field to provide insight into how bacterial pathogens can utilize multifunctional metal acquisition systems to compete with host nutritional immunity to cause infection.

5.3 Future directions

Why are two unique import systems required for yersiniabactin transport into the cell?

Several studies have indicated that Ybt is a diastereomer that can isomerize into a racemic mixture (69, 197). Despite the previous evidence that Ybt cannot bind to Zn (178, 197), Zn-binding by Ybt was tested with a new method. Native spray metal metabolomics and Zn titration with proton nuclear magnetic resonance (Fig. 5-2) characterized that Ybt does bind to Zn (69). Importantly, one of the identified diastereomers is found to preferentially bind to Zn over Fe (69), which is known to occur for some siderophores. In Pyochelin, a siderophore produced by *Burkholderia* and *Pseudomonas* with a similar structure to Ybt exists as two diastereomers and only one can bind to Fe (335). Importantly, Fe import by Ybt is fully understood, yet the outer membrane receptor for Zn import remains undefined. The Ybt-dependent Fe import consists of the Psn outer membrane receptor and YbtPQ (64, 176). The system for Ybt-dependent Zn import includes the inner membrane protein YbtX, but what receptor Ybt-Zn interacts with to reach the periplasmic space is unknown (197). I hypothesize that the presence of two diastereomers could be the reason that *Y.*
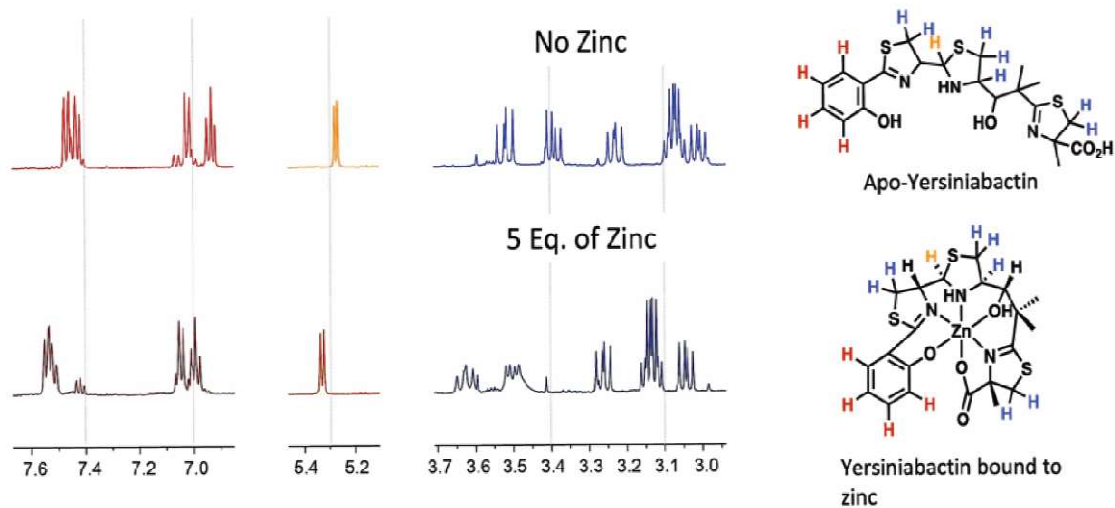
Figure 5-2. NMR confirms that Ybt can bind to Zn.

NMR spectra of Ybt in the presence of 0 equivalents of Zn or 5 equivalents of Zn. As increasing Zn is titrated into the solution, the signals that shift across the spectra correspond with protons that have electronic changes due to Zn^{2+} binding. The resulting NMR spectras lead to the predicted structures of apo-Ybt in the presence of no Zn and Ybt bound to Zn in the presence of 5 equivalents of Zn. Adapted from Behnsen, *et al*. (69).

pestis requires two distinctive metal import systems for Ybt, especially if the different diastereomers bind different metals, because the Ybt-Fe complex binds to the Psn outer membrane receptor for import into the cell. Hence, a change in structure of the molecule, whether it is a different diastereomer or altered structure due to Zn binding, may not be able to bind to Psn to be imported. Furthermore, the structure of Psn has been crystallized, therefore Psn can be co-crystallized with the Ybt-Fe complex and then docked to Ybt-Zn to determine why it cannot bind for import.

What is the receptor for yersiniabactin bound to zinc?

Our initial dTn-seq experiment only used one transposon library in the *znuBC* background, therefore we have five other libraries that can be used to increase our coverage in the genome and identify potential receptors for Ybt-Zn. I have established that dTn-seq can identify genes involved in Ybt synthesis and transport, dTn-seq can be used to determine the receptor for the Ybt-Zn complex, because while the psn receptor gene is encoded in the *ybt* locus, there is not a potential gene for a receptor for the Ybt-Zn complex. Based on the phenotype for the YbtX importer in the screen, this mutant would have a similar growth defect in the batch and in the droplet, since import mutants cannot be trans-complemented by neighboring cells. We can evaluate proteins not only by this importer phenotype but also by using bioinformatics to determine putative function of a transporter and outer membrane location. Genes with the importer phenotype can be validated by generating mutants in the *znuBC* background, then testing for growth in Zn-limited media and Zn uptake by ICPMS. Ybt-Zn outer membrane receptor mutants should show attenuated growth compared to *znuBC* and similar growth to *znuBC ybtX* in Zn-limited media. Regarding Zn uptake, mutants will have decreased Zn uptake compared to a *znuBC* mutant and show similar uptake levels as a *znuBC ybtX* mutant. Additionally, the potential receptor protein can be crystallized and tested for binding to the Ybt-Zn complex.

How is metal removed from yersiniabactin?

Although Ybt has been studied for over 30 years, the mechanism that removes metal from the metallophore remains unknown. There are three potential ways that metal is removed from Ybt. First, since metal binds to Ybt with a high affinity, an enzymatic reaction could occur to strip the

metal off or degrade Ybt to release the metal. Next, low pH has been shown to remove metal from Ybt, so an acidic environment could pull the metal off, but the likelihood of this environment inside a prokaryotic cell is low. Last, there is evidence that the inner membrane transporters, YbtPQ or YbtX, could remove the metal before Ybt reaches the cytoplasm, the metal is sent in the cytoplasm, and that Ybt is recycled back out from the periplasmic space (177) (Fig. 1-1C). Currently, there is no evidence of a specific mechanism to detach metal from any siderophore, thus identifying this mechanism will have a broad implication on understanding how many bacteria acquire metals.

If an enzyme removes the metal or degrades Ybt, our dTn-seq screen could be applied to identify this gene. Again, transposon mutants in genes involved in removing metal would show the same phenotype as an importer (*ybtX*) mutant, as they cannot be trans-complemented by cells in the batch culture. Therefore, when trying to identify the receptor for the Ybt-Zn complex, the screen can also be used to identify genes involved in this system. Further, the location of metal removal is not clear, yet some evidence shows metal is removed in the periplasm where Ybt can be sent back out of the cell before entering the cytoplasm (177). By determining what removes the metal off Ybt, we can further define this mechanism and the location that it occurs in the cell.

<u>What is the secondary secretion mechanism for yersiniabactin?</u>

Based on my data, the AcrAB-TolC efflux system Y0702-Y0704 is the primary Ybt secretion mechanism but a secondary system exists. I considered that other AcrAB systems in *Y. pestis* may be playing this supporting role, but the three other AcrAB homologs encoded in the *Y. pestis* genome are not attenuated in Zn-limited media (Fig. 2-5), demonstrating that the secondary system is not any of the AcrAB systems found in *Y. pestis*. Additionally, these data demonstrate that secretion of Ybt by Y0702-Y0704 does have specificity and cannot be done by any AcrAB homolog. Furthermore, inactivation of the two additional TolC homologs, Y3560 and Y3516 also did not show a Zn-phenotype in metal limitation (data not shown; work completed by Taylor Garrison). These data suggest another system is contributing to Ybt secretion. Efflux pumps are categorized by energy source and structure into more than 250 protein families (336). There are two main groups of efflux pumps by structure: three component assemblies that span from the cytoplasm to the

extracellular space (RND and ABC efflux pumps) and single-component inner membrane transporters (MFS, the small multidrug resistance family (SMR), the aromatic acid exporter family (ArAE), and the multi-antimicrobial extrusion (MATE) pumps) (286, 336, 337) (Fig. 5-3). Efflux pumps have been linked to the secretion of siderophores in several Gram-negative bacteria. The efflux of enterobactin had been well-established in *E. coli* to involve multiple efflux pumps. First, an MFS efflux pump, EntS, sends enterobactin across the inner membrane to the periplasm (338), where several RND efflux pumps (AcrAB, AcrAD, MdtABC, MdtEF, and AcrEF) can efflux the siderophore across the outer membrane (339, 340). In *V. cholerae*, six different system for RND efflux pumps were deleted to inhibit the secretion of vibriobactin and show decreased growth in iron limitation (183). In both *E. coli* and *V. cholerae,* these systems show functional redundancy for exporting siderophores, and multiple systems must be eliminated to inhibit secretion. Overall, *Y. pestis* has 34 efflux pump homologs, including RND, ABC, MATE, ArAE, and MFS, that have been identified in *E. coli* (286) that could be candidates for the secondary secretion system. Deletion of these systems would be a large undertaking, but luckily, efflux pumps are a mechanism for antibiotic resistance, so there are many therapeutics that have been classified to block the action of efflux pumps to allow for better antibiotic treatment. Thus, an efflux pump inhibitor can be used to attempt to block Ybt secretion. If Ybt secretion is blocked by an efflux inhibitor, this would indicate another efflux system is contribubting to Ybt secretion. Moreover, efflux inhibitors have broad spectrum and more specific activity for the variety of efflux pumps, therefore application of these different inhibitory levels can help distinguish which specific systems are playing a role in Ybt secretion.

A secondary approach to identify specific genes of the secondary system is altering our dTn-seq screen. By changing the background of our library to *znuBC y0702-y0704*, we can try to decrease these significant gene hits to a smaller pool and home in specifically on genes involved in secretion of Ybt. However, there is a possibility that more than one other system is contributing, like for the secretion of vibriobactin in *V. chlorerae* (183). In this instance, we may not be able to identify all potential systems in the screen and would need to take another approach. Since Fe
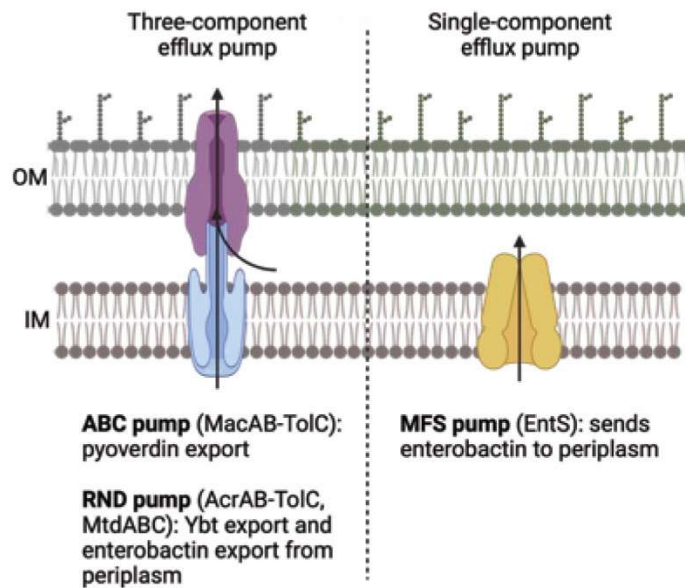
Figure 5-3. Schematic of the two families of efflux pumps by structure, three-component and single-component.

Three-component efflux pumps span from the cytoplasm to outside the cell and have been show to export pyoverdine and Ybt. Single-component efflux pumps transport across the inner membrane from the cytoplasm to the periplasm and have been implicated in the export of enterobactin. In some cases, like with enterobactin, compounds can be sent out from the periplasm with three-component pumps.

uptake by Ybt is a requirement for virulence, it is not a surprise that more than one system would contribute to Ybt secretion.

Further, the Ybt import system, YbtPQ, could play a role in Ybt export (341). In *E. coli*, YbtPQ can adopt the structure of a type IV ABC exporter that has been identified in multidrug ABC transporters (341, 342). There is substantial evidence in both *Y. pestis* and *E. coli* that the YbtPQ transporter imports the Ybt-Fe or Ybt-Cu complex (176, 177, 341, 343), however, the role of YbtPQ as a Ybt exporter has not been well-studied. To determine if YbtPQ play a role in Ybt secretion, an *ybtPQ y0702-y0704* mutant could be tested for measurement of Ybt secretion by LC/MS and growth in Zn-limited media. Although Wang *et al.* showed conformational changes as YbtPQ binds to Ybt for import (341), further structural analysis needs to be done to show the complete transport cycle YbtPQ, which may include export of Ybt. Because of YbtPQ's potential as an exporter, YbtX should undergo further analysis for a role in Ybt export. If YbtPQ or YbtX play a role in secretion of Ybt, another transporter would be required to export Ybt from the periplasm to the cytosol.

How is the secretion of yersiniabactin regulated?

Identification of the mechanism to induce Ybt is important to further understand how *Y. pestis* overcomes metal limitation. Further, defining how *y0702-y0704* is regulated could help identify the other secretion system(s), since they are likely controlled under the same mechanism. *Y. pestis* has two well-described systems to regulate expression of metal transporters, Fur and Zur. The *ybt* locus is regulated by Fur. Potentially, Zur and/or Fur could regulate the expression of Y0702-Y0704 to secrete Ybt out of the bacterial cell. However, *y0702-y0704* lacks a Fur box upstream of the operon, indicating that Fur likely cannot bind for repression and did not appear in the Li *et al.* that shows all genes from a microarray analysis impacted by Zur regulation (196). In other Gram-negative bacteria, the repressor AcrR negatively regulates *acrAB* and global transcriptional activators MarA and SoxS positively regulate the system (344, 345). These are likely candidates in *Y. pestis* but it's unclear how metal limitation would impact these regulators.

What is the importance of yersiniabactin-dependent zinc acquisition to other pathogens?

In 1987, Ybt was identified in *Y. enterocolitica* and *Y. pseudotuberculosis* (162). *Y. enterocolitica* and *Y. pseudotuberculosis* are not alone among gastrointestinal derived *Enterobacteriaceae* that encode for the Ybt system, and the pathogens *Klebsiella pneumoniae* and *E. coli* also synthesize Ybt. In fact, the high pathogenicity island that Ybt is located on is conserved across many bacteria in *Enterobacteriaceae*. Clinical studies have shown hypervirulent *Klebsiella* isolates produce Ybt (253–255, 346). In the lab setting, Ybt has been shown to evade lipocalin and support virulence of *K. pneumoniae* during pulmonary infection (235, 252). Ybt production by *K. pneumoniae* can also induce a change in nutritional immunity as ferroportin is unregulated in cells infected by *K. pneumoniae* (347). These data support that Fe acquisition by Ybt is important for *Klebsiella* pathogenesis but Zn acquisition by Ybt for *Klebsiella* remains undefined.

Ybt is part of the *Y. pestis* genome that descended from *Y. pseudotuberculosis*, which is a gastrointestinal pathogen, like *E. coli* and *K. pneumoniae*. Thus, *Y. pseudotuberculosis* survival throughout the gastrointestinal tract relies of adapting to pH changes in the gut and competing for nutrients against other bacteria of the microbiome. Suitably, Ybt preferentially binds Zn at high pH (pH 10) and binds Fe at low pH (pH 4) (69). The pH-dependent metal selectivity of Ybt may allow *Y. pestis* and other bacteria that use Ybt to adapt under various physiological conditions or different colonization niches during infection. Based on Behnsen *et al*., *E. coli* Nissile uses the ability of Ybt to bind to Zn to outcompete *S.* Typhimurium for Zn in the gut in the midst of inflammation and calprotectin secretion from the host (69). Although *E. coli* Nissile is not a pathogenic bacterium, I suspect this is a mechanism used by many gut pathogens to outcompete the host microbiota and to find a nutritional niche. Moreover, the Ybt system is conserved in *Klebsiella* and *E. coli* and the YbtX protein remains in the locus. This indicates that Ybt is likely to be used for Zn acquisition in *Klebsiella* similar to *Y. pestis* and *E. coli*. Future studies with *Klebsiella* will help determine if Ybt plays a role in zinc acquisition for infection.

Additionally, other bacteria potentially will utilize a similar secretion mechanism for Ybt to Y0702-Y0704 since it remains undefined in these bacteria, and especially because these bacteria encode for homologs to RND efflux pumps. Therefore, the identification of the secretion mechanism

of Ybt in *Y. pestis* has directly impacted our understanding of virulence determinants in more clinically relevant bacteria, such as *K. pneumoniae*.

<u>How do ZnuABC and yersiniabactin work together to compete with zinc nutritional immunity?</u>

My work and previous studies support the redundancy of ZnuABC and Ybt for Zn acquisition. This raises the question of how these systems work together to acquire Zn during infection. Overall, these two Zn acquisition systems are unique in the functionality. ZnuABC is a stationary membrane bound system that works for a single bacterium to acquire Zn. On the other hand, Ybt is a secreted molecule that is a common good shared amongst a bacterial population and even with other bacteria that can use Ybt. I hypothesize that early during infection, ZnuABC plays an early role in Zn uptake, but as the infection progresses and a larger population of bacteria are present, Ybt begins to contribute to Zn acquisition.

I believe Ybt plays a greater role in the presence of a dense community of *Y. pestis* bacteria for a couple of reasons. First, if we imagine a single *Y. pestis* bacterium in the host secreting Ybt, that singular secreted Ybt is most likely not going to reach that bacterium that secreted it. For the Ybt system to be upregulated, the regulator YbtA must bind to Ybt (168). Thus, if there are only a few bacteria secreting Ybt, the likelihood of YbtA inducing the system is low. Alternatively, with more bacteria present, there would be a domino effect leading to an increase in Ybt to positively regulate Ybt synthesis. Second, there is evidence that Ybt can play a role as a quorum sensing molecule and that the system is upregulated at higher cell densities (348). This leds to the concept that Ybt positively regulates the *ybt* locus and Ybt is needed in the environment to induce the system. Regardless of when Ybt and ZnuABC are used during the timeline of infection, the presence of these two redundant systems solidifies how important Zn acquisition is for *Y. pestis*.

<u>What immune mechanism does *Y. pestis* encounter at the site of infection in the dermis for bubonic infection that inhibits replication?</u>

Based on my data using an intradermal infection model, *Y. pestis* is repressed at the site of infection in the skin. A few bacteria can disseminate from the skin through the lymphatics to reach

the draining lymph node, to replicate to high numbers. This dissemination pattern and bottleneck have been reported previously and are supported by my data (268, 311). Further, I would like to define what host mechanisms are specifically preventing *Y. pestis* replication at the site of infection or if this is a bacteria driven mechanism to further evade the host immune system.

My data completed with S100A9$^{-/-}$ (deficient in calprotectin) mice indicates that calprotectin is the main zinc barrier to *Y. pestis* infection (Fig. 2-6). Additionally, my data from our intradermal model confirmed that the calprotectin barrier is present at the site of infection (Fig. 4-3). Therefore, I hypothesize that nutritional restriction inhibits *Y. pestis* replication in the dermis, because metal acquisition is not established entering the infection. To test my hypothesis, *Y. pestis* could be passed through metal limitation before incubation with MNAs for intradermal infection. Zn and Fe limitation have been shown to activate ZnuABC and Ybt, respectively (148, 239). Thus, the systems will be primed for metal acquisition and if immediate activity of metal acquisition can challenge the calprotectin nutritional barrier, *Y. pestis* will be able to replicate more efficiently in the dermis of the ear. The replication events should take place earlier than what has previously been reported and may recapitulate the findings in S100A9$^{-/-}$ mice, that lack the calprotectin barrier.

Furthermore, it is expected that the neutrophil influx is the main source of calprotectin secretion. However, other cells types, such as the epithelium and macrophages, can secrete calprotectin (104, 106) and could be the source of calprotectin restricting infection. To determine if neutrophils are secreting calprotectin at the site of infection, mice could be infected with *Y. pestis* intradermally in the ear. Then at early timepoints (2-4 h post infection), ears could be collected and evaluated for neutrophil influx and calprotectin secretion by microscopy. Mice lacking neutrophils could be used to compare calprotectin secretion with and without neutrophils present. Although these experiments can confirm whether neutrophils are the main source of calprotectin, I believe neutrophils are the main contributors, based on the data I have collected and data from other studies.

<u>What role do other components of nutritional immunity play in preventing *Y. pestis* infection?</u>

Although my work indicates that calprotectin is the main Zn barrier to *Y. pestis* infection, other facets of nutritional immunity may play a role in inhibiting pathogenesis. From our screen of nutritional immunity transcripts during bubonic plague, we know that lipocalin, haptoglobin, lactoferrin, and the two subunits of calprotectin are upregulated in the lymph nodes (Fig. 2-4). This supports data from Comer *et al*. that there is an increase in both calprotectin subunits in the in the lymph nodes of rats infected with *Y. pestis* (259). In an infection with *Y. pestis*' close relative the enteric pathogen *Y. pseudotuberculosis,* Nuss *et al*. reported increased transcription of these genes in the Peyer's patches (260). We chose to focus on calprotectin because of its Zn-restrictive properties, but *Y. pestis* must face these other secreted components of nutritional immunity during infection. Since *Y. pestis* must compete with these factors, it would be interesting to determine if lipocalin, haptoglobin, and lactoferrin impact *Y. pestis* growth. Lipocalin does not bind to Ybt, like it does other siderophores, (252) therefore it is unlikely to attenuate growth. Lactoferrin is secreted by neutrophils during infection and considering the interactions that occur between *Y. pestis* and neutrophils, I would expect that lactoferrin does play a role in inhibiting infection. Additionally, secretion of these proteins could be evaluated during pneumonic plague.

Moreover, on the cellular level, it would be interesting to define metal restrictive mechanisms that *Y. pestis* encounters during intracellular infection. For survival in the host, *Y. pestis* uses virulence mechanisms to invade host immune cells and hijacks normal phagolysosome functions. Based on studies with other bacteria, nutritional immunity mechanisms, such as Nramp1 and ZIP, will sequester Fe, Mn, and Zn to inhibit growth (93, 116, 117). The impact of Nramp1 or ZIP on *Y. pestis* during growth in the phagolysosome in macrophages has not been identified. By determining these interactions, it will further define how *Y. pestis* interacts and competes with nutritional immunity in the mammalian host.

What is the zinc availability inside the flea for *Y. pestis* colonization?

Metal homeostasis is better understood in vertebrates than insects, thus interpreting what nutrient barriers *Y. pestis* encounters during flea colonization is difficult. Insect cells do have ferritin and transferrin to transport and store Fe (256, 349). In a *Drosophila melanogaster* model system,

it has been shown that *Pseudomonas aeruginosa* must compete with transferrin 1 for Fe (257). There is also evidence that some insects have ZIP transporters for Zn influx and efflux in cells (350). These data suggest that insects could have some conserved aspects of mammalian nutritional immunity. More specifically to *Y. pestis*, in the flea midgut, some studies have shown how metal concentrations change after a blood meal (30), but the availability of these metals to *Y. pestis* for uptake has not been studied. Notably, fleas have hemolymph which is a nutrient rich fluid found throughout their whole body that would be available to *Y. pestis*, (351, 352) as well as mammalian blood in the midgut brought in through the blood meal. Although there are nutrients present, specific mechanisms for nutrient sequestration in the flea are unresolved. A study completed by Driscoll, *et al.* has the first sequence of the flea genome (258) and by using this resource genes with homology to nutritional immunity genes in the mammalian host could be identified.

Our studies using zinc acquisition mutants have probed the flea midgut to suggest that there is Zn limitation in the flea (Fig. 2-3). To further identify what nutrients are restricted in the flea host, a transcriptional analysis of *Y. pestis* during flea infection could be completed, analyzed, and compared to *Y. pestis* grown under metal-limitation (Fe, Zn, or Mn). Vadyvaloo *et al.* did identify genes involved in adapting to the environment inside the flea, but they focused on PhoPQ regulated genes (353). Development of a greater understanding of the flea midgut environment is important to evaluating how *Y. pestis* colonizes the insect vector that is a key component to the bacteria's enzootic cycle.

Application of nutritional immunity and yersiniabactin for vaccine design to combat plague

Currently, *Y. pestis* does not have an FDA-approved vaccine to prevent disease. Since *Y. pestis* is a reemerging, deadly pathogen, identifying a vaccine to treat susceptible populations that do not have prompt access to antibiotics is of high importance. Research has been completed to use different attenuated strains of *Y. pestis* or antigens for plague vaccine design (261, 262, 354–356) and previous studies have used administrations of live EV76-based vaccines to protect against plague (354). This vaccine is designed based on deletion of the pigmentation locus (*pgm*),

which results in iron acquisition deficiency due to elimination of Ybt, and elicits a strong adaptive protective immune response (174, 354). In Zauberman *et al.*, protective antibodies were recognized against this vaccine at 24 h post inoculation, thus to understand what anti-microbial activity was occurring so early after vaccination, they used mass spectrometry to identify the proteins (354). Surprisingly, two nutritional immunity proteins, hemopexin and transferrin were eluted in the antibacterial active fractions (354). This vaccination provided protection against disease in the mouse model and this rapid nutritional immunity response was followed by the development of innate and adaptive immune responses later in the infection (354). Further, co-administration of the vaccine and virulent *Y. pestis* subcutaneously showed that this early innate response by nutritional immunity inhibited dissemination of virulent *Y. pestis* by IVIS-imaging (354). Thus, protection by a live attenuated vaccine against plague can be attributed to a nutritional immunity response.

In my work, I attempted to use an avirulent strain *znuA ybtX* delivered by intradermal vaccination to prevent pneumonic plague and I was able to see a slight delay in disease progression. However, further work needs to be completed to alter our vaccine strategy with this model. For instance, based on Zauberman *et al.*, administration of the vaccine strain and lethal strain via the same route of inoculation may show more protection against disease. Moreover, we did not test for antibodies or a nutritional immune response to the vaccination strain. Additional time between the vaccination and infection or a boost immunization could help support more antibody responses. To improve this vaccine strategy, understanding the initial immune response to the inoculation in the dermis would also be helpful.

A different strategy to combatting bacterial infections is administration of siderophores as a potential treatment and vaccine against Gram-negative pathogens. Siderophores have been conjugated with a variety of antimicrobial agents, often call the trojan-horse strategy, to improve uptake of antibiotics in *Pseudomonas aeruginosa* and *Acenitobacter baumannii* (357, 358). Additionally, synthesized conjugates of siderophores and microbial proteins have been used as an immunization strategy against future infections for pathogens like *Salmonella* (359). In this study, enterobactin was conjugated with immunogenic carrier protein cholera toxin subunit B, because

this toxin induces a strong immune response (359). This strategy elicited a mucosal immune response with antibodies against enterobactin and another siderophore salmochelin that reduced gut colonization from *Salmonella* infection (359). A similar strategy could be attempted with Ybt to protect against plague infections. Psn, the receptor for the Ybt-Fe, has been shown to induce an immune response against plague so this could be conjugated to Ybt for delivery (355, 356). It should be noted that lipocalin 2 was produced as a response to the enterobactin vaccination and may have played a role in protection against the future infection (359). Since Ybt is not impacted by lipocalin 2, it is unclear how this response may differ. Although, we have shown that lipocalin is secreted at high concentrations during bubonic infection in the lymph nodes (Fig. 2-4).

5.4 Conclusions

My work and proposed future directions will further enhance our knowledge of how the Ybt system functions to not only allow *Y. pestis* to acquire Fe, but also Zn. Based on my work and collaborations, we have shown that Ybt is able to bind to Zn. Ybt has two diastereomers and they each prefer Zn or Fe binding. Although the mechanisms for the Ybt-Zn complex uptake and metal removal from Ybt remain poorly understood, we now have the tools with dTn-seq to define these essential functions. Importantly, dTn-seq allowed me to define the primary mechanism for Ybt secretion as an RND efflux pump but we know a secondary system(s) is also supporting Ybt secretion. Likely, the secondary system is also another efflux pump since redundancy for these systems has been shown in other bacteria for siderophore export.

Alongside Ybt, ZnuABC functions to support Zn acquisition during infection to compete with calprotectin. *Y. pestis* encounters calprotectin at the site of infection and this prevents rapid replication. It is unclear where calprotectin comes from and if nutrient restriction from calprotectin is responsible for inhibiting replication at the site of infection. Other nutritional immunity mechanisms in vertebrates that may challenge *Y. pestis* virulence remain undefined and an area of new research. Moreover, our data suggests a Zn nutritional barrier in the flea midgut that *Y. pestis* overcomes by using ZnuABC and Ybt to acquire Zn. However, nutrient availability in the flea

midgut is an understudied area but an important research space for us to understand how *Y. pestis* colonizes the flea.

Importantly, my research has led to future proposed tools to combat plague infections. My application of an intradermal vaccine with an attenuated Zn acquisition strain to prevent pneumonic plague infection shows potential and can be altered to test for an innate nutritional immune response that can protect against future infections. Furthermore, utilizing Ybt as a vaccine remains a promising area of research. Since the main mechanism for Ybt secretion is an RND efflux pump, my research indicates that Ybt export can potentially serve as anti-virulence drug target, since therapeutics can block the action of efflux pumps. Notably, my work reaches across many other bacterial pathogens that use the conserved Ybt system.

REFERENCES

1. M. Achtman, *et al.*, *Yersinia pestis*, the cause of plague, is a recently emerged clone of *Yersinia pseudotuberculosis*. *Proc. Natl. Acad. Sci.* **96**, 14043–14048 (1999).

2. J. Parkhill, *et al.*, Genome sequence of *Yersinia pestis*, the causative agent of plague. *Nature* **413**, 523–527 (2001).

3. P. S. G. Chain, *et al.*, Insights into the evolution of *Yersinia pestis* through whole-genome comparison with Yersinia pseudotuberculosis. *Proc. Natl. Acad. Sci. U. S. A.* **101**, 13826–13831 (2004).

4. R. D. Perry, J. D. Fetherston, *Yersinia pestis* - etiologic agent of plague. *Clin Microbiol Rev* **10**, 35–66 (1997).

5. N. C. Stenseth, *et al.*, Plague: past, present, and future. *PLoS Med.* **5**, e3 (2008).

6. A. Yersin, [Bubonic plague in Hong Kong. 1894]. *Rev. Med. Suisse Romande* **114**, 393–395 (1994).

7. L. Kartman, M. I. Goldenberg, W. T. Hubbert, Recent observations on the epidemiology of plague in the United States. *Am. J. Public Health Nations Health* **56**, 1554–1569 (1966).

8. V. Andrianaivoarimanana, *et al.*, Understanding the Persistence of Plague Foci in Madagascar. *PLoS Negl. Trop. Dis.* **7**, e2382 (2013).

9. T. Butler, Plague Gives Surprises in the First Decade of the 21st Century in the United States and Worldwide. *Am. J. Trop. Med. Hyg.* **89**, 788–793 (2013).

10. R. Pollitzer, Plague studies. *Bull. World Health Organ.* **4**, 475–533 (1951).

11. T. V. Inglesby, *et al.*, Plague as a biological weapon: medical and public health management. Working Group on Civilian Biodefense. *JAMA* **283**, 2281–2290 (2000).

12. T. Butler, Plague history: Yersin's discovery of the causative bacterium in 1894 enabled, in the subsequent century, scientific progress in understanding the disease and the development of treatments and vaccines. *Clin. Microbiol. Infect.* **20**, 202–209 (2014).

13. B. J. Hinnebusch, The Evolution of Flea-Borne Transmission in *Yersinia pestis. Curr. Issues Mol. Biol.* **7**, 197–212 (2005).

14. C. B. Beard, J. F. Butler, D. W. Hall, Prevalence and Biology of Endosymbionts of Fleas (Siphonaptera: Pulicidae) from Dogs and Cats in Alachua County, Florida. *J. Med. Entomol.* **27**, 1050–1061 (1990).

15. A. L. Burroughs, Sylvatic plague studies. *J. Hyg. (Lond.)* **45**, 371–396 (1947).

16. B. J. Hinnebusch, Bubonic plague: a molecular genetic case history of the emergence of an infectious disease. *J. Mol. Med. Berl. Ger.* **75**, 645–652 (1997).

17. L. D. Crook, B. Tempest, Plague: A Clinical Review of 27 Cases. *Arch. Intern. Med.* **152**, 1253–1256 (1992).

18. B. J. Hinnebusch, Interactions of *Yersinia pestis* with its flea vector that lead to the transmission of plague. *Microbe-Vector Interact. Vector-Borne Dis.*, 331–343 (2004).

19. S. J. Ajl, J. S. Reedal, E. L. Durrum, J. Warren, STUDIES ON PLAGUE. *J. Bacteriol.* **70**, 158–169 (1955).

20. Y. Du, E. Galyov, A. Forsberg, Genetic analysis of virulence determinants unique to *Yersinia pestis. Contrib. Microbiol. Immunol.* **13**, 321–324 (1995).

21. B. J. Hinnebusch, *et al.*, Role of Yersinia murine toxin in survival of *Yersinia pestis* in the midgut of the flea vector. *Science* **296**, 733–735 (2002).

22. S. Jackson, T. W. Burrows, The Virulence-enhancing Effect of Iron on Non-pigmented Mutants of Virulent Strains of Pasteurella pestis. *Br. J. Exp. Pathol.* **37**, 577–583 (1956).

23. M. J. Surgalla, E. D. Beesley, Congo Red-Agar Plating Medium for Detecting Pigmentation in Pasteurella pestis. *Appl. Microbiol.* **18**, 834–837 (1969).

24. C. Buchrieser, M. Prentice, E. Carniel, The 102-kilobase unstable region of *Yersinia pestis* comprises a high-pathogenicity island linked to a pigmentation segment which undergoes internal rearrangement. *J. Bacteriol.* **180**, 2321–2329 (1998).

25. B. J. Hinnebusch, R. D. Perry, T. G. Schwan, Role of the *Yersinia pestis* hemin storage (hms) locus in the transmission of plague by fleas. *Science* **273**, 367–370 (1996).

26. B. J. Hinnebusch, E. R. Fischer, T. G. Schwan, Evaluation of the Role of the *Yersinia pestis* Plasminogen Activator and Other Plasmid-Encoded Factors in Temperature-Dependent Blockage of the Flea. *J. Infect. Dis.* **178**, 1406–1415 (1998).

27. C. O. Jarrett, *et al.*, Transmission of *Yersinia pestis* from an infectious biofilm in the flea vector. *J. Infect. Dis.* **190**, 783–792 (2004).

28. A. W. Bacot, C. J. Martin, LXVII. Observations on the mechanism of the transmission of plague by fleas. *J. Hyg. (Lond.)* **13**, 423–439 (1914).

29. A. W. Bacot, LXXXI. Further notes on the mechanism of the transmission of plague by fleas. *J. Hyg. (Lond.)* **14**, 774-776.3 (1915).

30. R. Rebeil, *et al.*, Induction of the *Yersinia pestis* PhoP-PhoQ regulatory system in the flea and its role in producing a transmissible infection. *J. Bacteriol.* **195**, 1920–1930 (2013).

31. K. Lähteenmäki, R. Virkola, A. Sarén, L. Emödy, T. K. Korhonen, Expression of Plasminogen Activator Pla of *Yersinia pestis* Enhances Bacterial Attachment to the Mammalian Extracellular Matrix. *Infect. Immun.* **66**, 5755–5762 (1998).

32. O. A. Sodeinde, *et al.*, A surface protease and the invasive character of plague. *Science* **258**, 1004–1007 (1992).

33. E. Bohn, M. Sonnabend, K. Klein, I. B. Autenrieth, Bacterial adhesion and host cell factors leading to effector protein injection by type III secretion system. *Int. J. Med. Microbiol. IJMM* **309**, 344–350 (2019).

34. T. Bergsbaken, B. T. Cookson, Innate immune response during Yersinia infection: critical modulation of cell death mechanisms through phagocyte activation. *J. Leukoc. Biol.* **86**, 1153–1158 (2009).

35. K. Pha, L. Navarro, Yersinia type III effectors perturb host innate immune responses. *World J. Biol. Chem.* **7**, 1–13 (2016).

36. D. M. Bland, D. M. Anderson, Imaging early pathogenesis of bubonic plague: are neutrophils commandeered for lymphatic transport of bacteria? *mBio* **4**, e00837-00813 (2013).

37. C. F. Bosio, C. O. Jarrett, D. Gardner, B. J. Hinnebusch, Kinetics of Innate Immune Response to *Yersinia pestis* after Intradermal Infection in a Mouse Model. *Infect. Immun.* **80**, 4034–4045 (2012).

38. J. E. Trosky, A. D. B. Liverman, K. Orth, Yersinia outer proteins: Yops. *Cell. Microbiol.* **10**, 557–565 (2008).

39. G. I. Viboud, J. B. Bliska, Yersinia outer proteins: role in modulation of host cell signaling responses and pathogenesis. *Annu. Rev. Microbiol.* **59**, 69–89 (2005).

40. C. Pujol, J. B. Bliska, Turning Yersinia pathogenesis outside in: subversion of macrophage function by intracellular yersiniae. *Clin. Immunol. Orlando Fla* **114**, 216–226 (2005).

41. M. M. Marketon, R. W. DePaolo, K. L. DeBord, B. Jabri, O. Schneewind, Plague Bacteria Target Immune Cells During Infection. *Science* **309**, 1739–1741 (2005).

42. A. R. Pulsifer, *et al.*, Redundant and Cooperative Roles for *Yersinia pestis* Yop Effectors in the Inhibition of Human Neutrophil Exocytic Responses Revealed by Gain-of-Function Approach. *Infect. Immun.* **88**, e00909-19 (2020).

43. R. Rosqvist, K. E. Magnusson, H. Wolf-Watz, Target cell contact triggers expression and polarized transfer of Yersinia YopE cytotoxin into mammalian cells. *EMBO J.* **13**, 964–972 (1994).

44. G. V. Plano, K. Schesser, The *Yersinia pestis* type III secretion system: expression, assembly and role in the evasion of host defenses. *Immunol. Res.* **57**, 237–245 (2013).

45. U. Von Pawel-Rammingen, *et al.*, GAP activity of the Yersinia YopE cytotoxin specifically targets the Rho pathway: a mechanism for disruption of actin microfilament structure. *Mol. Microbiol.* **36**, 737–748 (2000).

46. C. Persson, N. Carballeira, H. Wolf-Watz, M. Fällman, The PTPase YopH inhibits uptake of Yersinia, tyrosine phosphorylation of p130Cas and FAK, and the associated accumulation of these proteins in peripheral focal adhesions. *EMBO J.* **16**, 2307–2318 (1997).

47. F. Shao, J. E. Dixon, YopT is a cysteine protease cleaving Rho family GTPases. *Adv. Exp. Med. Biol.* **529**, 79–84 (2003).

48. J. M. Blander, R. Medzhitov, Toll-dependent selection of microbial antigens for presentation by dendritic cells. *Nature* **440**, 808–12 (2006).

49. M. V. Telepnev, *et al.*, Tetraacylated lipopolysaccharide of *Yersinia pestis* can inhibit multiple Toll-like receptor-mediated signaling pathways in human dendritic cells. *J. Infect. Dis.* **200**, 1694–1702 (2009).

50. N. Maeshima, R. C. Fernandez, Recognition of lipid A variants by the TLR4-MD-2 receptor complex. *Front. Cell. Infect. Microbiol.* **3**, 3 (2013).

51. I. Zanoni, *et al.*, CD14 controls the LPS-induced endocytosis of Toll-like receptor 4. *Cell* **147**, 868–880 (2011).

52. Y. A. Knirel, *et al.*, Temperature-dependent variations and intraspecies diversity of the structure of the lipopolysaccharide of Yersinia pestis. *Biochemistry* **44**, 1731–1743 (2005).

53. Y. A. Knirel, A. P. Anisimov, Lipopolysaccharide of *Yersinia pestis*, the Cause of Plague: Structure, Genetics, Biological Properties. *Acta Naturae* **4**, 46–58 (2012).

54. M. A. Tito, *et al.*, Macromolecular organization of the *Yersinia pestis* capsular F1 antigen: insights from time-of-flight mass spectrometry. *Protein Sci. Publ. Protein Soc.* **10**, 2408–2413 (2001).

55. A. Soliakov, J. R. Harris, A. Watkinson, J. H. Lakey, The structure of *Yersinia pestis* Caf1 polymer in free and adjuvant bound states. *Vaccine* **28**, 5746–5754 (2010).

56. L. M. Runco, S. Myrczek, J. B. Bliska, D. G. Thanassi, Biogenesis of the fraction 1 capsule and analysis of the ultrastructure of *Yersinia pestis*. *J. Bacteriol.* **190**, 3381–3385 (2008).

57. D. C. Cavanaugh, R. Randall, The role of multiplication of Pasteurella pestis in mononuclear phagocytes in the pathogenesis of flea-borne plague. *J. Immunol. Baltim. Md 1950* **83**, 348–363 (1959).

58. E. M. Galván, M. A. S. Lasaro, D. M. Schifferli, Capsular antigen fraction 1 and Pla modulate the susceptibility of Yersinia pestis to pulmonary antimicrobial peptides such as cathelicidin. *Infect. Immun.* **76**, 1456–1464 (2008).

59. A. M. Friedlander, *et al.*, Relationship between virulence and immunity as revealed in recent studies of the F1 capsule of *Yersinia pestis*. *Clin. Infect. Dis. Off. Publ. Infect. Dis. Soc. Am.* **21 Suppl 2**, S178-181 (1995).

60. K. J. Davis, *et al.*, Pathology of experimental pneumonic plague produced by fraction 1-positive and fraction 1-negative *Yersinia pestis* in African green monkeys (Cercopithecus aethiops). *Arch. Pathol. Lab. Med.* **120**, 156–163 (1996).

61. P. L. Worsham, M. P. Stein, S. L. Welkos, Construction of defined F1 negative mutants of virulent *Yersinia pestis*. *Contrib. Microbiol. Immunol.* **13**, 325–328 (1995).

62. S. L. Welkos, K. M. Davis, L. M. Pitt, P. L. Worsham, A. M. Freidlander, Studies on the contribution of the F1 capsule-associated plasmid pFra to the virulence of *Yersinia pestis*. *Contrib. Microbiol. Immunol.* **13**, 299–305 (1995).

63. S. W. Bearden, J. D. Fetherston, R. D. Perry, Genetic organization of the yersiniabactin biosynthetic region and construction of avirulent mutants in *Yersinia pestis*. *Infect. Immun.* **65**, 1659–1668 (1997).

64. J. D. Fetherston, O. Kirillina, A. G. Bobrov, J. T. Paulley, R. D. Perry, The yersiniabactin transport system is critical for the pathogenesis of bubonic and pneumonic plague. *Infect. Immun.* **78**, 2045–2052 (2010).

65. L. E. Quenee, *et al.*, Hereditary hemochromatosis restores the virulence of plague vaccine strains. *J. Infect. Dis.* **206**, 1050–1058 (2012).

66. C. Andreini, I. Bertini, G. Cavallaro, G. L. Holliday, J. M. Thornton, Metal ions in biological catalysis: from enzyme databases to general principles. *J. Biol. Inorg. Chem. JBIC Publ. Soc. Biol. Inorg. Chem.* **13**, 1205–1218 (2008).

67. A. J. Monteith, E. P. Skaar, The impact of metal availability on immune function during infection. *Trends Endocrinol. Metab. TEM* **32**, 916–928 (2021).

68. E. P. Skaar Raffatellu, M., Metals in infectious diseases and nutritional immunity. *Metallomics* **7**, 926–8 (2015).

69. J. Behnsen, *et al.*, Siderophore-mediated zinc acquisition enhances enterobacterial colonization of the inflamed gut. *Nat. Commun.* **12**, 7016 (2021).

70. C. A. Lopez Skaar, Eric P., The Impact of Dietary Transition Metals on Host-Bacterial Interactions. *Cell Host Microbe* **23**, 737–748 (2018).

71. T. Kehl-Fie Skaar, E., Nutritional immunity beyond iron: a role for manganese and zinc. *Curr Opin Chem Biol* **14**, 218–224 (2010).

72. C. C. Murdoch, E. P. Skaar, Nutritional immunity: the battle for nutrient metals at the host-pathogen interface. *Nat. Rev. Microbiol.* **20**, 657–670 (2022).

73. I. Iteman, *et al.*, Relationship between loss of pigmentation and deletion of the chromosomal iron-regulated irp2 gene in *Yersinia pestis*: evidence for separate but related events. *Infect. Immun.* **61**, 2717–2722 (1993).

74. J. E. Williams, *et al.*, Atypical plague bacilli isolated from rodents, fleas, and man. *Am. J. Public Health* **68**, 262–264 (1978).

75. F. Sebbane, C. Jarrett, D. Gardner, D. Long, B. J. Hinnebusch, Role of the *Yersinia pestis* yersiniabactin iron acquisition system in the incidence of flea-borne plague. *PLoS One* **5**, e14379 (2010).

76. N. C. Andrews, Iron homeostasis: insights from genetics and animal models. *Nat. Rev. Genet.* **1**, 208–217 (2000).

77. H. Tapiero, K. D. Tew, Trace elements in human physiology and pathology: zinc and metallothioneins. *Biomed. Pharmacother. Biomedecine Pharmacother.* **57**, 399–411 (2003).

78. J. C. King, Zinc: an essential but elusive nutrient. *Am. J. Clin. Nutr.* **94**, 679S–84S (2011).

79. C. L. Keen, J. L. Ensunsa, M. S. Clegg, Manganese metabolism in animals and humans including the toxicity of manganese. *Met. Ions Biol. Syst.* **37**, 89–121 (2000).

80. A. Donovan, *et al.*, The iron exporter ferroportin/Slc40a1 is essential for iron homeostasis. *Cell Metab.* **1**, 191–200 (2005).

81. A. Donovan, *et al.*, Positional cloning of zebrafish ferroportin1 identifies a conserved vertebrate iron exporter. *Nature* **403**, 776–781 (2000).

82. S. Abboud, D. J. Haile, A novel mammalian iron-regulated protein involved in intracellular iron metabolism. *J. Biol. Chem.* **275**, 19906–19912 (2000).

83. A. T. McKie, *et al.*, A novel duodenal iron-regulated transporter, IREG1, implicated in the basolateral transfer of iron to the circulation. *Mol. Cell* **5**, 299–309 (2000).

84. H. Drakesmith, A. M. Prentice, Hepcidin and the iron-infection axis. *Science* **338**, 768–772 (2012).

85. H. K. Miller, L. Schwiesow, W. Au-Yeung, V. Auerbuch, Hereditary Hemochromatosis Predisposes Mice to *Yersinia pseudotuberculosis* Infection Even in the Absence of the Type III Secretion System. *Front Cell Infect Microbiol* **6**, 69 (2016).

86. F. W. Huang, J. L. Pinkus, G. S. Pinkus, M. D. Fleming, N. C. Andrews, A mouse model of juvenile hemochromatosis. *J Clin Invest* **115**, 2187–91 (2005).

87. M. Vadillo, X. Corbella, V. Pac, P. Fernandez-Viladrich, R. Pujol, Multiple liver abscesses due to *Yersinia enterocolitica* discloses primary hemochromatosis: three cases reports and review. *Clin. Infect. Dis. Off. Publ. Infect. Dis. Soc. Am.* **18**, 938–941 (1994).

88. R. Zapata, P. García, Multiple hepatosplenic abscesses caused by *Yersinia enterocolitica* in a patient with hemochromatosis. *Rev. Med. Chil.* **125**, 917–921 (1997).

89. K. M. Frank, O. Schneewind, W.-J. Shieh, Investigation of a researcher's death due to septicemic plague. *N. Engl. J. Med.* **364**, 2563–2564 (2011).

90. H. Haase, L. Rink, Zinc signals and immune function. *BioFactors* **40**, 27–40 (2014).

91. H. Haase, L. Rink, Functional significance of zinc-related signaling pathways in immune cells. *Annu. Rev. Nutr.* **29**, 133–152 (2009).

92. T. Hirano, *et al.*, Roles of zinc and zinc signaling in immunity: zinc as an intracellular signaling molecule. *Adv. Immunol.* **97**, 149–176 (2008).

93. M. F. Cellier, P. Courville, C. Campion, Nramp1 phagocyte intracellular metal withdrawal defense. *Microbes Infect.* **9**, 1662–1670 (2007).

94. O. L. Champion, *et al.*, *Yersinia pseudotuberculosis* mntH functions in intracellular manganese accumulation, which is essential for virulence and survival in cells expressing functional Nramp1. *Microbiology* **157**, 1115–22 (2011).

95. M. Wessling-Resnick, Nramp1 and Other Transporters Involved in Metal Withholding during Infection. *J. Biol. Chem.* **290**, 18984–18990 (2015).

96. Y. Brenz, D. Ohnezeit, H. C. Winther-Larsen, M. Hagedorn, Nramp1 and NrampB Contribute to Resistance against Francisella in Dictyostelium. *Front. Cell. Infect. Microbiol.* **7**, 282 (2017).

97. O. Cunrath, D. Bumann, Host resistance factor SLC11A1 restricts Salmonella growth through magnesium deprivation. *Science* **366**, 995–999 (2019).

98. S. T. Ong, J. Z. S. Ho, B. Ho, J. L. Ding, Iron-withholding strategy in innate immunity. *Immunobiology* **211**, 295–314 (2006).

99. K. Gkouvatsos, G. Papanikolaou, K. Pantopoulos, Regulation of iron transport and the role of transferrin. *Biochim. Biophys. Acta* **1820**, 188–202 (2012).

100. S. Farnaud, R. W. Evans, Lactoferrin--a multifunctional protein with antimicrobial properties. *Mol. Immunol.* **40**, 395–405 (2003).

101. K. Okubo, *et al.*, Lactoferrin Suppresses Neutrophil Extracellular Traps Release in Inflammation. *EBioMedicine* **10**, 204–215 (2016).

102. S. M. Damo, *et al.*, Molecular basis for manganese sequestration by calprotectin and roles in the innate immune response to invading bacterial pathogens. *Proc Natl Acad Sci U A* **110**, 3841–6 (2013).

103. T. G. Nakashige, E. M. Zygiel, C. L. Drennan, E. M. Nolan, Nickel Sequestration by the Host-Defense Protein Human Calprotectin. *J. Am. Chem. Soc.* **139**, 8828–8836 (2017).

104. T. G. Nakashige, B. Zhang, C. Krebs, E. M. Nolan, Human calprotectin is an iron-sequestering host-defense protein. *Nat. Chem. Biol.* **11**, 765–771 (2015).

105. J. Edgeworth, M. Gorman, R. Bennett, P. Freemont, N. Hogg, Identification of p8,14 as a highly abundant heterodimeric calcium binding protein complex of myeloid cells. *J. Biol. Chem.* **266**, 7706–7713 (1991).

106. A. N. Besold, *et al.*, Antimicrobial action of calprotectin that does not involve metal withholding. *Met. Integr. Biometal Sci.* **10**, 1728–1742 (2018).

107. B. D. Corbin, *et al.*, Metal chelation and inhibition of bacterial growth in tissue abscesses. *Science* **319**, 962–965 (2008).

108. T. E. Kehl-Fie, *et al.*, MntABC and MntH Contribute to Systemic *Staphylococcus aureus* Infection by Competing with Calprotectin for Nutrient Manganese. *Infect. Immun.* **81**, 3395–3405 (2013).

109. M. I. Hood, *et al.*, Identification of an *Acinetobacter baumannii* zinc acquisition system that facilitates resistance to calprotectin-mediated zinc sequestration. *PLoS Pathog* **8**, e1003068 (2012).

110. J. P. Zackular, *et al.*, Dietary zinc alters the microbiota and decreases resistance to *Clostridium difficile* infection. *Nat Med* **22**, 1330–1334 (2016).

111. J. A. Gaddy, *et al.*, The host protein calprotectin modulates the *Helicobacter pylori* cag type IV secretion system via zinc sequestration. *PLoS Pathog.* **10**, e1004450 (2014).

112. A. Dow, *et al.*, Zinc limitation triggers anticipatory adaptations in *Mycobacterium tuberculosis*. *PLoS Pathog.* **17**, e1009570 (2021).

113. T. H. Flo, *et al.*, Lipocalin 2 mediates an innate immune response to bacterial infection by sequestrating iron. *Nature* **432**, 917–921 (2004).

114. M. A. Bachman, *et al.*, *Klebsiella pneumoniae* yersiniabactin promotes respiratory tract infection through evasion of lipocalin 2. *Infect. Immun.* **79**, 3309–3316 (2011).

115. K. Subramanian Vignesh, J. A. Landero Figueroa, A. Porollo, J. A. Caruso, G. S. Deepe, Granulocyte macrophage-colony stimulating factor induced Zn sequestration enhances macrophage superoxide and limits intracellular pathogen survival. *Immunity* **39**, 697–710 (2013).

116. S. C. Hall, *et al.*, Critical Role of Zinc Transporter (ZIP8) in Myeloid Innate Immune Cell Function and the Host Response against Bacterial Pneumonia. *J. Immunol. Baltim. Md 1950* **207**, 1357–1370 (2021).

117. M.-J. Liu, *et al.*, ZIP8 regulates host defense through zinc-mediated inhibition of NF-κB. *Cell Rep.* **3**, 386–400 (2013).

118. L. A. Finney, T. V. O'Halloran, Transition metal speciation in the cell: insights from the chemistry of metal ion receptors. *Science* **300**, 931–936 (2003).

119. D. K. Blencowe, A. P. Morby, Zn(II) metabolism in prokaryotes. *FEMS Microbiol. Rev.* **27**, 291–311 (2003).

120. S. Silver, Bacterial resistances to toxic metal ions--a review. *Gene* **179**, 9–19 (1996).

121. C. A. McDevitt, *et al.*, A molecular mechanism for bacterial susceptibility to zinc. *PLoS Pathog.* **7**, e1002357 (2011).

122. B. A. Eijkelkamp, *et al.*, Extracellular zinc competitively inhibits manganese uptake and compromises oxidative stress management in *Streptococcus pneumoniae*. *PloS One* **9**, e89427 (2014).

123. C. Y. Ong, M. J. Walker, A. G. McEwan, Zinc disrupts central carbon metabolism and capsule biosynthesis in *Streptococcus pyogenes*. *Sci. Rep.* **5**, 10799 (2015).

124. M. Valko, H. Morris, M. T. D. Cronin, Metals, toxicity and oxidative stress. *Curr. Med. Chem.* **12**, 1161–1208 (2005).

125. J. A. Imlay, The mismetallation of enzymes during oxidative stress. *J. Biol. Chem.* **289**, 28121–28128 (2014).

126. F. F. Xu, J. A. Imlay, Silver(I), mercury(II), cadmium(II), and zinc(II) target exposed enzymic iron-sulfur clusters when they toxify *Escherichia coli*. *Appl. Environ. Microbiol.* **78**, 3614–3621 (2012).

127. K. A. Hassan, *et al.*, Zinc stress induces copper depletion in *Acinetobacter baumannii*. *BMC Microbiol.* **17**, 59 (2017).

128. H. Botella, *et al.*, Mycobacterial p(1)-type ATPases mediate resistance to zinc poisoning in human macrophages. *Cell Host Microbe* **10**, 248–259 (2011).

129. R. Kapetanovic, *et al.*, Salmonella employs multiple mechanisms to subvert the TLR-inducible zinc-mediated antimicrobial response of human macrophages. *FASEB J. Off. Publ. Fed. Am. Soc. Exp. Biol.* **30**, 1901–1912 (2016).

130. C. J. Stocks, *et al.*, Uropathogenic *Escherichia coli* employs both evasion and resistance to subvert innate immune-mediated zinc toxicity for dissemination. *Proc. Natl. Acad. Sci. U. S. A.* **116**, 6341–6350 (2019).

131. C. J. Stocks, *et al.*, Frontline Science: LPS-inducible SLC30A1 drives human macrophage-mediated zinc toxicity against intracellular *Escherichia coli*. *J. Leukoc. Biol.* **109**, 287–297 (2021).

132. C. Y. Ong, C. M. Gillen, T. C. Barnett, M. J. Walker, A. G. McEwan, An antimicrobial role for zinc in innate immune defense against group A streptococcus. *J. Infect. Dis.* **209**, 1500–1508 (2014).

133. N. Z. Gammoh, L. Rink, Zinc in Infection and Inflammation. *Nutrients* **9**, 624 (2017).

134. V. Ducret, M. R. Gonzalez, S. Leoni, M. Valentini, K. Perron, The CzcCBA Efflux System Requires the CadA P-Type ATPase for Timely Expression Upon Zinc Excess in *Pseudomonas aeruginosa*. *Front. Microbiol.* **11**, 911 (2020).

135. S. F. Alquethamy, *et al.*, The Role of Zinc Efflux during *Acinetobacter baumannii* Infection. *ACS Infect. Dis.* **6**, 150–158 (2020).

136. E. B. Brazel, *et al.*, Dysregulation of *Streptococcus pneumoniae* zinc homeostasis breaks ampicillin resistance in a pneumonia infection model. *Cell Rep.* **38**, 110202 (2022).

137. D. Osman, *et al.*, Bacterial sensors define intracellular free energies for correct enzyme metalation. *Nat. Chem. Biol.* **15**, 241–249 (2019).

138. K. A. Baksh, D. B. Zamble, Allosteric control of metal-responsive transcriptional regulators in bacteria. *J. Biol. Chem.* **295**, 1673–1684 (2020).

139. K. Hantke, Regulation of ferric iron transport in *Escherichia coli* K12: isolation of a constitutive mutant. *Mol. Gen. Genet. MGG* **182**, 288–292 (1981).

140. A. Bagg, J. B. Neilands, Ferric uptake regulation protein acts as a repressor, employing iron (II) as a cofactor to bind the operator of an iron transport operon in *Escherichia coli*. *Biochemistry* **26**, 5471–5477 (1987).

141. M. Coy, J. B. Neilands, Structural dynamics and functional domains of the fur protein. *Biochemistry* **30**, 8201–8210 (1991).

142. I. Michaud-Soret, *et al.*, Electrospray ionization mass spectrometry analysis of the apo- and metal-substituted forms of the Fur protein. *FEBS Lett.* **413**, 473–476 (1997).

143. C. Daniel, S. Haentjens, M. C. Bissinger, R. J. Courcol, Characterization of the *Acinetobacter baumannii* Fur regulator: cloning and sequencing of the fur homolog gene. *FEMS Microbiol. Lett.* **170**, 199–209 (1999).

144. R. W. Prince, C. D. Cox, M. L. Vasil, Coordinate regulation of siderophore and exotoxin A production: molecular cloning and sequencing of the *Pseudomonas aeruginosa* fur gene. *J. Bacteriol.* **175**, 2589–2598 (1993).

145. K. G. Wooldridge, P. H. Williams, J. M. Ketley, Iron-responsive genetic regulation in *Campylobacter jejuni*: cloning and characterization of a fur homolog. *J. Bacteriol.* **176**, 5852–5856 (1994).

146. T. M. Staggs, R. D. Perry, Identification and cloning of a fur regulatory gene in *Yersinia pestis*. *J. Bacteriol.* **173**, 417–425 (1991).

147. H. Gao, *et al.*, The iron-responsive Fur regulon in *Yersinia pestis*. *J. Bacteriol.* **190**, 3063–3075 (2008).

148. D. C. Desrosiers, *et al.*, Znu is the predominant zinc importer in *Yersinia pestis* during in vitro growth but is not essential for virulence. *Infect. Immun.* **78**, 5163–5177 (2010).

149. S. I. Patzer, K. Hantke, The ZnuABC high-affinity zinc uptake system and its regulator Zur in *Escherichia coli*. *Mol. Microbiol.* **28**, 1199–1210 (1998).

150. K. Hantke, Bacterial zinc uptake and regulators. *Curr. Opin. Microbiol.* **8**, 196–202 (2005).

151. S. W. Bearden, R. D. Perry, The Yfe system of *Yersinia pestis* transports iron and manganese and is required for full virulence of plague. *Mol. Microbiol.* **32**, 403–414 (1999).

152. J. D. Fetherston, I. Mier, H. Truszczynska, R. D. Perry, The Yfe and Feo transporters are involved in microaerobic growth and virulence of *Yersinia pestis* in bubonic plague. *Infect. Immun.* **80**, 3880–3891 (2012).

153. R. D. Perry, I. Mier Jr., J. D. Fetherston, Roles of the Yfe and Feo transporters of *Yersinia pestis* in iron uptake and intracellular growth. *Biometals* **20**, 699–703 (2007).

154. S. W. Bearden, T. M. Staggs, R. D. Perry, An ABC Transporter System of *Yersinia pestis* Allows Utilization of Chelated Iron by Escherichia coli SAB11. *J. Bacteriol.* **180**, 1135–1147 (1998).

155. S. Gong, S. W. Bearden, V. A. Geoffroy, J. D. Fetherston, R. D. Perry, Characterization of the *Yersinia pestis* Yfu ABC inorganic iron transport system. *Infect Immun* **69**, 2829–37 (2001).

156. O. Kirillina, A. G. Bobrov, J. D. Fetherston, R. D. Perry, Hierarchy of Iron Uptake Systems: Yfu and Yiu Are Functional in *Yersinia pestis*. *Infect. Immun.* **74**, 6171–6178 (2006).

157. J. M. Thompson, H. A. Jones, R. D. Perry, Molecular Characterization of the Hemin Uptake Locus (hmu) from *Yersinia pestis* and Analysis of hmu Mutants for Hemin and Hemoprotein Utilization. *Infect. Immun.* **67**, 3879–3892 (1999).

158. J. M. Hornung, H. A. Jones, R. D. Perry, The hmu locus of *Yersinia pestis* is essential for utilization of free haemin and haem--protein complexes as iron sources. *Mol. Microbiol.* **20**, 725–739 (1996).

159. J. M. Thompson, H. A. Jones, R. D. Perry, Molecular characterization of the hemin uptake locus (hmu) from *Yersinia pestis* and analysis of hmu mutants for hemin and hemoprotein utilization. *Infect. Immun.* **67**, 3879–3892 (1999).

160. A. M. Albrecht-Gary, A. L. Crumbliss, Coordination chemistry of siderophores: thermodynamics and kinetics of iron chelation and release. *Met. Ions Biol. Syst.* **35**, 239–327 (1998).

161. H. Haag, *et al.*, Purification of yersiniabactin: a siderophore and possible virulence factor of *Yersinia enterocolitica*. *J. Gen. Microbiol.* **139**, 2159–2165 (1993).

162. J. Heesemann, *et al.*, Virulence of *Yersinia enterocolitica* is closely associated with siderophore production, expression of an iron-repressible outer membrane polypeptide of 65,000 Da and pesticin sensitivity. *Mol. Microbiol.* **8**, 397–408 (1993).

163. A. Rakin, C. Noelting, S. Schubert, J. Heesemann, Common and Specific Characteristics of the High-Pathogenicity Island of *Yersinia enterocolitica*. *Infect. Immun.* **67**, 5265–5274 (1999).

164. H. Karch, *et al.*, A genomic island, termed high-pathogenicity island, is present in certain non-O157 Shiga toxin-producing *Escherichia coli* clonal lineages. *Infect. Immun.* **67**, 5994–6001 (1999).

165. S. Schubert, A. Rakin, H. Karch, E. Carniel, J. Heesemann, Prevalence of the "high-pathogenicity island" of Yersinia species among *Escherichia coli* strains that are pathogenic to humans. *Infect. Immun.* **66**, 480–485 (1998).

166. S. Bach, A. de Almeida, E. Carniel, The Yersinia high-pathogenicity island is present in different members of the family Enterobacteriaceae. *FEMS Microbiol. Lett.* **183**, 289–294 (2000).

167. S. D. Himpsl, *et al.*, Proteobactin and a yersiniabactin-related siderophore mediate iron acquisition in *Proteus mirabilis*. *Mol. Microbiol.* **78**, 138–157 (2010).

168. J. D. Fetherston, S. W. Bearden, R. D. Perry, YbtA, an AraC-type regulator of the *Yersinia pestis* pesticin/yersiniabactin receptor. *Mol. Microbiol.* **22**, 315–325 (1996).

169. R. Anisimov, D. Brem, J. Heesemann, A. Rakin, Transcriptional regulation of high pathogenicity island iron uptake genes by YbtA. *Int. J. Med. Microbiol. IJMM* **295**, 19–28 (2005).

170. A. M. Gehring, *et al.*, Iron acquisition in plague: modular logic in enzymatic biogenesis of yersiniabactin by *Yersinia pestis*. *Chem. Biol.* **5**, 573–586 (1998).

171. A. M. Gehring, I. Mori, R. D. Perry, C. T. Walsh, The nonribosomal peptide synthetase HMWP2 forms a thiazoline ring during biogenesis of yersiniabactin, an iron-chelating virulence factor of *Yersinia pestis*. *Biochemistry* **37**, 11637–11650 (1998).

172. V. A. Geoffroy, J. D. Fetherston, R. D. Perry, *Yersinia pestis* YbtU and YbtT Are Involved in Synthesis of the Siderophore Yersiniabactin but Have Different Effects on Regulation. *Infect. Immun.* **68**, 4452–4461 (2000).

173. D. M. Ferber, J. M. Fowler, R. R. Brubaker, Mutations to tolerance and resistance to pesticin and colicins in *Escherichia coli* phi. *J. Bacteriol.* **146**, 506–511 (1981).

174. J. D. Fetherston, R. D. Perry, The pigmentation locus of *Yersinia pestis* KIM6+ is flanked by an insertion sequence and includes the structural genes for pesticin sensitivity and HMWP2. *Mol. Microbiol.* **13**, 697–708 (1994).

175. A. Rakin, E. Saken, D. Harmsen, J. Heesemann, The pesticin receptor of *Yersinia enterocolitica*: a novel virulence factor with dual function. *Mol. Microbiol.* **13**, 253–263 (1994).

176. J. D. Fetherston, V. J. Bertolino, R. D. Perry, YbtP and YbtQ: two ABC transporters required for iron uptake in *Yersinia pestis*. *Mol. Microbiol.* **32**, 289–299 (1999).

177. E. I. Koh, A. E. Robinson, N. Bandara, B. E. Rogers, J. P. Henderson, Copper import in *Escherichia coli* by the yersiniabactin metallophore system. *Nat. Chem. Biol.* **13**, 1016–1021 (2017).

178. E. I. Koh, *et al.*, Metal selectivity by the virulence-associated yersiniabactin metallophore system. *Metallomics* **7**, 1011–22 (2015).

179. K. S. Chaturvedi, C. S. Hung, J. R. Crowley, A. E. Stapleton, J. P. Henderson, The siderophore yersiniabactin binds copper to protect pathogens during infection. *Nat. Chem. Biol.* **8**, 731–736 (2012).

180. A. E. Robinson, J. E. Lowe, E.-I. Koh, J. P. Henderson, Uropathogenic enterobacteria use the yersiniabactin metallophore system to acquire nickel. *J. Biol. Chem.* **293**, 14953–14961 (2018).

181. L. M. Bogomolnaya, R. Tilvawala, J. R. Elfenbein, J. D. Cirillo, H. L. Andrews-Polymenis, Linearized Siderophore Products Secreted via MacAB Efflux Pump Protect *Salmonella enterica* Serovar Typhimurium from Oxidative Stress. *mBio* **11**, e00528-20 (2020).

182. T. Henríquez, N. V. Stein, H. Jung, PvdRT-OpmQ and MdtABC-OpmB efflux systems are involved in pyoverdine secretion in *Pseudomonas putida* KT2440. *Environ. Microbiol. Rep.* **11**, 98–106 (2019).

183. D. E. Kunkle, X. R. Bina, J. E. Bina, The *Vibrio cholerae* VexGH RND Efflux System Maintains Cellular Homeostasis by Effluxing Vibriobactin. *mBio* **8**, e00126-17 (2017).

184. R. M. Wells, *et al.*, Discovery of a siderophore export system essential for virulence of *Mycobacterium tuberculosis*. *PLoS Pathog.* **9**, e1003120 (2013).

185. T. Horiyama, K. Nishino, AcrB, AcrD, and MdtABC multidrug efflux systems are involved in enterobactin export in *Escherichia coli*. *PloS One* **9**, e108642 (2014).

186. M. S. Lawlor, C. O'connor, V. L. Miller, Yersiniabactin is a virulence factor for *Klebsiella pneumoniae* during pulmonary infection. *Infect. Immun.* **75**, 1463–1472 (2007).

187. G. Dalmasso, *et al.*, Yersiniabactin Siderophore of Crohn's Disease-Associated Adherent-Invasive *Escherichia coli* Is Involved in Autophagy Activation in Host Cells. *Int. J. Mol. Sci.* **22**, 3512 (2021).

188. A. R. Brumbaugh, *et al.*, Blocking yersiniabactin import attenuates extraintestinal pathogenic *Escherichia coli* in cystitis and pyelonephritis and represents a novel target to prevent urinary tract infection. *Infect. Immun.* **83**, 1443–1450 (2015).

189. A. Paauw, M. A. Leverstein-van Hall, K. P. M. van Kessel, J. Verhoef, A. C. Fluit, Yersiniabactin reduces the respiratory oxidative stress response of innate immune cells. *PloS One* **4**, e8240 (2009).

190. M. L. Zaharik, B. B. Finlay, Mn2+ and bacterial pathogenesis. *Front. Biosci. J. Virtual Libr.* **9**, 1035–1042 (2004).

191. N. S. Jakubovics, H. F. Jenkinson, Out of the iron age: new insights into the critical role of manganese homeostasis in bacteria. *Microbiol. Read. Engl.* **147**, 1709–1718 (2001).

192. D. G. Kehres, M. E. Maguire, Emerging themes in manganese transport, biochemistry and pathogenesis in bacteria. *FEMS Microbiol. Rev.* **27**, 263–290 (2003).

193. R. D. Perry, *et al.*, Manganese transporters Yfe and MntH are Fur-regulated and important for the virulence of *Yersinia pestis*. *Microbiology* **158**, 804–15 (2012).

194. S. S. Merchant, J. D. Helmann, Elemental economy: microbial strategies for optimizing growth in the face of nutrient limitation. *Adv. Microb. Physiol.* **60**, 91–210 (2012).

195. C. Andreini, L. Banci, I. Bertini, A. Rosato, Zinc through the three domains of life. *J. Proteome Res.* **5**, 3173–3178 (2006).

196. Y. Li, *et al.*, Characterization of Zur-dependent genes and direct Zur targets in *Yersinia pestis*. *BMC Microbiol* **9**, 128 (2009).

197. A. G. Bobrov, *et al.*, Zinc transporters YbtX and ZnuABC are required for the virulence of *Yersinia pestis* in bubonic and pneumonic plague in mice. *Met. Integr. Biometal Sci.* **9**, 757–772 (2017).

198. F. Sebbane, *et al.*, Adaptive response of *Yersinia pestis* to extracellular effectors of innate immunity during bubonic plague. *Proc. Natl. Acad. Sci.* **103**, 11766–11771 (2006).

199. V. Vadyvaloo, C. Jarrett, D. E. Sturdevant, F. Sebbane, B. J. Hinnebusch, Transit through the flea vector induces a pretransmission innate immunity resistance phenotype in *Yersinia pestis*. *PLoS Pathog.* **6**, e1000783 (2010).

200. S. Ammendola, *et al.*, High-affinity Zn2+ uptake system ZnuABC is required for bacterial zinc homeostasis in intracellular environments and contributes to the virulence of *Salmonella enterica*. *Infect. Immun.* **75**, 5867–5876 (2007).

201. S. Campoy, *et al.*, Role of the high-affinity zinc uptake znuABC system in *Salmonella enterica* serovar typhimurium virulence. *Infect. Immun.* **70**, 4721–4725 (2002).

202. L. M. Davis, T. Kakuda, V. J. DiRita, A *Campylobacter jejuni* znuA orthologue is essential for growth in low-zinc environments and chick colonization. *J. Bacteriol.* **191**, 1631–1640 (2009).

203. L. E. Hesse, Z. R. Lonergan, W. N. Beavers, E. P. Skaar, The *Acinetobacter baumannii* Znu System Overcomes Host-Imposed Nutrient Zinc Limitation. *Infect. Immun.* **87**, e00746-19 (2019).

204. S. Kim, K. Watanabe, T. Shirahata, M. Watarai, Zinc uptake system (znuA locus) of *Brucella abortus* is essential for intracellular survival and virulence in mice. *J. Vet. Med. Sci.* **66**, 1059–1063 (2004).

205. P. Petrarca, S. Ammendola, P. Pasquali, A. Battistoni, The Zur-Regulated ZinT Protein Is an Auxiliary Component of the High-Affinity ZnuABC Zinc Transporter That Facilitates Metal Recruitment during Severe Zinc Shortage. *J. Bacteriol.* **192**, 1553–1564 (2010).

206. L. A. Yatsunyk, *et al.*, Structure and metal binding properties of ZnuA, a periplasmic zinc transporter from *Escherichia coli*. *J. Biol. Inorg. Chem. JBIC Publ. Soc. Biol. Inorg. Chem.* **13**, 271–288 (2008).

207. A. I. Graham, *et al.*, Severe zinc depletion of *Escherichia coli*: roles for high affinity zinc binding by ZinT, zinc transport and zinc-independent proteins. *J. Biol. Chem.* **284**, 18377–18389 (2009).

208. M. Cerasi, S. Ammendola, A. Battistoni, Competition for zinc binding in the host-pathogen interaction. *Front. Cell. Infect. Microbiol.* **3**, 108 (2013).

209. A. G. Bobrov, *et al.*, The *Yersinia pestis* siderophore, yersiniabactin, and the ZnuABC system both contribute to zinc acquisition and the development of lethal septicaemic plague in mice. *Mol. Microbiol.* **93**, 759–775 (2014).

210. Z. A. Youard, N. Wenner, C. Reimmann, Iron acquisition with the natural siderophore enantiomers pyochelin and enantio-pyochelin in Pseudomonas species. *Biometals Int. J. Role Met. Ions Biol. Biochem. Med.* **24**, 513–522 (2011).

211. L. Remy, *et al.*, The *Staphylococcus aureus* Opp1 ABC transporter imports nickel and cobalt in zinc-depleted conditions and contributes to virulence. *Mol. Microbiol.* **87**, 730–743 (2013).

212. G. Ghssein, *et al.*, Biosynthesis of a broad-spectrum nicotianamine-like metallophore in *Staphylococcus aureus*. *Science* **352**, 1105–1109 (2016).

213. C. Demeure, *et al.*, *Yersinia pestis* and plague: an updated view on evolution, virulence determinants, immune subversion, vaccination and diagnostics. *Microbes Infect.* **21**, 202–212 (2019).

214. R. J. Eisen, *et al.*, Early-phase transmission of *Yersinia pestis* by unblocked fleas as a mechanism explaining rapidly spreading plague epizootics. *Proc. Natl. Acad. Sci. U. S. A.* **103**, 15380–15385 (2006).

215. R. D. Pechous, V. Sivaraman, N. M. Stasulli, W. E. Goldman, Pneumonic Plague: The Darker Side of *Yersinia pestis*. *Trends Microbiol.* **24**, 190–197 (2016).

216. W. W. Lathem, S. D. Crosby, V. L. Miller, W. E. Goldman, Progression of primary pneumonic plague: a mouse model of infection, pathology, and bacterial transcriptional activity. *Proc. Natl. Acad. Sci. U. S. A.* **102**, 17786–17791 (2005).

217. K. W. Becker, E. P. Skaar, Metal limitation and toxicity at the interface between host and pathogen. *FEMS Microbiol. Rev.* **38**, 1235–1249 (2014).

218. V. E. Diaz-Ochoa, S. Jellbauer, S. Klaus, M. Raffatellu, Transition metal ions at the crossroads of mucosal immunity and microbial pathogenesis. *Front. Cell. Infect. Microbiol.* **4**, 2 (2014).

219. M. I. Hood, E. P. Skaar, Nutritional immunity: transition metals at the pathogen-host interface. *Nat. Rev. Microbiol.* **10**, 525–537 (2012).

220. Z. R. Lonergan, E. P. Skaar, Nutrient Zinc at the Host-Pathogen Interface. *Trends Biochem Sci* (2019) https://doi.org/10.1016/j.tibs.2019.06.010.

221. L. D. Palmer Skaar, E. P., Transition Metals and Virulence in Bacteria. *Annu Rev Genet* **50**, 67–91 (2016).

222. V. Brinkmann, A. Zychlinsky, Neutrophil extracellular traps: is immunity the second function of chromatin? *J. Cell Biol.* **198**, 773–783 (2012).

223. V. Brinkmann, et al., Neutrophil Extracellular Traps Kill Bacteria. *Science* **303**, 1532–1535 (2004).

224. C. F. Urban, *et al.*, Neutrophil extracellular traps contain calprotectin, a cytosolic protein complex involved in host defense against *Candida albicans*. *PLoS Pathog* **5**, e1000639 (2009).

225. K. Odink, *et al.*, Two calcium-binding proteins in infiltrate macrophages of rheumatoid arthritis. *Nature* **330**, 80–82 (1987).

226. J. P. Zackular, W. J. Chazin, E. P. Skaar, Nutritional Immunity: S100 Proteins at the Host-Pathogen Interface. *J. Biol. Chem.* **290**, 18991–18998 (2015).

227. P. Sohnle Hunter, M. ,. Hahn, B. ,. Chazin, W., Zinc-Reversible Antimicrobial Activity of Recombinant Calprotectin (Migration Inhibitory Factor–Related Proteins 8 and 14). *J. Infect. Dis.* **182**, 1272–1275 (2000).

228. T. E. Kehl-Fie, *et al.*, Nutrient metal sequestration by calprotectin inhibits bacterial superoxide defense, enhancing neutrophil killing of *Staphylococcus aureus*. *Cell Host Microbe* **10**, 158–164 (2011).

229. J. L. Kelliher, T. E. Kehl-Fie, Competition for Manganese at the Host-Pathogen Interface. *Prog. Mol. Biol. Transl. Sci.* **142**, 1–25 (2016).

230. C. A. Lopez, *et al.*, The Immune Protein Calprotectin Impacts *Clostridioides difficile* Metabolism through Zinc Limitation. *MBio* **10** (2019).

231. J. Z. Liu, *et al.*, Zinc sequestration by the neutrophil protein calprotectin enhances Salmonella growth in the inflamed gut. *Cell Host Microbe* **11**, 227–39 (2012).

232. B. R. Wilson, A. R. Bogdan, M. Miyazawa, K. Hashimoto, Y. Tsuji, Siderophores in Iron Metabolism: From Mechanism to Therapy Potential. *Trends Mol. Med.* **22**, 1077–1090 (2016).

233. A. Rakin, L. Schneider, O. Podladchikova, Hunger for iron: the alternative siderophore iron scavenging systems in highly virulent Yersinia. *Front Cell Infect Microbiol* **2**, 151 (2012).

234. R. D. Perry Fetherston, J. D., Yersiniabactin iron uptake: mechanisms and role in *Yersinia pestis* pathogenesis. *Microbes Infect* **13**, 808–17 (2011).

235. M. S. Lawlor, C. O'Connor, V. L. Miller, Yersiniabactin Is a Virulence Factor for *Klebsiella pneumoniae* during Pulmonary Infection. *Infect. Immun.* **75**, 1463–1472 (2007).

236. E. C. Garcia, A. R. Brumbaugh, H. L. T. Mobley, Redundancy and specificity of *Escherichia coli* iron acquisition systems during urinary tract infection. *Infect. Immun.* **79**, 1225–1235 (2011).

237. D. H. Wellawa, B. Allan, A. P. White, W. Köster, Iron-Uptake Systems of Chicken-Associated Salmonella Serovars and Their Role in Colonizing the Avian Host. *Microorganisms* **8**, 1203 (2020).

238. J. Mokracka, R. Koczura, A. Kaznowski, Yersiniabactin and other siderophores produced by clinical isolates of Enterobacter spp. and Citrobacter spp. *FEMS Immunol. Med. Microbiol.* **40**, 51–55 (2004).

239. R. D. Perry, P. B. Balbo, H. A. Jones, J. D. Fetherston, E. DeMoll, Yersiniabactin from *Yersinia pestis*: biochemical characterization of the siderophore and its role in iron transport and regulation. *Microbiology* **145**, 1181–1190 (1999).

240. M. C. Miller, S. Parkin, J. D. Fetherston, R. D. Perry, E. DeMoll, Crystal structure of ferric-yersiniabactin, a virulence factor of *Yersinia pestis*. *J. Inorg. Biochem.* **100**, 1495–1500 (2006).

241. M. C. Miller, *et al.*, Reduced synthesis of the Ybt siderophore or production of aberrant Ybt-like molecules activates transcription of yersiniabactin genes in *Yersinia pestis*. *Microbiol. Read. Engl.* **156**, 2226–2238 (2010).

242. J. D. Fetherston, J. W. Lillard, R. D. Perry, Analysis of the pesticin receptor from *Yersinia pestis*: role in iron-deficient growth and possible regulation by its siderophore. *J. Bacteriol.* **177**, 1824–1833 (1995).

243. A. Lemon, A. Silva-Rohwer, J. Sagawa, V. Vadyvaloo, Co-infection Assay to Determine *Yersinia pestis* Competitive Fitness in Fleas. *Methods Mol. Biol. Clifton NJ* **2010**, 153–166 (2019).

244. L. C. Martínez-Chavarría, *et al.*, Putative Horizontally Acquired Genes, Highly Transcribed during *Yersinia pestis* Flea Infection, Are Induced by Hyperosmotic Stress and Function in Aromatic Amino Acid Metabolism. *J. Bacteriol.* **202**, e00733-19 (2020).

245. Y. Sun, M. G. Connor, J. M. Pennington, M. B. Lawrenz, Development of bioluminescent bioreporters for in vitro and in vivo tracking of *Yersinia pestis*. *PloS One* **7**, e47123 (2012).

246. I. P. Korndörfer, F. Brueckner, A. Skerra, The crystal structure of the human (S100A8/S100A9)2 heterotetramer, calprotectin, illustrates how conformational changes of interacting alpha-helices can determine specific association of two EF-hand proteins. *J. Mol. Biol.* **370**, 887–898 (2007).

247. D. E. Brodersen, J. Nyborg, M. Kjeldgaard, Zinc-binding site of an S100 protein revealed. Two crystal structures of Ca^{2+}-bound human psoriasin (S100A7) in the Zn^{2+}-loaded and Zn^{2+}-free states. *Biochemistry* **38**, 1695–1704 (1999).

248. O. V. Moroz, E. V. Blagova, A. J. Wilkinson, K. S. Wilson, I. B. Bronstein, The crystal structures of human S100A12 in apo form and in complex with zinc: new insights into S100A12 oligomerisation. *J. Mol. Biol.* **391**, 536–551 (2009).

249. M. P. Manitz, *et al.*, Loss of S100A9 (MRP14) Results in Reduced Interleukin-8-Induced CD11b Surface Expression, a Polarized Microfilament System, and Diminished Responsiveness to Chemoattractants In Vitro. *Mol. Cell. Biol.* **23**, 1034–1043 (2003).

250. J. Kramer, O. Ozkaya, R. Kummerli, Bacterial siderophores in community and host interactions. *Nat Rev Microbiol* (2019) https:/doi.org/10.1038/s41579-019-0284-4.

251. N. J. Moscatello, B. A. Pfeifer, Yersiniabactin metal binding characterization and removal of nickel from industrial wastewater. *Biotechnol. Prog.* **33**, 1548–1554 (2017).

252. M. A. Bachman, *et al.*, *Klebsiella pneumoniae* Yersiniabactin Promotes Respiratory Tract Infection through Evasion of Lipocalin 2. *Infect. Immun.* **79**, 3309–3316 (2011).

253. A. C. Souza Lopes, *et al.*, Occurrence and analysis of *irp2* virulence gene in isolates of *Klebsiella pneumoniae* and Enterobacter spp. from microbiota and hospital and community-acquired infections. *Microb. Pathog.* **96**, 15–19 (2016).

254. L. Wisgrill, *et al.*, Outbreak of Yersiniabactin-producing *Klebsiella pneumoniae* in a Neonatal Intensive Care Unit. *Pediatr. Infect. Dis. J.* **38**, 638–642 (2019).

255. C. Shankar, *et al.*, Whole genome analysis of hypervirulent *Klebsiella pneumoniae* isolates from community and hospital acquired bloodstream infection. *BMC Microbiol.* **18**, 6 (2018).

256. D. L. Geiser, J. J. Winzerling, Insect transferrins: multifunctional proteins. *Biochim. Biophys. Acta* **1820**, 437–451 (2012).

257. I. Iatsenko, A. Marra, J.-P. Boquete, J. Peña, B. Lemaitre, Iron sequestration by transferrin 1 mediates nutritional immunity in *Drosophila melanogaster*. *Proc. Natl. Acad. Sci. U. S. A.* **117**, 7317–7325 (2020).

258. T. P. Driscoll, *et al.*, A chromosome-level assembly of the cat flea genome uncovers rampant gene duplication and genome size plasticity. *BMC Biol.* **18**, 70 (2020).

259. J. E. Comer, *et al.*, Transcriptomic and innate immune responses to *Yersinia pestis* in the lymph node during bubonic plague. *Infect. Immun.* **78**, 5086–5098 (2010).

260. A. M. Nuss, *et al.*, Tissue dual RNA-seq allows fast discovery of infection-specific functions and riboregulators shaping host-pathogen transcriptomes. *Proc. Natl. Acad. Sci. U. S. A.* **114**, E791–E800 (2017).

261. G. Dinc, J. M. Pennington, E. S. Yolcu, M. B. Lawrenz, H. Shirwan, Improving the Th1 cellular efficacy of the lead *Yersinia pestis* rF1-V subunit vaccine using SA-4-1BBL as a novel adjuvant. *Vaccine* **32**, 5035–40 (2014).

262. W. Bowen, *et al.*, Robust Th1 cellular and humoral responses generated by the *Yersinia pestis* rF1-V subunit vaccine formulated to contain an agonist of the CD137 pathway do not translate into increased protection against pneumonic plague. *Vaccine* **37**, 5708–5716 (2019).

263. K. Cao, *et al.*, The mechanism of iron-compensation for manganese deficiency of *Streptococcus pneumoniae*. *J. Proteomics* **184**, 62–70 (2018).

264. K. P. Grim, *et al.*, The Metallophore Staphylopine Enables *Staphylococcus aureus* To Compete with the Host for Zinc and Overcome Nutritional Immunity. *mBio* **8**, e01281-17 (2017).

265. P. A. Clohessy, B. E. Golden, Calprotectin-mediated zinc chelation as a biostatic mechanism in host defence. *Scand. J. Immunol.* **42**, 551–556 (1995).

266. H. L. Clark, *et al.*, Zinc and Manganese Chelation by Neutrophil S100A8/A9 (Calprotectin) Limits Extracellular *Aspergillus fumigatus* Hyphal Growth and Corneal Infection. *J. Immunol. Baltim. Md 1950* **196**, 336–344 (2016).

267. J. G. Shannon, B. J. Hinnebusch, Antibody Opsonization Enhances Early Interactions between *Yersinia pestis* and Neutrophils in the Skin and Draining Lymph Node in a Mouse Model of Bubonic Plague. *Infect. Immun.* **89**, e00061-20 (2020).

268. R. J. Gonzalez, M. C. Lane, N. J. Wagner, E. H. Weening, V. L. Miller, Dissemination of a Highly Virulent Pathogen: Tracking The Early Events That Define Infection. *PLoS Pathog.* **11**, e1004587 (2015).

269. Y. Vagima, *et al.*, Circumventing *Y. pestis* Virulence by Early Recruitment of Neutrophils to the Lungs during Pneumonic Plague. *PLoS Pathog.* **11**, e1004893 (2015).

270. J. N. Radin, J. L. Kelliher, P. K. Parraga Solorzano, T. E. Kehl-Fie, The Two-Component System ArlRS and Alterations in Metabolism Enable *Staphylococcus aureus* to Resist Calprotectin-Induced Manganese Starvation. *PLoS Pathog* **12**, e1006040 (2016).

271. S. A. Handley, P. H. Dube, V. L. Miller, Histamine signaling through the H(2) receptor in the Peyer's patch is important for controlling *Yersinia enterocolitica* infection. *Proc. Natl. Acad. Sci. U. S. A.* **103**, 9268–9273 (2006).

272. R. D. Pechous, Intranasal Inoculation of Mice with *Yersinia pestis* and Processing of Pulmonary Tissue for Analysis. *Methods Mol. Biol. Clifton NJ* **2010**, 17–28 (2019).

273. K. R. O. Hazlett, *et al.*, The *Treponema pallidum tro* operon encodes a multiple metal transporter, a zinc-dependent transcriptional repressor, and a semi-autonomously expressed phosphoglycerate mutase. *J. Biol. Chem.* **278**, 20687–20694 (2003).

274. J. M. Doll, *et al.*, Cat-transmitted fatal pneumonic plague in a person who traveled from Colorado to Arizona. *Am. J. Trop. Med. Hyg.* **51**, 109–114 (1994).

275. T. V. Inglesby, *et al.*, Plague as a biological weapon: medical and public health management. *J Amer Med Assoc* **283**, 2281–2290 (2000).

276. M. I. Hood, E. P. Skaar, Nutritional immunity: transition metals at the pathogen-host interface. *Nat Rev Microbiol* **10**, 525–37 (2012).

277. J. D. Fetherston, O. Kirillina, A. G. Bobrov, J. T. Paulley, R. D. Perry, The yersiniabactin transport system is critical for the pathogenesis of bubonic and pneumonic plague. *Infect Immun* **78**, 2045–52 (2010).

278. S. L. Price, *et al.*, Yersiniabactin contributes to overcoming zinc restriction during *Yersinia pestis* infection of mammalian and insect hosts. *Proc. Natl. Acad. Sci. U. S. A.* **118**, e2104073118 (2021).

279. A. G. Bobrov, O. Kirillina, J. D. Fetherston, M. C. Miller, J. A. Burlison, R. D. Perry, The *Yersinia pestis* siderophore, yersiniabactin, and the ZnuABC system both contribute to zinc acquisition and the development of lethal septicaemic plague in mice. *Mol Microbiol* **93**, 759–75 (2014).

280. T. A. Oelschlaeger, *et al.*, The high-pathogenicity island is absent in human pathogens of *Salmonella enterica* subspecies I but present in isolates of subspecies III and VI. *J. Bacteriol.* **185**, 1107–1111 (2003).

281. T. van Opijnen, K. L. Bodi, A. Camilli, Tn-seq: high-throughput parallel sequencing for fitness and genetic interaction studies in microorganisms. *Nat. Methods* **6**, 767–772 (2009).

282. D. Thibault, *et al.*, Droplet Tn-Seq combines microfluidics with Tn-Seq for identifying complex single-cell phenotypes. *Nat. Commun.* **10**, 5729 (2019).

283. M. G. Gutierrez, D. R. Yoder-Himes, J. M. Warawa, Comprehensive identification of virulence factors required for respiratory melioidosis using Tn-seq mutagenesis. *Front. Cell. Infect. Microbiol.* **5**, 78 (2015).

284. J. Hunt, *et al.*, The Use of 4-(2-Pyridylazo)resorcinol in Studies of Zinc Relase from *Escherichia coli* Aspartate Transcarbamoylase. *Anal. Biochem.* **146**, 150–157 (1985).

285. M. C. Miller, E. DeMoll, Extraction, purification, and identification of yersiniabactin, the siderophore of *Yersinia pestis*. *Curr Protoc Microbiol* **Chapter 5**, Unit5B 3 (2011).

286. K. L. Stirrett, *et al.*, A multicopy suppressor screening approach as a means to identify antibiotic resistance determinant candidates in Yersinia pestis. *BMC Microbiol.* **8**, 122 (2008).

287. R. L. Guest, E. A. Court, J. L. Waldon, K. A. Schock, T. L. Raivio, Impaired Efflux of the Siderophore Enterobactin Induces Envelope Stress in *Escherichia coli*. *Front. Microbiol.* **10**, 2776 (2019).

288. G. Aviv, *et al.*, A unique megaplasmid contributes to stress tolerance and pathogenicity of an emergent *Salmonella enterica* serovar Infantis strain. *Environ. Microbiol.* **16**, 977–994 (2014).

289. E. Riera, *et al.*, *Pseudomonas aeruginosa* carbapenem resistance mechanisms in Spain: impact on the activity of imipenem, meropenem and doripenem. *J. Antimicrob. Chemother.* **66**, 2022–2027 (2011).

290. M. F. Lin, Y. Y. Lin, C. C. Tu, C. Y. Lan, Distribution of different efflux pump genes in clinical isolates of multidrug-resistant *Acinetobacter baumannii* and their correlation with antimicrobial resistance. *J. Microbiol. Immunol. Infect. Wei Mian Yu Gan Ran Za Zhi* **50**, 224–231 (2017).

291. J. Nowak, H. Seifert, P. G. Higgins, Prevalence of eight resistance-nodulation-division efflux pump genes in epidemiologically characterized *Acinetobacter baumannii* of worldwide origin. *J. Med. Microbiol.* **64**, 630–635 (2015).

292. C. Kosmidis, *et al.*, Expression of multidrug resistance efflux pump genes in clinical and environmental isolates of *Staphylococcus aureus*. *Int. J. Antimicrob. Agents* **40**, 204–209 (2012).

293. D. Ma, D. N. Cook, J. E. Hearst, H. Nikaido, Efflux pumps and drug resistance in Gram-negative bacteria. *Trends Microbiol.* **2**, 489–493 (1994).

294. H. Nikaido, M. Basina, V. Nguyen, E. Y. Rosenberg, Multidrug Efflux Pump AcrAB of Salmonella typhimurium Excretes Only Those β-Lactam Antibiotics Containing Lipophilic Side Chains. *J. Bacteriol.* **180**, 4686–4692 (1998).

295. A. Schumacher, *et al.*, Effect of 1-(1-naphthylmethyl)-piperazine, a novel putative efflux pump inhibitor, on antimicrobial drug susceptibility in clinical isolates of Enterobacteriaceae other than *Escherichia coli*. *J. Antimicrob. Chemother.* **57**, 344–348 (2006).

296. D. H. Adamson, V. Krikstopaityte, P. J. Coote, Enhanced efficacy of putative efflux pump inhibitor/antibiotic combination treatments versus MDR strains of *Pseudomonas aeruginosa* in a *Galleria mellonella in vivo* infection model. *J. Antimicrob. Chemother.* **70**, 2271–2278 (2015).

297. G. W. Kaatz, V. V. Moudgal, S. M. Seo, J. B. Hansen, J. E. Kristiansen, Phenylpiperidine selective serotonin reuptake inhibitors interfere with multidrug efflux pump activity in *Staphylococcus aureus*. *Int. J. Antimicrob. Agents* **22**, 254–261 (2003).

298. J. Nzakizwanayo, *et al.*, Fluoxetine and thioridazine inhibit efflux and attenuate crystalline biofilm formation by *Proteus mirabilis*. *Sci. Rep.* **7**, 12222 (2017).

299. J. R. Aeschlimann, L. D. Dresser, G. W. Kaatz, M. J. Rybak, Effects of NorA Inhibitors on *in vitro* Antibacterial Activities and Postantibiotic Effects of Levofloxacin, Ciprofloxacin, and Norfloxacin in Genetically Related Strains of *Staphylococcus aureus*. *Antimicrob. Agents Chemother.* **43**, 335–340 (1999).

300. I. M. S. Torres, E. B. Bento, L. da C. Almeida, L. Z. C. M. de Sá, E. M. Lima, Preparation, characterization and *in vitro* antimicrobial activity of liposomal ceftazidime and cefepime against *Pseudomonas aeruginosa* strains. *Braz. J. Microbiol.* **43**, 984–992 (2012).

301. J. J. Merriam, R. Mathur, R. Maxfield-Boumil, R. R. Isberg, Analysis of the *Legionella pneumophila fliI* gene: intracellular growth of a defined mutant defective for flagellum biosynthesis. *Infect. Immun.* **65**, 2497–2501 (1997).

302. K. A. Walker, V. L. Miller, Regulation of the Ysa Type III Secretion System of *Yersinia enterocolitica* by YsaE/SycB and YsrS/YsrR. *J. Bacteriol.* **186**, 4056–4066 (2004).

303. S. Al-Khodor, C. T. Price, F. Habyarimana, A. Kalia, Y. Abu Kwaik, A Dot/Icm-translocated ankyrin protein of *Legionella pneumophila* is required for intracellular proliferation within human macrophages and protozoa. *Mol. Microbiol.* **70**, 908–923 (2008).

304. K. M. McCoy, M. L. Antonio, T. van Opijnen, MAGenTA: a Galaxy implemented tool for complete Tn-Seq analysis and data visualization. *Bioinformatics* **33**, 2781–2783 (2017).

305. J. S. Anthony, T. van Opijnen, A DAG computation server for fully integrated and automated massively parallel sequencing analyses. (2019).

306. Y. Sun, M. G. Connor, J. M. Pennington, M. B. Lawrenz, Development of bioluminescent bioreporters for *in vitro* and *in vivo* tracking of *Yersinia pestis*. *PLoS One* **7**, e47123 (2012).

307. J. D. Fetherston, P. Schuetze, R. D. Perry, Loss of the pigmentation phenotype in *Yersinia pestis* is due to the spontaneous deletion of 102 kb of chromosomal DNA which is flanked by a repetitive element. *Mol. Microbiol.* **6**, 2693–2704 (1992).

308. K. I. Bos, *et al.*, A draft genome of *Yersinia pestis* from victims of the Black Death. *Nature* **478**, 506–510 (2011).

309. F. Sebbane, C. O. Jarrett, D. Gardner, D. Long, B. J. Hinnebusch, Role of the *Yersinia pestis* plasminogen activator in the incidence of distinct septicemic and bubonic forms of flea-borne plague. *Proc. Natl. Acad. Sci. U. S. A.* **103**, 5526–5530 (2006).

310. R. J. Gonzalez, M. C. Lane, N. J. Wagner, E. H. Weening, V. L. Miller, Dissemination of a highly virulent pathogen: tracking the early events that define infection. *PLoS Pathog* **11**, e1004587 (2015).

311. J. G. Shannon, *et al.*, *Yersinia pestis* Subverts the Dermal Neutrophil Response in a Mouse Model of Bubonic Plague. *mBio* **4**, e00170-13 (2013).

312. F. Sebbane, D. Gardner, D. Long, B. B. Gowen, B. J. Hinnebusch, Kinetics of Disease Progression and Host Response in a Rat Model of Bubonic Plague. *Am. J. Pathol.* **166**, 1427–1439 (2005).

313. R. J. Gonzalez, E. H. Weening, M. C. Lane, V. L. Miller, Comparison of Models for Bubonic Plague Reveals Unique Pathogen Adaptations to the Dermis. *Infect Immun* **83**, 2855–61 (2015).

314. F. Guinet, P. Avé, L. Jones, M. Huerre, E. Carniel, Defective Innate Cell Response and Lymph Node Infiltration Specify *Yersinia pestis* Infection. *PLoS ONE* **3**, e1688 (2008).

315. A. N. Besold, *et al.*, Role of Calprotectin in Withholding Zinc and Copper from *Candida albicans*. *Infect. Immun.* **86**, e00779-17 (2018).

316. S. Ammendola, *et al.*, Zinc-binding metallophores protect *Pseudomonas aeruginosa* from calprotectin-mediated metal starvation. *FEMS Microbiol. Lett.* **369**, fnac071 (2022).

317. Q. Zeng, J. M. Gammon, L. H. Tostanoski, Y.-C. Chiu, C. M. Jewell, In Vivo Expansion of Melanoma-Specific T Cells Using Microneedle Arrays Coated with Immune-Polyelectrolyte Multilayers. *ACS Biomater. Sci. Eng.* **3**, 195–205 (2017).

318. R. F. Donnelly, *et al.*, Microneedle arrays allow lower microbial penetration than hypodermic needles in vitro. *Pharm. Res.* **26**, 2513–2522 (2009).

319. N. G. Rouphael, *et al.*, The safety, immunogenicity, and acceptability of inactivated influenza vaccine delivered by microneedle patch (TIV-MNP 2015): a randomised, partly blinded, placebo-controlled, phase 1 trial. *Lancet Lond. Engl.* **390**, 649–658 (2017).

320. C. E. Chandler, *et al.*, *In vivo* Intradermal Delivery of Bacteria by Using Microneedle Arrays. *Infect Immun* **86** (2018).

321. J. Ziesmer, *et al.*, Vancomycin-Loaded Microneedle Arrays against Methicillin-Resistant *Staphylococcus aureus* Skin Infections. *Adv. Mater. Technol.* **6**, 2001307 (2021).

322. Q. Zhu, *et al.*, Immunization by vaccine-coated microneedle arrays protects against lethal influenza virus challenge. *Proc. Natl. Acad. Sci.* **106**, 7968–7973 (2009).

323. M. E. Turvey, *et al.*, Microneedle-based intradermal delivery of stabilized dengue virus. *Bioeng. Transl. Med.* **4**, e10127 (2019).

324. R. J. Gonzalez, E. H. Weening, R. Frothingham, G. D. Sempowski, V. L. Miller, Bioluminescence imaging to track bacterial dissemination of *Yersinia pestis* using different routes of infection in mice. *BMC Microbiol.* **12**, 147 (2012).

325. M. L. Bookstaver, S. J. Tsai, J. S. Bromberg, C. M. Jewell, Improving Vaccine and Immunotherapy Design Using Biomaterials. *Trends Immunol.* **39**, 135–150 (2018).

326. J. G. Shannon, C. F. Bosio, B. J. Hinnebusch, Dermal Neutrophil, Macrophage and Dendritic Cell Responses to *Yersinia pestis* Transmitted by Fleas. *PLoS Pathog.* **11**, e1004734 (2015).

327. I. Dale, M. K. Fagerhol, I. Naesgaard, Purification and Partial Characterization of a Highly Immunogenic Human Leukocyte Protein, the L1 Antigen. *Eur. J. Biochem.* **134**, 1–6 (1983).

328. S. Z. Chong, M. Evrard, L. G. Ng, Lights, Camera, and Action: Vertebrate Skin Sets the Stage for Immune Cell Interaction with Arthropod-Vectored Pathogens. *Front. Immunol.* **4** (2013).

329. F. Guinet, E. Carniel, A technique of intradermal injection of Yersinia to study *Y. pestis* physiopathology. *Adv. Exp. Med. Biol.* **529**, 73–78 (2003).

330. C. F. Bosio, C. O. Jarrett, D. Gardner, B. J. Hinnebusch, Kinetics of innate immune response to *Yersinia pestis* after intradermal infection in a mouse model. *Infect. Immun.* **80**, 4034–4045 (2012).

331. S. O'Mahony, *et al.*, Finding an optimal method for imaging lymphatic vessels of the upper limb. *Eur. J. Nucl. Med. Mol. Imaging* **31**, 555–563 (2004).

332. R. Cubas, *et al.*, Virus-like particle (VLP) Lymphatic Trafficking and Immune Response Generation after Immunization by Different Routes. *J. Immunother. Hagerstown Md 1997* **32**, 118–128 (2009).

333. C. Liard, *et al.*, Targeting of HIV-p24 particle-based vaccine into differential skin layers induces distinct arms of the immune responses. *Vaccine* **29**, 6379–6391 (2011).

334. B. Bonnotte, *et al.*, Intradermal injection, as opposed to subcutaneous injection, enhances immunogenicity and suppresses tumorigenicity of tumor cells. *Cancer Res.* **63**, 2145–2149 (2003).

335. H. Hayen, D. A. Volmer, Different iron-chelating properties of pyochelin diastereoisomers revealed by LC/MS. *Anal. Bioanal. Chem.* **385**, 606–611 (2006).

336. T. Teelucksingh, L. K. Thompson, G. Cox, The Evolutionary Conservation of *Escherichia coli* Drug Efflux Pumps Supports Physiological Functions. *J. Bacteriol.* **202**, e00367-20 (2020).

337. M. Alcalde-Rico, S. Hernando-Amado, P. Blanco, J. L. Martínez, Multidrug Efflux Pumps at the Crossroad between Antibiotic Resistance and Bacterial Virulence. *Front. Microbiol.* **7**, 1483 (2016).

338. J. L. Furrer, D. N. Sanders, I. G. Hook-Barnard, M. A. McIntosh, Export of the siderophore enterobactin in *Escherichia coli*: involvement of a 43 kDa membrane exporter. *Mol. Microbiol.* **44**, 1225–1234 (2002).

339. T. Horiyama, K. Nishino, AcrB, AcrD, and MdtABC multidrug efflux systems are involved in enterobactin export in *Escherichia coli*. *PloS One* **9**, e108642 (2014).

340. C. Bleuel, *et al.*, TolC is involved in enterobactin efflux across the outer membrane of *Escherichia coli*. *J. Bacteriol.* **187**, 6701–6707 (2005).

341. Z. Wang, W. Hu, H. Zheng, Pathogenic siderophore ABC importer YbtPQ adopts a surprising fold of exporter. *Sci. Adv.* **6**, eaay7997 (2020).

342. R. J. P. Dawson, K. P. Locher, Structure of a bacterial multidrug ABC transporter. *Nature* **443**, 180–185 (2006).

343. E. I. Koh, C. S. Hung, J. P. Henderson, The Yersiniabactin-Associated ATP Binding Cassette Proteins YbtP and YbtQ Enhance *Escherichia coli* Fitness during High-Titer Cystitis. *Infect. Immun.* **84**, 1312–1319 (2016).

344. H. Okusu, D. Ma, H. Nikaido, AcrAB efflux pump plays a major role in the antibiotic resistance phenotype of *Escherichia coli* multiple-antibiotic-resistance (Mar) mutants. *J. Bacteriol.* **178**, 306–308 (1996).

345. M. T. Gallegos, R. Schleif, A. Bairoch, K. Hofmann, J. L. Ramos, Arac/XylS family of transcriptional regulators. *Microbiol. Mol. Biol. Rev.* **61**, 393–410 (1997).

346. A. Rakotondrasoa, *et al.*, Characterization of *Klebsiella pneumoniae* isolated from patients suspected of pulmonary or bubonic plague during the Madagascar epidemic in 2017. *Sci. Rep.* **12**, 6871 (2022).

347. P. Grubwieser, *et al.*, Airway Epithelial Cells Differentially Adapt Their Iron Metabolism to Infection With *Klebsiella pneumoniae* and *Escherichia coli in vitro*. *Front. Cell. Infect. Microbiol.* **12**, 875543 (2022).

348. J. R. Heffernan, G. L. Katumba, W. H. McCoy, J. P. Henderson, Yersiniabactin is a quorum sensing autoinducer and siderophore in uropathogenic *Escherichia coli*. *BioRxiv Prepr. Serv. Biol.*, 2023.02.09.527953 (2023).

349. M. J. Gorman, Iron Homeostasis in Insects. *Annu. Rev. Entomol.* **68**, 51–67 (2023).

350. S. Yin, Q. Qin, B. Zhou, Functional studies of Drosophila zinc transporters reveal the mechanism for zinc excretion in Malpighian tubules. *BMC Biol.* **15**, 12 (2017).

351. G. R. Wyatt, The Biochemistry of Insect Hemolymph. *Annu. Rev. Entomol.* **6**, 75–102 (1961).

352. F. Blow, A. E. Douglas, The hemolymph microbiome of insects. *J. Insect Physiol.* **115**, 33–39 (2019).

353. V. Vadyvaloo, *et al.*, Role of the PhoP-PhoQ gene regulatory system in adaptation of *Yersinia pestis* to environmental stress in the flea digestive tract. *Microbiol. Read. Engl.* **161**, 1198–1210 (2015).

354. A. Zauberman, *et al.*, Host Iron Nutritional Immunity Induced by a Live *Yersinia pestis* Vaccine Strain Is Associated with Immediate Protection against Plague. *Front Cell Infect Microbiol* **7**, 277 (2017).

355. C. G. Branger, J. D. Fetherston, R. D. Perry, R. Curtiss, Oral vaccination with different antigens from *Yersinia pestis* KIM delivered by live attenuated Salmonella typhimurium elicits a protective immune response against plague. *Adv. Exp. Med. Biol.* **603**, 387–399 (2007).

356. C. G. Branger, *et al.*, Evaluation of Psn, HmuR and a modified LcrV protein delivered to mice by live attenuated Salmonella as a vaccine against bubonic and pneumonic *Yersinia pestis* challenge. *Vaccine* **29**, 274–282 (2010).

357. L. N. Yaeger, V. E. Coles, D. C. K. Chan, L. L. Burrows, How to kill Pseudomonas-emerging therapies for a challenging pathogen. *Ann. N. Y. Acad. Sci.* **1496**, 59–81 (2021).

358. P. J. Simner, R. Patel, Cefiderocol Antimicrobial Susceptibility Testing Considerations: the Achilles' Heel of the Trojan Horse? *J. Clin. Microbiol.* **59**, e00951-20 (2020).

359. M. Sassone-Corsi, *et al.*, Siderophore-based immunization strategy to inhibit growth of enteric pathogens. *Proc. Natl. Acad. Sci. U. S. A.* **113**, 13462–13467 (2016).

CURRICULUM VITA

Sarah Price

University of Louisville School of Medicine
Clinical and Translational Research Building Rm 633
505 S. Hancock St.
Louisville, KY 40202

EDUCATION

2008- 2012   B.S. in Microbiology, University of Tennessee, Knoxville, TN
2016- 2018   M.S. in Microbiology and Immunology, University of Louisville, Louisville, KY
2016- current   Ph.D. in Microbiology and Immunology, University of Louisville, Louisville, KY

RESEARCH POSTIONS

2011- 2012   Undergraduate Student Internship
              Center for Environmental Biotechnology
              University of Tennessee
              Knoxville, TN

2012   Research Technician
              Center for Environmental Biotechnology
              University of Tennessee
              Knoxville, TN

2012- 2016   Research Technologist
              Retrovirus Laboratory
              Johns Hopkins University School of Medicine
              Baltimore, MD

2016- current   Graduate Student Research Assistant
              Department of Microbiology and Immunology
              University of Louisville
              Louisville, KY

HONORS AND AWARDS

2008- 2012   Phi Eta Sigma National Honor Society
2011   Undergraduate Microbiology Summer Fellowship, University of Tennessee

2017	University of Louisville Graduate Student Council Travel Award
2019	University of Louisville Graduate Student Council Travel Award
2019	Mid Atlantic Microbial Pathogenesis Student Travel Award
2019	Predoctoral T32 Fellowship in Inflammation and Pathogenesis
2019	Midwest Microbial Pathogenesis Conference Student Travel Award
2020- 2022	Ruth L. Kirschstein Predoctoral Individual National Research Service Award
2020	Louisville chapter of the American Association of University Women Luncheon Student Award
2020	American Society of Microbiology Biothreats Conference Travel Award
2020	CIRTL Network MOOC, *An Introduction to Evidence-Based Undergraduate STEM Teaching*, completed with distinction
2020	American Society of Microbiology KY-TN Fall 2020 Branch Meeting: 1st place presentation
2021	CIRTL Network MOOC, *Advancing Learning Through Evidence-based STEM Teaching*, completed with distinction
2021	American Society of Microbiology KY-TN Spring 2021 Branch Meeting: 1st place presentation
2021	The Richard and Mary Finkelstein Student Travel Award for American Society of Microbiology World Microbe 2021
2021	FASEB Microbial Pathogenesis Conference: Mechanisms of Infectious Disease Poster Award
2021	FASEB Microbial Pathogenesis Conference: Mechanisms of Infectious Disease Student Travel Award
2021	FASEB The Nutrition, Immunity, and Inflammation Conference: From Model Systems to Human Trials Student Travel Award
2021	Midwest Microbial Pathogenesis Conference Student Travel Award
2021	Research Louisville Basic Science Graduate Student Poster Finalist
2022	St. Jude Future Fellow Research Conference Invited Student
2022	University of Louisville Graduate Student Council Travel Award
2022	Mid Atlantic Microbial Pathogenesis Student Travel Award
2023	Graduate Dean's Citation
2023	The Guy Stevenson Award for Excellence in Graduate Studies

TEACHING EXPERIENCE

2017- 2022	Research Methods in Microbiology and Immunology, University of Louisville, *In vivo* Selection of Mutants
2020	Nursing School, University of Louisville, Infectious Disease Training
2021- 2022	First Year Graduate Student Learning Discussion Group, University of Louisville, *Teach Yourself How to Learn*
2022	Jedi Mindset: Discussing Effective Learning Strategies with Students, University of Louisville, Celebration of Teaching and Learning: The Ripple Effect

MENTORSHIP

Shane Reeves: Undergraduate research assistant; 2017-2019
Stephanie Lunn: Master's student; 2017-2018
Tyrell Jamison: Rotation student; 2018
Hannah Hanford: Rotation student; 2019
Michelle Hallenbeck: Rotation student; 2021
Taylor Garrison: Rotation student; 2021

PROFESSIONAL DEVELOPMENT

2018	University of Louisville, *Instructional Strategies in Teaching Science Education*

2020	Center for the Integration of Research Teaching and Learning, *An Introduction to Evidence-Based Undergraduate STEM Teaching*
2021	Center for the Integration of Research Teaching and Learning, *Advancing Learning Through Evidence-based Undergraduate STEM Teaching*
2021	NIH Becoming a Resilient Scientist, University of Louisville
2021	University of Louisville Graduate School Mentoring Academy

LEADERSHIP

2011- 2012	Phi Eta Sigma National Honor Society, University of Tennessee: President
2017- 2019	Association for Women in Science Kentucky: Communications Coordinator
2017- 2018	Microbiology and Immunology Student Organization: Treasurer
2018- 2021	CRAFT Seminar Series Student Representative
2018- 2019	Microbiology and Immunology Student Organization: President
2018- 2021	Louisville Science Pathways Program Director
2019- 2022	Association for Women in Science Kentucky: Secretary
2019- 2020	Microbiology and Immunology Student Organization: Admissions Committee Student Representative
2020- 2022	Academic Achievement Discussion Group: Lead Facilitator
2021- 2022	T32 Steering Committee Student Representative

PROFESSIONAL MEMBERSHIPS

2008- 2012	Phi Eta Sigma National Honor Society
2011- current	American Society for Microbiology
2016- current	Association for Women in Science
2021-current	Microbiology Society

COMMUNITY OUTREACH

2017	Biosafety Incident Response Training with Louisville Fire Department and Public Safety
2018	DuPont Manual Regional Science Fair Judge
2018- 2021	Louisville Science Pathways Program Director
2020- 2022	Academic Achievement Discussion Group with Louis Stokes Alliances for Minority Participation at the University of Louisville

GRANTS AND CONTRACTS

Previous Support
NIH-1F31AI147404-01
Price, S (PI) Lawrenz, M (Mentor)   01/2020-12/2022
Proposal Title: Identification of a novel zinc acquisition system in *Yersinia pestis*
Goal: To biochemically define a novel zincophore secreted by *Yersinia pestis* and define its role in plague.
Role: PI

NIH/NIAID-T32 AI132146-01A1
Shirwan, H (PI)   08/2018-08/2023
Proposal Title: Inflammation and Pathogenesis T32 Training Grant
Role: Fellow (08/2019-12/2019)

Genentech Local Initiatives ($25,000)
Gritton, M, Price, S, Johnson, D   06/2019-08/2019
Proposal Title: SummerWorks and Louisville Science Pathways Project

Goal: To fund and provide a stipend for ten high school students to obtain research experience by working in research labs at the University of Louisville.
Role: Co-PI

PUBLICATIONS

1. Close, D. M., Xu, T., Smartt, A., **Price, S. L.**, Ripp, S. A., and Sayler, G. S.(2012). Expression of non-native genes in a surrogate host organism, Genetic Engineering - Basics, New Applications and Responsibilities. Ed. Barrera-Saldana HA. Rijeka, Croatia: Intech Publishers. 3-34.

2. Close, D. M., Xu, T., Smartt, A., Rogers, A., Crossley, R., **Price, S. L.**, Ripp, S. A., and Sayler, G. S.(2012). "The evolution of the bacterial luciferase gene cassette (lux) as a real-time bioreporter." *Sensors (Basel)* **12**(1): 732-752.

3. Xu, T., Close, D. M., Webb, J D., **Price, S. L.**, Ripp, S. A., and Sayler, G. S. (2013). "Continuous, real-time bioimaging of chemical bioavailability and toxicology using autonomously bioluminescent human cell lines." *Proc SPIE Int Soc Opt Eng* **8723**: 872310.

4. Abreu, C. M., **Price, S. L.**, Shirk, E. N., Cunha, R. D., Pianowski, L. F., Clements, J. E., Tanuri, A., and Gama, L. (2014). "Dual role of novel ingenol derivatives from Euphorbia tirucalli in HIV replication: inhibition of de novo infection and activation of viral LTR." *PLoS One* **9**(5): e97257.

5. Avalos, C. R., **Price**, S. L., Forsyth, E. R., Pin, J. N., Shirk, E. N., Bullock, B. T., Queen, S. E., Li, M., Gellerup, D., O'Connor, S. L., Zink, M. C., Mankowski, J. L., Gama, L., and Clements, J. E. (2016). "Quantitation of Productively Infected Monocytes and Macrophages of Simian Immunodeficiency Virus-Infected Macaques." *J Virol* **90**(12): 5643-5656.

6. Gama, L., Abreu, C. M., Shirk, E. N., **Price, S. L.**, Li, M., Laird, G. M., Pate, K. A., Wietgrefe, S. W., O'Connor, S. L., Pianowski, L., Haase, A. T., Van Lint, C., Siliciano, R. F., Clements, J. E., and L.-S. S. Group (2017). "Reactivation of simian immunodeficiency virus reservoirs in the brain of virally suppressed macaques." *AIDS* **31**(1): 5-14.

7. Hou, J., Brouwer, W. P., Kreefft, K., Gama, L., **Price, S. L.**, Janssen, H. L. A., French, P. J., Vanwolleghem, T., and Boonstra, A. (2017). "Unique intrahepatic transcriptomics profiles discriminate the clinical phases of a chronic HBV infection." *PLoS One* **12**(6): e0179920.

8. Avalos, C. R., Abreu, C. M., Queen, S. E., Li, M., **Price, S. L.**, E. N. Shirk, E. L. Engle, E. Forsyth, B. T. Bullock, F. Mac Gabhann, S. W. Wietgrefe, A. T. Haase, M. C. Zink, J. L. Mankowski, J. E. Clements and L. Gama (2017). "Brain Macrophages in Simian Immunodeficiency Virus-Infected, Antiretroviral-Suppressed Macaques: a Functional Latent Reservoir." *MBio* **8**(4).

9. **Price, S. L.**, Vadyvaloo, V., DeMarco, J. K., Brady, A., Kehl-Fie, T. E., Garneau-Tsodikova, S., Perry, R. D., and Lawrenz, M. B. **(2021). Y**ersiniabactin contributes to overcoming zinc restriction during *Yersinia pestis* infection of mammalian and insect hosts. *Proc Natl Acad Sci U S A* 118(44).

10. Behnsen, J., Zhi, H., Aron, A. T., Subramanian, V., Santus, W., Lee, M. H., Gerner, R. R., Petras, D., Liu, J. Z., Green, K. D., **Price, S. L.,** Camacho, J., Hillman, H., Tjokrosurjo, J., Montaldo, N. P., Hoover, E. M., Treacy-Abarca, S., Gilston, B. A., Skaar, E. P., Chazin, W. J., Garneau-Tsodikova, S., Lawrenz, M. B., Perry, R. D., Nuccio, S. P., Dorrestein, P. C., and Raffatellu, M. (2021). Siderophore-mediated zinc acquisition enhances enterobacterial colonization of the inflamed gut. *Nature communications*, *12*(1), 7016.

11. Kumar, A., Yang, T., Chakravorty, S., Majumdar, A., Nairn, B. L., Six, D. A., Marcondes Dos Santos, N., **Price, S. L.**, Lawrenz, M. B., Actis, L. A., Marques, M., Russo, T. A., Newton, S. M., &

Klebba, P. E. (2022). Fluorescent sensors of siderophores produced by bacterial pathogens. *The Journal of biological chemistry*, *298*(3), 101651.

12. **Price, S. L.**, Thibault, D., Garrison, T. M., Brady, A., Guo, H., Kehl-Fie, T. E., Garneau-Tsodikova, S., Perry, R. D., van Opijnen, T., and Lawrenz, M. B. (2023). DropletTn-Seq identifies the primary secretion mechanism for yersiniabactin in *Yersinia pestis. (Under review with EMBO reports).*

13. **Price, S. L.**, Oakes, R., Gonzalez, R., DeMarco, J. K., Brady, A., Jewell, C. M., and Lawrenz, M. B. (2023). Application of microneedle arrays to study *Yersinia pestis* pathogenesis. *(In submission).*

14. Brady, A., Pulsifer, A. R., **Price, S. L.**, Maddipati, K. R., Bodduluri, S. R., Pan, J., Rai, S. N., Haribabu, B., Uriarte, S. M., and Lawrenz, M. B. (2023). Inhibition of Type-3 Secretion induced LTB4 production by Yop effectors: A mechanism for early immune evasion by *Yersinia pestis. (In revision with Plos Pathogens).*

INVITED PRESENTATIONS

1. Midwest Microbial Pathogenesis Conference, Toledo, OH (2019). "Yersiniabactin contributes to *Yersinia pestis* virulence independent of iron acquisition." **(Travel Award)**

2. American Society of Microbiology Biothreats Conference, Arlington, VA (2020). "Identification of a novel zinc acquisition system in *Yersinia pestis.*" **(Travel Award)**

3. University of Louisville Community Engagement Symposium, Louisville, KY (2021). "Louisville Science Pathways."

4. American Society of Microbiology, World Microbe, Virtual (2021). "An RND Efflux System Is the Primary Secretion Mechanism for Yersiniabactin in *Yersinia pestis*." **(The Richard and Mary Finkelstein Student Travel Award)**

5. FASEB The Nutrition, Immunity, and Inflammation Conference: From Model Systems to Human Trials, Virtual (2021). "Got Zinc? A Role for Yersiniabactin in Zinc Acquisition during *Yersinia pestis* Infection."
(Travel Award)

6. Midwest Area Biosafety Network Symposium, Louisville, KY (2021). "Role for Yersiniabactin in zinc acquisition during *Yersinia pestis* infection."

7. Mid-Atlantic Microbial Pathogenesis Meeting, Wintergreen, VA (2022). "Novel Tn-seq approach identifies primary secretion system for yersiniabactin." **(Travel Award)**

8. Microbiology Society Annual Meeting, Belfast, United Kingdom (2022). "Novel Tn-seq approach identifies primary secretion system for yersiniabactin."

ORAL PRESENTATIONS

1. Department of Microbiology and Immunology Seminar, University of Louisville, Louisville, KY (2018). "Identification of a novel zinc acquisition system in *Yersinia pestis*."

2. Department of Microbiology and Immunology Seminar, University of Louisville, Louisville, KY (2020). "Got Zinc? A novel role for Yersiniabactin in zinc acquisition."

3. American Society of Microbiology, KY-TN Branch Meeting, Virtual (2020). "Role for Yersiniabactin in zinc acquisition during *Yersinia pestis* infection."

4. American Society of Microbiology, KY-TN Branch Meeting, Virtual (2021). "An RND Efflux System Is the Primary Secretion Mechanism for Yersiniabactin in *Yersinia pestis*."

5. Department of Microbiology and Immunology Seminar, University of Louisville, Louisville, KY (2021). "Ironing out the yersiniabactin system: New discoveries about an old siderophore."

6. Louisville Science Pathways Seminar Series, Louisville, KY (2021). "Role for Yersiniabactin in zinc acquisition during *Yersinia pestis* infection."

7. University of Louisville Celebration of Teaching and Learning Conference, Louisville, KY (2022). "Jedi Mindset: Discussing Effective Learning Strategies with Students."

8. Louisville Science Pathways Seminar Series, Louisville, KY (2022). "Role for Yersiniabactin in zinc acquisition during *Yersinia pestis* infection."

9. Vanderbilt University, Nashville, TN (2022). "Ironing out the yersiniabactin system: New discoveries about an old siderophore."

10. St. Jude Children's Research Hospital, Memphis, TN (2022). "Ironing out the yersiniabactin system: New discoveries about an old siderophore."

11. University of California- Davis, Davis, CA (2022). "Ironing out the yersiniabactin system: New discoveries about an old siderophore."

12. Dartmouth College, Hanover, NH (2022). "Ironing out the yersiniabactin system: New discoveries about an old siderophore."

13. University of Texas Southwestern Medical Center, Dallas, TX (2022). "Ironing out the yersiniabactin system: New discoveries about an old siderophore."

POSTER PRESENTATIONS (*presenter)

1. American Society of Microbiology KY-TN Branch Meeting, Gallatin, TN (2011). "Development of a bacterial luciferase gene cassette as a mammalian bioreporter." **Sarah Price***, Tingting Xu, Dan Close, Steven Ripp and Gary Sayler.

2. American Society of Microbiology KY-TN Branch Meeting, Maryville, TN (2012). "Optimization of a bacterial bioluminescent-based mammalian bioreporter for estrogenicity detection." **Sarah Price***, Tingting Xu, Dan Close, Steven Ripp and Gary Sayler.

3. Exhibition of Undergraduate Research and Creative Achievement, Knoxville, TN (2012). "Optimization of a bacterial bioluminescent-based mammalian bioreporter for estrogenicity detection." **Sarah Price***, Tingting Xu, Dan Close, Steven Ripp and Gary Sayler.

4. Research Louisville, Louisville, KY (2018). "Identification of a novel zinc acquisition system in *Yersinia pestis*." **Sarah Price***, Marina Fosso Yatchang, Derek Thibault, Viveka Vadyvaloo, Alex Bobrov, Sylvie Garneau-Tsodikova, Tim van Opijnen, Robert Perry, Matthew Lawrenz.

5. Mid Atlantic Microbial Pathogenesis Meeting, Wintergreen, VA (2019). "Identification of a novel zinc acquisition system in *Yersinia pestis*." **Sarah Price***, Marina Fosso Yatchang, Derek Thibault, Viveka Vadyvaloo, Alex Bobrov, Sylvie Garneau-Tsodikova, Tim van Opijnen, Robert Perry, Matthew Lawrenz.

6. Gordon Research Conference, Phagocytes, Waterville Valley, NH (2019). "Gain of function approach reveals hidden contributions of Yop effectors during *Yersinia pestis* infection of human neutrophils"; Amanda R. Pulsifer, Aruna Vashishta, **Sarah L. Price**, Shane A. Reeves, Jennifer K. Wolfe, Samantha G. Palace, Jon D. Goguen, Sobha R. Bodduluri, Haribabu Bodduluri, Silvia M. Uriarte, and Matthew B. Lawrenz*.

7. American Society of Microbiology Biothreats Conference, Arlington, VA (2020). "Identification of a novel zinc acquisition system in *Yersinia pestis*." **Sarah Price***, Keith Green, Derek Thibault, Viveka Vadyvaloo, Sylvie Garneau-Tsodikova, Tim van Opijnen, Robert Perry, Matthew Lawrenz.

8. FASEB Microbial Pathogenesis Conference: Mechanisms of Infectious Disease, Virtual (2021). "Novel Tn-seq approach identifies primary secretion system for yersiniabactin." **Sarah L. Price***, Derek M. Thibault, Tim van Opijnen, Thomas E. Kehl-Fie, Taylor M. Garrison, Michelle K. Hallenbeck, Sylvie Garneau-Tsodikova, Robert D. Perry, and Matthew B. Lawrenz.

9. FASEB The Nutrition, Immunity, and Inflammation Conference: From Model Systems to Human Trials, Virtual (2021). "Got Zinc? A Role for Yersiniabactin in Zinc Acquisition during *Yersinia pestis* Infection." **Sarah L. Price***, Keith Green, Viveka Vadyvaloo, Sylvie Garneau-Tsodikova, Thomas E. Kehl-Fie, Robert D. Perry, and Matthew B. Lawrenz.

10. Midwest Microbial Pathogenesis Conference, East Lansing, MI (2021). "Novel Tn-seq approach identifies primary secretion system for yersiniabactin." **Sarah L. Price***, Derek M. Thibault, Tim van Opijnen, Thomas E. Kehl-Fie, Taylor M. Garrison, Michelle K. Hallenbeck, Sylvie Garneau-Tsodikova, Robert D. Perry, and Matthew B. Lawrenz.

11. Research Louisville, Louisville, KY (2021). "Novel Tn-seq approach identifies primary secretion system for yersiniabactin." **Sarah L. Price***, Derek M. Thibault, Tim van Opijnen, Thomas E. Kehl-Fie, Taylor M. Garrison, Sylvie Garneau-Tsodikova, Robert D. Perry, and Matthew B. Lawrenz.

12. American Society of Microbiology KY-TN Branch Meeting, Cookeville, TN (2022). "The Role of AcrAB efflux Systems in Yersiniabactin Secretion." Taylor M. Garrison[*], **Sarah L. Price**, Michelle Hallenbeck, and Matthew B. Lawrenz.

13. St. Jude Future Fellow Research Conference, Memphis, TN (2022). "Novel Tn-seq approach identifies primary secretion system for yersiniabactin." **Sarah L. Price***, Derek M. Thibault, Tim van Opijnen, Thomas E. Kehl-Fie, Taylor M. Garrison, Sylvie Garneau-Tsodikova, Robert D. Perry, and Matthew B. Lawrenz.

14. Gordon Research Conference, Toxins and Pathogenesis, Southbridge, MA (2022). "Novel Tn-seq approach identifies primary secretion system for yersiniabactin." **Sarah L. Price***, Derek M. Thibault, Tim van Opijnen, Thomas E. Kehl-Fie, Taylor M. Garrison, Sylvie Garneau-Tsodikova, Robert D. Perry, and Matthew B. Lawrenz.

15. Gordon Research Conference, Toxins and Pathogenesis, Southbridge, MA (2022). "Application of microneedle arrays to study *Yersinia pestis* pathogenesis." **Sarah L. Price,** Robert S. Oakes, Jennifer K. DeMarco, Amanda Brady, Thomas E. Kehl-Fie, Christopher M. Jewell, Robert K. Ernst, and Matthew B. Lawrenz*.